WASHINGTON UNIVERSITY IN ST. LOUIS

Division of Biology and Biomedical Sciences
Molecular Cell Biology

Dissertation Examination Committee:
Dr. Phyllis Hanson, Chair
Dr. Robert Mecham, Co-Chair
Dr. Michael Mueckler
Dr. Daniel Ory
Dr. Philip Stahl

Mechanisms of Extracellular Vesicle Biogenesis

by
Charles E. Jackson

A dissertation presented to the
Graduate School of Arts & Sciences
of Washington University in
partial fulfillment of the
requirements for the degree
of Doctor of Philosophy

August 2016
St. Louis, Missouri

Table of Contents

List of Figures iv
Acknowledgments v
Abstract vii
Chapter 1: Introduction 1
1.1 Overview: What is an extracellular vesicle? 1
1.1.1 Cells release different types of EVs 2
1.1.2 Current methods of investigating EVs 3
1.2 EV functions 9
1.3 EV biogenesis 13
1.3.1 ESCRT 14
1.3.2 Tetraspanins 17
1.3.3 Lipids 19
1.3.4 Ubiquitin 21
1.3.5 Actin 23
1.3.6 MVB secretion 24
1.4 Aims of the thesis 29
References 33
Figures 64
Chapter 2: Inhibiting VPS4 impairs extracellular vesicle biogenesis and demonstrates a broad role for ESCRTs in exosome and ectosome release 66
Abstract 66
Introduction 67
Methods 69
Results 72
Discussion 80
References 84
Figures 95
Chapter 3: Rab27b is a selective and pH sensitive marker of exocytic MVBs 103
Abstract 103

Introduction 103
Methods 105
Results and discussion 106
References 111
Figures 114
Chapter 4: Preliminary data and future directions 119
4.1 CD63 and CD9 as markers for distinguishing exosomes versus ectosomes 119
4.2 Extended analysis of EV cargo proteins 121
Methods 124
References 126
Chapter 4 Figures 130
Chapter 5: Summary and discussion 136
Summary of the thesis 136
Discussion 139
References 144

List of Figures

Figure 1-1: Cells release different types of extracellular vesicles..... 65
Figure 2-1: CD63 and CD9 are released on distinct EVs..... 96
Figure 2-2: Comparison of PEG/ConA and ultracentrifugation EV collection methods..... 97
Figure 2-3: CD63 and CD9 EVs depend on VPS4 98
Figure 2-4: VPS4-dependant release of miRNAs and membrane vesicles 99
Figure 2-5: Characteristics of serum-triggered EV release 100
Figure 2-6: CD63 EV release depends on polymerized microtubules 101
Figure 2-7: Serum-triggered release of surface-localized CD63..... 102
Figure 3-1: Rab27b localizes to endosomes in different cell types..... 115
Figure 3-2: Rab27b localizes to a subset of CD63+ endosomes in U87 cells..... 116
Figure 3-3: Rab27b marks non-acidic endosomes 117
Figure 3-4: Neutral endosome pH enhances Rab27b recruitment 118
Figure 4-1: Nanosight particle tracking analysis of HEK293 EVs 131
Figure 4-2: HEK293 cells expressing fluorescent tetraspanins..... 132
Figure 4-3: Fluorescently tagged tetraspanins are released on EVs..... 133
Figure 4-4: VPS4 inhibition alters EV protein composition 134
Figure 4-5: ESCRT-III is incorporated into EVs.....135

Acknowledgments

I would like to thank my mentor, Dr. Phyllis Hanson, for her support, advice, and most of all her patience. I also thank my committee for their support and advice. Collaborators include Dr. Benjamin Scruggs who performed the qPCR experiments in Chapter 2, and Dr. Jean Schaffer who introduced me to Ben, and who always had thought-provoking advice and perspectives. I also extend my appreciation to past and present members of the Hanson lab. In particular, I must thank Dr. Anil Cashikar, Teri Naismith and Dr. Abigail Buchwalter. Anil is a passionate and thoughtful scientist. His openness to new ideas and techniques is inspiring. Teri is an excellent and trustworthy collaborator and friend. Abigail was encouraging and I thank her for many inspiring scientific conversations.

The friendship and support of all my DBBS classmates has been especially invaluable. Each and every one has made a special contribution to this journey, and I will be forever grateful for our time together. Thank you for being a friend.

Finally, I must thank my partner in life, Jon Roche. He has made this journey right by my side. As such, he has shared in every twist, turn, frustration, fall, and recovery. Jon is my rock. Thank you for standing by me and giving me strength when I needed it most.

ABSTRACT OF THE DISSERTATION

Mechanisms of Extracellular Vesicle Biogenesis

by

Charles E. Jackson

Doctor of Philosophy in Biology and Biomedical Sciences

Molecular Cell Biology

Washington University in St. Louis, 2016

Dr. Phyllis I. Hanson, Chair

Dr. Robert Mecham, Co-Chair

Extracellular vesicles (EVs) are important mediators of intercellular communication. Different types of EVs are released from cells by either fusion of late endsomal multivesicular bodies with the plasma membrane (exosomes) or direct budding from the plasma membrane (ectosomes). Topologically equivalent processes including intralumenal vesicle formation for degradation in the endosomal pathway and virus budding from the plasma membrane depend on the ATPase VPS4 and its Endosomal Sorting Complex Required for Transport (ESCRT)-III substrates for membrane fission and release. Whether this machinery is generally required for EV biogenesis has, however, been the subject of debate. Studies of the EV proteome from a variety of cell types consistently find ESCRT-III subunits, thus providing further impetus for studying their function in EV biogenesis. Detailed understanding of the mechanisms underlying EV biogenesis is critical to testing their proposed functions. Monitoring EV release, however, remains technically challenging. To this end, I developed a protocol for efficiently isolating EVs from small numbers of cultured cells. Using this together with complementary standard techniques, I found that inhibiting VPS4 reduced release of both protein and miRNA in EVs.

Notably, VPS4 activity was required for the release of two proteins – the tetraspanins CD63 and CD9 – that preferentially reside on different membranes and are enriched on separate EV populations. I establish that CD63 is enriched on and preferentially marks endosome-derived exosomes while CD9 is a primary marker of plasma membrane-derived ectosomes. An important question in the cell biology of exosome release is what distinguishes exocytic from degradative MVBs. I identified Rab27b as a selective marker of a subset of less acidic and likely exocytic MVBs. Neutralizing endosomal pH increased Rab27b recruitment to CD63 containing MVBs, pointing toward an important role for pH in regulating Rab27b recruitment. Returning to the role of VPS4 and ESCRT-III, our data broadly implicate VPS4 and ESCRT-III in biogenesis of both exosomes and ectosomes. I established cell lines expressing fluorescent CD63 and CD9 singly or in combination in order to further probe their segregation to different EV populations. Intriguingly, inhibiting VPS4 increased the concentration of ESCRT-III protein recovered in EVs despite the significant decrease in total vesicle release. This suggests a role for ESCRT-III disassembly during EV fission. Altogether, the work presented here sets the stage for future studies aimed at understanding multiple aspects of exosome and ectosome biogenesis.

Chapter 1

Introduction

1.1 Overview: What is an extracellular vesicle?

Extracellular vesicles (EVs) are secreted from cells as sub-micron sized spherical mosaic lipid bilayers that contain transmembrane and peripherally associated membrane proteins. The vesicles encapsulate both soluble proteins and nucleic acids. EV topology is like that of the cell that produced it: the vesicle lumen is comprised of cytosol, and proteins at the surface are in the same orientation as at the plasma membrane. Hence, EVs can be thought of as nano-organelles that, like cells, are capable of interacting with the environment and with other cells. Knowledge about these interactions is still growing, but it has become clear since the first descriptions of EV expulsion nearly 50 years ago that these organelles have broad functions in intercellular communication.

The ability of cells to release EVs appears to be an evolutionarily conserved phenomenon. They have been described in a variety of multicellular organisms, such as *Drosophila Melanogaster* and *Caenorhabtitis Elegans* (1, 2). Single-celled fungi and even archaebacteria have been shown to release EVs (3-5). Studies performed in these systems generally corroborate mechanisms of EV biogenesis and EV functions found in human cells (6-8). These findings highlight the ubiquity and evolutionary conservation of EV release and provide strong evidence supporting their physiologic importance.

EVs are found in many human bio-fluids including blood, saliva, urine and cerebral spinal fluid to name a few (9-11). Since virtually all cell types investigated to date secrete EVs, it is likely that body fluid EVs derive from multiple origins. Several proteins are common to EVs released by all cells, while others are uniquely associated with the secreting cell. In addition, even a single cell can produce different types of EVs that derive from different intracellular membranes. Thus, all EV source fluids contain heterogeneous mixtures of EV types. This EV heterogeneity is a major factor complicating investigation of EV functions and mechanisms of biogenesis. A great deal of attention has recently been placed on efforts to identify molecules that are representative of different EV classes. The following chapter provides a broad overview of extracellular vesicle biology placing emphasis on what is known about formation and function of different vesicle populations, in particular exosomes and ectosomes.

1.1.1 Cells release different types of EVs

In 1967, membranous particles termed “platelet dust” were probably the first described EVs. They possessed coagulation properties similar to those of the platelets from which they derive (12). The term prostasome was coined some years later to describe small prostate epithelia-derived vesicles found in seminal fluid (13). More recently, vesicles shed by tumor cells have been referred to as oncosomes (14). These are a few examples of cell-type specific EV descriptions. While EV content and function differ among cell types, all cells appear able to release two general types of EVs as defined by their intracellular membrane of origin (Figure 1-1). Exosomes bud into the lumen of endocytic multivesicular bodies (MVBs) and are expelled from the cell upon MVB fusion with the plasma membrane. Ectosomes, in contrast, are released in a single step by budding directly from the cell surface. The fact that different EV populations are released from a single cell raises the question of whether these different EV types play distinct functional roles. Differing subcellular distribution of EV cargo correlates with the mode

by which it is released, and manipulations that affect both subcellular distribution and release strengthen such claims. However, identifying clear markers of either EV class remains a major challenge (15-17).

1.1.2 Current Methods of Investigating EVs

The list of available approaches for analyzing EVs has expanded in recent years. Global EV–omics studies provide a broad picture of EV content and lead to assays that directly monitor a cargo of interest. Cell imaging reveals details about cargo molecule trafficking and EV release. Particle analyses provide information about EV size, number and concentration. The following discussion reviews the current state of methodologies used for EV research.

Assessing quality of EV preparations—The International Society of Extracellular Vesicles recently published a minimal set of criteria to guide distinction between EV and non-EV material (18). These guidelines are meant to help standardize what is described as an EV (rather than distinguishing among different types of EVs, e.g. exosomes vs. ectosomes). The first criterion logically requires that the EV material is isolated from extracellular fluid. Second, the need to identify proteins enriched in EVs compared to the EV-producing cells is highlighted. Examples of such proteins include integral membrane proteins, such as the tetraspanins, and cytosolic proteins that are known to interact with receptors or with membranes giving rise to EVs. In addition, intracellular proteins that reside in organelles from which EVs *do not* arise (e.g. Golgi, ER or nucleus) are expected to be de-enriched in EV preparations. The final criterion considered is some type of single vesicle analysis. Both direct visualization (e.g. transmission electron microscopy, high resolution fluorescence microscopy) and diffusion-based technologies (e.g. dynamic light scattering, nanoparticle tracking) can provide overviews of the size distribution of EVs.

Isolating EVs—EVs can be isolated using several methods that are generally based on either size or content. These methods provide a range of specificities, yields and purity. Comparative analyses demonstrate these differences, and different methods can be combined to separate EVs with different properties. To date, there is no robust method for physical separation of exosomes and ectosomes, in part because of the overlap between plasma membrane and endosomal membrane content.

Differential centrifugation is the most common method for isolating EVs from a variety of source fluids. The basis for vesicle separation is size. Typically, extracellular fluids are subject to an initial clearing step in which cells and large debris are sedimented at low g-force. Micron-sized vesicles are then sedimented at a range of 10,000-12,000 × g. A filtration step is often added to clear particles above a size range of 200-500nm. Finally, smaller vesicles are sedimented by prolonged centrifugation at 100,000-110,000 × g. In some cases, this protocol is modified to pellet micro- and nano-vesicles together. Differential centrifugation is capable of isolating vesicles for a variety of downstream applications. Among these are immunoblotting, RT-PCR, imaging by optical methods or electron microscopy, mass-spectrometry and cell uptake assays. A major downfall of differential centrifugation is the requirement for large volumes of source fluid (19). High yields can be obtained by increasing the source volume, but even then recovery efficiency is often only moderate (20). Furthermore, non-EV material including protein aggregates and lipoproteins can co-sediment with EVs isolated by this technique. Still, differential centrifugation is the current method of choice for collecting EVs and is an acceptable standard when coupled with stringent characterization of the pelleted material. Based on the average ILV size in mammals (~50nm), 40-150nm diameter vesicles are often considered to be exosomes (21). Vesicles larger than ~150nm are assumed to originate from the plasma

membrane and are referred to variously as microvesicles or ectosomes. Notably, however, smaller ectosomes are not readily distinguishable from exosomes using standard techniques, and it is likely that EVs prepared by differential centrifugation contain a mixture of vesicle types.

Density equilibrium floatation is widely used to demonstrate that a particular secreted molecule is associated with EVs. Applying the gradient over the sample allows buoyant membrane and membrane-associated molecules to float to equilibrium leaving behind soluble contaminants. This is in contrast to density equilibrium sedimentation, in which the sample is applied to the top of the gradient. Density equilibrium floatation can also distinguish among vesicles with different buoyant properties (22). A sucrose density between 1.15 and 1.19 g/ml is characteristic of exosomes based on the fractionation of proteins such as CD63, ALIX and TSG101 known to be associated with MVBs. Once again, however, the presence of ectosomes with similar protein content cannot be ruled out. EVs larger than 150nm exhibit higher densities (23), and proteomic analysis revealed that these larger EVs uniquely associate with extracellular matrix components and are likely to originate from the plasma membrane.

Affinity purification isolates EVs based on the presence of defined molecule(s) on their surface. Therefore, this method is ideal for characterizing specific EV sub-classes. EVs collected by immuno-affinity isolation have been used for downstream applications such as immunoblotting, fluorescence cytometry and mass spectrometry. Comparative analyses demonstrate that immuno-affinity isolation exhibits superior efficiency and purity compared to differential centrifugation and density floatation (24). Several commercial kits are available for immuno-capture, and this approach is an obvious choice for developing clinical diagnostic applications. Known differences in intracellular localization (e.g. endosomes vs. plasma membrane) can be a predictor for identifying proteins released on distinct types of vesicles.

Proteomic studies of immuno-affinity purified EVs has provided insight into the composition of different EV populations (25,23).

EVs can be concentrated based on size using membrane filters with micron-sized pores that retain EVs with diameters larger than the pores. Recently, EVs produced by LIM1863 cells were fractionated by sequential filtration through PVDF membranes with pore sized ranging from 0.65µm to 0.1µm (26). The authors found only two EV size classes. EVs ~300-1000nm were retained by the largest pore size filter, and EVs ~30-100nm remained in the filtrate after passage through the smallest pore size. EM and dynamic light scattering confirmed the size of EVs in each fraction. Limitations to this approach include an inability to separate EVs from large proteins and aggregates and difficulties recovering EVs from the surface and/or pores of the filter.

Size exclusion chromatography (SEC) is another approach that has been used to isolate EVs (20, 27, 28). Vesicles isolated by this method are relatively pure but a second step (either centrifugation or filter-based concentration is needed) to concentrate EVs for most downstream applications. The ensuing losses limit the efficiency of this isolation protocol.

Quantifying EVs—Methods to quantify EVs are necessary in order to study their biology and gain insight into the factors involved in EV release. An early and general approach is to determine the total protein concentration in EV isolates, but this provides no information about changes in protein composition or vesicle numbers (19). Immunoblotting for EV proteins is commonly employed to assess changes in the protein profile of EV isolates. However, changes in the number of EVs can only be inferred. The following section discusses methods for directly

counting EVs. Each has limitations and advantages, and it is clear that new approaches are still needed.

Direct visualization allows distinction between individual membrane vesicles and other types of particles such as large protein aggregates. Electron microscopy has been the choice method for observing EVs because of their small size. Immunolabeling coupled with EM can provide information about protein distribution (29). EM can also provide an estimate of the size range of EVs obtained by a given isolation procedure. It is not, however, suitable for counting EVs.

Dynamic light scattering is an optics-based method for determining the size and number of particles in suspension. A laser illuminates a volume of the medium, and the particles present in suspension scatter light in a pattern that depends on their size, shape and molecular interactions (30). Fluctuations in light scattering occur over time due to particle movement. These measurements are used to generate a mathematical model of the change in scatter over time (the autocorrelation function), which can then be used to extrapolate particle size and number. The extrapolated parameters are an average computed from the contribution of all of the particles present in the illuminated volume. Scatter intensity depends on size, leading to a skewing of results toward larger particles. Thus, the polydispersity of most EV preparations (including non-EV particles) limits the utility of this approach for describing the size distribution of EVs.

Nanoparticle tracking analysis (NTA), in contrast to dynamic light scattering, is an optical method for determining particle size and number that is independent of light scatter intensities. A time-lapse series of images of particles moving under Brownian motion is used to

track individual particles. Size information for each particle is extrapolated from its movement, and particle concentration is determined by particle counts within the defined illumination volume. As with dynamic light scattering, NTA detects all light-scattering particles and therefore requires pure EV preparations. This limitation can be overcome by using fluorescent probes that selectively label EVs (31). The simplicity and rapid read-out of NTA makes this an appealing technology for both research and clinical applications.

Flow cytometry (FC) is another technique used to quantitate EVs. Early applications of this technique coupled EVs to micron-sized beads to increase particle size thereby allowing detection (29, 32). Importantly, this approach cannot provide information about EV size or absolute number. Conventional FC measuring forward and side light scatter can only resolve objects larger than 500nm, and is thus not appropriate for detecting smaller sized EVs. Recent advances in FC technology are enabling EV analysis by measuring light scattered at larger angles, using smaller probe volumes and slower flow rates (33). A major advantage to this approach is the ability to distinguish EVs from other particles by using fluorescence labeling with antibodies or lipophilic dyes. However, size estimation in this paradigm is hampered by lack of knowledge about number of labeled molecules per EV, which directly contributes to fluorescence intensity. It is worth noting that accurate size estimation also requires calibration standards (such as synthetic beads) with size and refractive indices similar to EVs (34). The sensitivity of FC toward the smallest of EVs is still a concern.

Resistive pulse sensing is another approach used to monitor the size and number of EVs, and works by detecting the movement of single particles through a pore. The pore is in a membrane across which a voltage is applied to create a current. Increases in resistance as the particles move through the pore and the frequency of resistance increases are used to estimate

particle size and number, respectively (34-36). In one study, the lower size limit of EV detection was ~50nm, but smaller EVs were readily observed in EM preparations (34). Pore clogging remains a major technical challenge, and pure EV preparations are needed since this method cannot distinguish between EVs and other EV-sized particles.

Monitoring EV release from cells—Direct observation of EV release is a major challenge in the field since the small size of EVs presents a challenge for conventional microscopy due to diffraction limits. Discriminating a release event among the behaviors of the entire population of organelles and domains labeled by a given marker is challenging even with sensitive high-resolution imaging. Attempts to address this obstacle include the use of total internal resonance fluorescence microscopy (TIRFM) to demonstrate delivery to and docking of MVBs to the plasma membrane (32). In the future, TIRFM could also provide an approach for monitoring ectosome release in a similar fashion to studies on HIV budding (37,38).

1.2 EV functions

EVs represent a unique intercellular communication system potentially capable of delivering hydrophobic and soluble cargo to influence signaling and other processes in cells both near and far. Their original and still best-studied functions are in the immune system, where exosomes participate in antigen presentation and stimulating immune responses (16). However, EVs have now been implicated as central players in progression of diseases as heterogeneous as metastatic cancer (39-42), neurodegeneration (43, 44) and autoimmune disorders (45). A few examples of recently defined roles are in breast cancer progression and therapy resistance (46), trophic support to neurons (47), transmitting pathogenic prions in the brain (44), and disposal of cholesterol in lysosomal storage disease (48). The potent but in many cases varied effects attributed to EVs provide strong justification for future experimentation in disease models and

suggest exciting therapeutic applications. The following section provides a brief discussion of the physiologic functions attributed to EVs. In addition, a recently proposed function for EVs in virus-independent propagation of viral genomic material is highlighted.

Cellular remodeling via EV release—Exosomes were initially described as a mechanism for eliminating membrane proteins employed by maturing reticulocytes (49, 50). During the maturation process, these erythroid precursors become enucleated, and unnecessary proteins are selected for mass exodus. Early studies demonstrated that transferrin receptor is internalized from the cell surface and sorted to MVBs before being exocytosed on exosomes. The *in vivo* relevance of this pathway is evidenced by the delayed reticulocyte maturation, accumulation of transferrin receptor and microcytic anemia exhibited by mice that are deficient in p53-regulated exosome secretion (51). The α4β1 integrin is cleared from reticulocytes via exosomes implicating them in down-regulation of cellular adhesive properties (52). These studies delineate exosome secretion as an alternative lysosome-independent means to control protein and cholesterol levels.

More recently, changes in cellular content brought about by EV secretion have been suggested for other cell types. Ectocytosis is proposed to regulate levels of the GPI-anchored CD24 receptor during B-cell maturation (53). Both cadherin and β-catenin are released in EVs in a manner that depends on expression of CD9 and CD82 tetraspanins (54). Thus, EVs may regulate Wnt signaling through modulating cellular levels of β-catenin. EVs can also modulate signaling in an autocrine fashion through polarized release of receptor ligands. For example, tumor cell intravasation occurs through directional movement that requires extracellular matrix degradation. Invadapodia are actin-based protrusions that facilitate this process, and these structures are hot spots for EV release (55). Matrix metalloproteases are EV cargos that promote

matrix clearance (56). Ligands such as fibronectin associate with the surface of EVs and may promote directional tumor cell movement (57). Thus, polarized release of EVs by tumor cells could literally pave the way for intravasating cells by clearing matrix and laying out a substrate across which the cell can traverse.

Immune regulation—The most well characterized function of EVs is modulating immune responses. EVs released from myriad cell types carry molecules that are involved in activation or suppression of immune cells. It is clear that changes in the molecular composition of EVs are able to dictate the type of response. Such changes correlate with the status of the EV producing cell. For example, EVs can announce exposure to microbial pathogens, and oncogenic transformation can quell EV immune-activating properties. The ability of EVs to transfer information over long distances compared to soluble secreted proteins allows broader surveillance of physiologic status. The contribution of EVs to immune biology has provided a foundation for several clinical trials utilizing EVs for therapeutic purposes (58).

The observation that EVs released by B-cells are capable of activating T-cells was a pivotal finding that launched studies leading to the current understanding of EVs as important mediators in intercellular communication (59). Since this discovery, it has become clear that other antigen presenting cells (dendritic cells; DCs and Macrophages; Macs) release EVs with similar properties. These cells capture and process foreign antigens for presentation on MHC I or II molecules upon activation. Peptide-MHC and co-stimulatory molecules are then released on EVs (59-61). Evidence suggests that T-cell priming by bystander antigen presenting cells is required for EV-mediated activation (62,63). While the source of antigen can be through direct contact of antigen presenting cells with pathogens, EVs can deliver antigens to immature antigen-presenting cells thereby potentiating T-cell activation. Antigen-exposed B-cells travel to

the spleen where DCs take up antigen for presentation to T-cells – a process that may be facilitated by B-cell EVs (64). Nonhematopoietic cells can also provide antigen-loaded EVs. For example, EVs from intestinal epithelium carry peptide-MHC II complexes that can transfer to DCs (65,66).

Immunosuppressive functions can convey immune privilege to the developing fetus as well as to tumors (67, 68). EVs derived from trophoblast cells are found in the uterine fluid and the blood of pregnant women. Similarly, EVs with tumor cell associated molecules are found in the circulation of individuals with cancer (69). In each case, immune modulation involves suppression of T-lymphocytes. Natural killer cell cytotoxicity is inhibited by EVs that engage NKG2D receptors via peptide-MHC I or truncated MHC I during pregnancy and cancer (70)(71). Furthermore, EVs from trophoblast and tumor cells carry FasL/TRAIL molecules that induce T-cell apoptosis (67, 72). Recent evidence points towards bi-directional EV-mediated communication during pregnancy (73). The authors found that trophoblast cells take up EVs from Macs, which results in increased secretion of IL-6, IL-8 and IL-10 cytokines. This finding implicates EVs as a mechanism by which the maternal immune system can communicate inflammatory conditions to the developing fetus. Whether the altered cytokine production in response to Mac EVs culminates in anti- or pro-inflammatory responses remains an open question. Given the parallels between EV-mediated communication during pregnancy and cancer it will be interesting to see if future studies reveal a role for immune cell EVs in altering tumor phenotypes. Taken together, the studies outlined here demonstrate that EVs play a critical role in immune surveillance and highlight a few of what are likely to be many dynamic responses mediated by EVs.

Viral genome transfer—EV contents include protein and nucleic acid cargo that can be transferred between cells via these vesicular shuttles. Notably, cells that are infected with bacterial or viral pathogens incorporate pathogen-derived molecules into their EVs (74,75). The role of this phenomenon in activating immune responses to combat infection is discussed in the previous section. Importantly, viruses can also highjack EVs in order to transfer molecules to uninfected cells thus manipulating their environment and allowing for their propagation. Such is the case for HIV, which induces apoptosis of uninfected cells through EV-mediated transfer of negative regulatory factor (76). The transfer of virus-derived molecules, including nucleic acids, further raises the question of whether EVs provide a mechanism by which viruses transfer their genome but remain undetected by the host immune system. This is particularly intriguing given that many viruses undergo latency periods during which they remain apparently dormant before viral loads rapidly increase. Several studies suggest EV-mediated infection mechanisms, but the similar size and biophysical properties of EVs and viruses make them difficult to separate and complicate investigation into this process (77, 78). In a recent study, Longatti and colleagues suggest that Hepatitis C viral RNA can transfer from cells incapable of forming viral particles (79). It will be interesting to see if future studies will confirm EV-mediated transfer of viral genomes and if this process extends to other types of viruses.

1.3 EV biogenesis

As discussed above, EVs are released through either fusion of MVBs with the plasma membrane (exosomes) or through direct budding of the plasma membrane (ectosomes). A host of factors have been described to regulate the initial steps of cargo sorting and membrane fission that are required to generate both exosomes and ectosomes. Some of these are unique to a specific EV type, while others are required for both. These mechanisms are discussed together in

sections 1.3.1 through 1.3.4. In contrast to ectosomes, exosome production involves a second obligate step: fusion of the MVB with the plasma membrane. The factors involved in this process are discussed in section 1.3.6.

1.3.1 ESCRT[1]

ESCRT complexes are modular but interconnected entities that most clearly act at the MVB to recognize and concentrate cargo, facilitate membrane deformation to initiate vesicle formation, and finally constrict vesicle necks to drive membrane scission. The modular nature of the ESCRT machinery provides flexibility in how their function can be harnessed to accomplish a range of activities. Models for how ESCRTs operate in MVB biogenesis as well as the topologically related processes of viral particle release and cytokinesis are explored in a number of reviews written over the past few years (80-83).

ESCRT proteins and the complexes they form are soluble and associate transiently with membranes, similar to other membrane trafficking and remodeling factors. In their best known role – delivering cargo protein into the vacuole or lysosome – ESCRT complexes can be divided into those that cooperatively bind ubiquitin, phosphatidylinositol 3-phosphate, and each other to recruit cargo and initiate membrane deformation and vesicle formation on the endosomal membrane (ESCRT-0, -I, and –II) and those that complete the release of vesicles into the MVB (ESCRT-III and Vps4). The numbering of the ESCRT complexes is based on the order in which they are recruited for vacuolar protein sorting in yeast although, as will be apparent in the following discussion, these are modular complexes that function in different combinations depending on the system involved. A brief description of ESCRT complexes follows. Excellent

[1] Hanson P. I., Jackson C. E., 2015. ESCRTing around the cell. *Encylopedia of Cell Biology* 2: 466-474.

in-depth reviews discussing ESCRT complex structure and organization can be found in (82, 84-86.

Early acting ESCRTs—ESCRT complexes implicated in cargo recognition and early stages of ILV formation include ESCRT-0 (composed of Vps27/Hrs and Hse1/STAM), ESCRT-I (composed of Vps23/Tsg101, Vps28, Mvb12 and Vps37), and ESCRT-II (composed of Vps36/EAP45, Snf8/EAP30 and Vps25/EAP20). Each of these complexes is a constitutive heterooligomeric complex and depletion of any single subunit destabilizes the whole complex. Important features of these early acting complexes include a number of low-affinity ubiquitin-binding motifs for cargo recognition (all three), phosphatidylinositol 3-phosphate binding sites for endosomal targeting (ESCRT-0 and ESCRT-II), and specific motifs that connect the complexes to each other and in the case of ESCRT-II to ESCRT-III. Other factors able to engage and activate ESCRT-III can replace some or all of these early acting ESCRT complexes, expanding the repertoire of molecular pathways into the MVB. The best studied of these are Bro1-domain containing proteins such as Alix that (like the early acting ESCRT complexes) bind both ubiquitin and CHMP4 family ESCRT-III proteins (87-89).

ESCRT-III & Vps4—ESCRT-III and its AAA ATPase Vps4 are the central players in ESCRT-driven membrane scission. The overall structure of individual ESCRT-III proteins (90-92) and the filamentous assemblies they form is established (93, 94). A number of models describing how rings and spirals on the membrane might facilitate membrane remodeling and scission have been proposed and are discussed further below. There are seven non-redundant ESCRT-III or ESCRT-III related proteins in the yeast *Saccharomyces cerevisiae* and twelve in humans, and a varying but generally similar complement in other eukaryotes. All are predicted to share a core molecular structure in which a helical hairpin is surrounded and regulated by short

C-terminal helices (90, 91). ESCRT-III proteins cycle between a closed or autoinhibited conformation in the cytoplasm and an open or activated conformation on the membrane that is primed for polymer assembly (95-97). ESCRT-II and Alix bind ESCRT-III proteins to initiate ESCRT-III polymer assembly. ESCRT-III then grows in a process for which mechanisms controlling composition and final size have yet to be defined. Assembled ESCRT-III polymers are intrinsically stable but because of Vps4-driven disassembly are short-lived in the cell (93, 98). Studies using RNAi to examine roles for individual ESCRT-III proteins support a general conclusion that particular ESCRT-III proteins are more or less essential in different settings. A general requirement for one protein related to Snf7/CHMP4 and one related to Vps2/CHMP2 appears to be conserved in most membrane remodeling processes (99). The reader is referred to original descriptions of ESCRT-III polymers cited above and previous reviews for additional details (81, 83, 100).

ESCRT and EVs—How involved the ESCRT machinery is in exosome (and more broadly EV) biogenesis is still an open question. Because of the topology of EV formation (budding away from the cytoplasm), an early and logical hypothesis was that EV formation would utilize the same machinery responsible for creating ILVs within MVBs *en route* to degradation; i.e. the ESCRTs. Proteomic studies abound in EV research, and many such studies identify ESCRT proteins as components of the EV proteome (101, 102). In fact, Tsg101 (ESCRT-I) and Alix are among the most common markers used to identify EVs (103). Despite interest in the role of the ESCRT machinery in EV biogenesis, it has remained unclear if ESCRT function is generally required for EV biogenesis. Seemingly straightforward experimental tests in different systems provide contradictory results (29, 104-106) leading to the idea that at least some EVs may be created without the help of ESCRTs (107, 108). However, while lipids clearly affect EV

biogenesis (104), ESCRT-independent pathways for controlling EV formation have not emerged. In fact, proteins recently implicated in EV biogenesis have each revealed new connections to the ESCRT machinery. In one example, the adaptor protein syntenin-1 binds syndecans and other transmembrane proteins and promotes their release in exosomes by recruiting Alix and ESCRT-III (106, 109). In another example, the arrestin domain protein ARRDC1 interacts with Tsg101 and ubiquitinated proteins at the plasma membrane to stimulate EV formation and release (110). A number of reports indicate that perturbing ESCRT function can affect EV number, content, or size (106, 110). Electron microscopy of artificial immunologic synapses showed that dominant-negative Vps4 inhibits release of ectosomes at the plasma membrane (111). Our finding that ESCRT spirals accumulate on the plasma membrane in Vps4 depleted cells suggests the possibility of similar release from other cultured cells (93). Further understanding of how the ESCRT machinery contributes to generating EVs will aid in developing tools to manipulate EV biogenesis.

1.3.2 Tetraspanins

Tetraspanins are small four-pass integral membrane proteins that organize protein networks to facilitate diverse processes such as receptor signaling, protein trafficking, cell adhesion and cell-cell fusion (112, 113). CD9, CD63 and CD81 are the most common tetraspanins identified in EVs and have broad tissue distribution in mammals (114). The roles tetraspanins play in EV biogenesis have been the subject of ongoing studies but still remain enigmatic. Some cargos depend on tetraspanins for incorporation into EVs. CD9 regulates the sorting of the CD10 metalloprotease in a manner that depends on the CD9 C-terminal tail (115). Furthermore, CD9 but not CD82 regulates β-catenin EV sorting (54). Knockout of CD81 diminishes secretion of several CD81 interaction partners in EVs (116). Melanocytes contain specialized secretory MVBs where the amylodogenic pigment cell-specific type I integral

membrane protein (PMEL) is sorted before secretion onto intralumenal vesicles. This sorting and release is reduced by CD63 depletion (105, 117).

How tetraspanin-based protein networks are organized is likely to be central to their functions in EV biogenesis. Tetraspanins consist of two extracellular loops and two short intracellular tails. The second larger extracellular loop is comprised of three clustered α-helices that are stabilized by disulfide bonding. This extracellular loop interacts with the extracellular regions of other proteins such as immunoglobulins, integrins and proteases (112). Cytoplasmic N- and C- terminal tails of tetraspanins interact with intracellular adaptor proteins to link them to signaling platforms and regulate their trafficking (113). Intracellular membrane-proximal cysteine residues are palmitoylated (118). This palmitoylation is important for oligomerization, interaction with partner proteins, protein stability (118-124).

Tetraspanins float in sucrose gradients when cells are homogenized with mild detergents revealing their propensity to form tetraspanin-enriched microdomains (TEM) (125). Tetraspanin interactions with other tetraspanins are typically preserved under these conditions. More hydrophobic detergents disrupt them, but preserve tetraspanin association with non-tetraspanin proteins. These observations have led to models of TEM organization whereby specific tetraspanins bind avidly to non-tetraspanin partners and form less stable associations with other tetraspanin complexes (126). Such organization is directly observed by cryo-electron microscopy of urothelial plaques, in which a pair of specialized tetraspanins forms stable hexagonal structures with a pair of type-I membrane proteins (127). Each tetraspanin binds tightly to a specific partner, and these heterodimers associate through tetraspanin-tetraspanin interactions (112, 127). In more recent studies, super-resolution analysis of TEMs in the plasma membrane showed that the tetraspanin CD53 remained largely segregated from the tetraspanins CD37,

CD81 and CD82 calling into question whether TEMs are primarily formed by interactions between the same or different tetraspanin species (128).

Despite the evidence implicating tetraspanins as important components of EV structure and composition, it is not known if and how TEM formation contributes to EV biogenesis. Details about TEM dynamics and intracellular trafficking are needed to understand how TEMs form and interact with each other and with other TEM protein constituents. Much of what is known about TEM dynamics comes from studies at the plasma membrane. Therefore, TEM organization on intracellular membranes is a topic of great interest.

1.3.3 Lipids

Combinations of different lipid species segregate into separate fluid phases *in vitro* (129-131). In the cell, this property is important for the formation of membrane domains with compositions and physical properties distinct from the surrounding bilayer. Membrane proteins are laterally organized within these domains through their affinity for specific lipids and for other proteins within the domain. Lipids are also important second messengers in signaling pathways that regulate membrane trafficking. As such, lipids and lipid metabolism play essential roles in the biogenesis of both exosomes and ectosomes.

Lipidomics studies have revealed a set of lipids that are typically enriched in EVs. Among these are sphingosine-based species such as sphingomyelin, gangliosides and ceramide (104, 132-134). Cholesterol is also enriched in EVs, and represents almost half of the total lipid in PC-3 cell EVs (134). Manipulating cholesterol levels causes changes in EV release (48). EVs released during different stages of reticulocyte maturation maintain constant cholesterol levels while sphingolipids vary (135). These observations are in line with the notion that cholesterol plays an important role in EV architecture. Sphingolipids and cholesterol comprise a major

component of lipid raft domains in the cell. Like TEMs, lipid rafts are detergent-resistant microdomains. Accordingly, B cell EVs exhibit degrees of detergent resistance (132). Cholesterol is an important component of both TEMs and lipid rafts (136). Imaging studies such as antibody co-patching, FRET and single-molecule labeling demonstrate segregation of TEMs and lipid rafts (124). In contrast, there is evidence that TEMs and lipid rafts interact during HIV budding (137). How this phenomenon contributes to viral maturation is unknown. Phosphotidylserine (PS), phosphatidylcholine (PC) and phosphatidylethanolamine (PE) predominate among phospholipids in EVs demonstrating PS exposure on the outer membrane leaflet (32, 134, 138).

In accordance with their abundance in EV membranes, sphingolipids, cholesterol and specific phospholipids are associated with several EV biogenesis mechanisms. Our knowledge of the roles lipids play in EV biogenesis comes from studies on the enzymes that modify and organize lipids in the cell. Neutral Sphingomyelinase 2 (nSMase2) was initially implicated in the biogenesis of exosomes bearing proteolipid protein and CD63 (104), and this mechanism has been verified for other cell types and cargos (43). nSMase2 hydrolyzes sphigomyelin to form ceramide and phosphatidylcholine. The observation that ceramide causes small vesicles to form within giant unilamelar vesicles provides a model for ceramide-driven MVB formation (104). Sphingosine 1-phosphate (S1P) activates S1P receptors at endosomes and promotes MVB formation, but details of the downstream signaling in this pathway are unknown (139). Phospholipase D hydrolyzes phosphatidylcholine to generate choline and phosphatidic acid. Phospholipase D2 (PLD2) is released on EVs, localizes to endosomes and regulates MVB formation and exosome secretion (140, 141). At the plasma membrane, flippase, floppase and scramblase enzymes use ATP hydrolysis to transfer lipids between leaflets of the bilayer and

maintain bilayer asymmetry. In *C. elegans* embryos, the TAT-5 ATPase prevents extracellular phosphatidyl ethanolamine exposure and negatively regulates ectosome budding (6). Despite these strides toward understanding lipids in EV biogenesis, much remains to be learned about how changes in lipid composition are localized and triggered during EV formation.

Few large-scale lipidomics studies have been reported for EVs compared to the vast amount of proteomics data. More such analyses are needed. Careful lipid characterization could identify less abundant species that might provide hints about EV origin. All of the lipids mentioned above are present at both the plasma membrane and on endosomes and thus cannot discriminate between EVs derived from these membranes. However, proportional lipid composition is expected to differ somewhat among EV types since proteins that preferentially bind ganglioside or phosphatidylserine concentrate EVs with different protein and RNA profiles (142). Phosphatidylinositol (PI) levels in EVs are similar to whole cell membranes, but only a subset of acyl chain length and saturation categories were identified in one study (134, 143). The inositol head group of PI is phosphorylated to different degrees, and these species are generally restricted to specific cell membranes where they are involved in trafficking regulation. Therefore, these lipids could potentially be relevant markers distinguishing exosomes and ectosomes.

1.3.4 Ubiquitin

Ubiquitination serves as an important sorting signal during endocytosis and MVB formation (144). Ubiquitin interactions with the ESCRT machinery, which comprises the primary sorting mechanism for ESCRT-dependent lysosomal degradation, are discussed in section 1.3.1. Similar interactions function in ESCRT-dependent enveloped virus budding from the cell surface (145). EVs contain ubiquitinated proteins, although one study found that the

majority is soluble suggesting that if ubiquitin is important for cargo sorting then either ubiquitin is removed from transmembrane proteins before vesicle budding or ubiquitinated soluble proteins interact with transmembrane proteins to provide the ubiquitin signal (146, 147). Evidence for specific roles for ubiquitination in EV biogenesis includes ARRDC1 ubiquitination by the WWP2 E3 ligase promoting formation of ARRDC1 ectosomes (110). Mouse macrophages release *M. tuberculosis* proteins in EVs in an ubiquitination-dependent manner during infection or after exposure to secreted *M. tuberculosis* proteins (148). Silencing the ubiquitin-binding ESCRT-0 protein Hrs dampened release of ubiquitinated proteins in EVs from dendritic cells (149). Intriguingly, MHC II ubiquitination is important for lysosomal degradation of MHC II but not for sorting it to exosomes (108, 150). However, MHC II interacts with several other proteins in EVs (151). Some of these, such as heat shock proteins and pyruvate kinase, were independently reported to be ubiquitinated in EVs (146). This opens the possibility that direct ubiquitination and interaction with certain ubiquitinated proteins could be competing mechanisms for delivering MHC II to lysosomes or exosomes. Such a hypothesis has yet to be explored for MHC II or for other cargos. An example of ubiquitin bridging is the ESCRT-dependent sorting of lumenal GPI-anchored proteins recently described in yeast. This bridging function is carried out by the Cos proteins (152). The Cos family is comprised of 11 heavily ubiquitinated, four-pass transmembrane proteins. It has been speculated that the unique Cos transmembrane domains could be important for organizing lipidated cargo into membrane domains. Computational studies suggest possible biophysical similarities between Cos and tetraspanin transmembrane domains (153). One missing aspect to this parallel is that few studies have reported tetraspanin ubiquitination (154). However, it is possible that this role could be fulfilled by cytosolic tetraspanin binding proteins that are ubiquitinated or interact with

ubiquitinated proteins. For example, the syntenin-1 PDZ adaptor protein binds to CD63, is ubiquitinated and interacts with ubiquitinated proteins (155, 156). It will be interesting to see if future studies identify ubiquitinated and ubiquitin interacting proteins that link functionally relevant cargo to EV budding machinery.

1.3.5 Actin

Actin forms a dense and dynamic filament network underneath the plasma membrane to which it is tightly coupled (157). An extensive number of proteins regulate actin dynamics including proteins that stabilize or destabilize filaments, promote filament branching and halt filament elongation. Actin and actin regulating proteins are likely to be important for EV biogenesis since actin dynamics is coordinated with endocytosis and secretion (158). The actin cortex is likely to play a direct role in ectosome budding. The Rho family GTPases govern actin dynamics and allow the cell to rapidly change its architecture in response to environmental cues (158). RhoA is implicated in EV release from several tumor cell lines. Constitutively active RhoA but not Ras, Rac, Cdc42 or other Rho isoforms cause an increase in the amount of tissue transglutaminase and flotillin-2 released on EVs (159). The major RhoA effector, Rho-associated coiled coil-containing kinase (ROCK), is involved in this pathway through activation of LIM kinase and subsequent phosphorylation of cofilin, which inhibits cofilin's actin-depolymerizing activity. These data suggest roles for regulated actin polymerization in EV release, although a direct mechanism has yet to be characterized. There are interesting parallels between this pathway and the pathway involved in regulation of plasma membrane blebbing (160). During non-apoptotic blebbing, myosin-based contraction of the actin cortex initiates detachment of the plasma membrane from the underlying cytoskeleton followed by flow of cytosol and lipids into an expanding membrane bleb. The actin cortex eventually reassembles inside the bleb, and myosin-based contraction causes retraction into the cell body (161). An alternative pathway

could promote abscission at the bleb neck downstream of actin polymerization. A few aspects of blebbing dynamics open other possibilities for EV release. Blebbing first requires an increase in membrane surface area, which could be provided by unfolding of microvilli structures or by exocytic vesicles (161). Exocytosis of MVBs would then give rise to exosome secretion. Whether exocytosis accompanies blebbing remains an open question. Likewise, membrane surface area decreases during retraction. Membrane refolding, endocytosis and ectosome shedding could be tactics for dealing with excess membrane. Blebbing is associated with a specific mode of cell migration particularly employed by tumor cells (162). Understanding how this process is coupled to EV expulsion awaits future studies that will likely reveal novel aspects of EV function.

1.3.6 MVB secretion

The ultimate step in exosome secretion is fusion of the MVB with the plasma membrane. The proteins and lipids involved in MVB formation were discussed in previous sections. Here, I will discuss the proteins that regulate endocytic trafficking and membrane fusion processes. An extensive network of soluble and membrane associated proteins regulates all of membrane trafficking. Several subclasses of the Ras family of GTPases mediate vesicle formation, transport and fusion across many aspects of membrane trafficking. These include Rab, Arf and Ral families, which act as molecular switches by cycling between active, GTP-bound and inactive, GDP-bound states. Guanine nucleotide exchange factors (GEFs) promote exchange of GDP for GTP, and GTPase activating proteins (GAPs) enhance Rab intrinsic GTPase activity. Effectors bind activated G proteins to mediate their functions. Effectors include coat proteins that function in vesicle formation, motor proteins that transport vesicles to their destination along microtubules and tethering proteins that link transport and target membranes. Once vesicles are tethered to their target membrane, SNARE proteins on both the target and transport vesicle

(tSNAREs and vSNAREs, respectively) interact and catalyze membrane fusion. SNAREs interact with Sec1/Munc18 (SM) proteins and tethering proteins that regulate the specificity and fidelity of the fusion reaction. Representatives of all of the proteins discussed above are implicated in exosome secretion.

Rab proteins—Rab5 identifies early endocytic vesicles and mediates their transport and homotypic fusion. Overexpressing GTP-locked Rab5 promotes fusion causing enlarged endosomes and inhibits recycling pathways (163). Not surprisingly, this mutant reduces exosome release from different cell types (104, 106). Early endosomes mature to late endosomes as Rab7 replaces Rab5, which is required for fusion with lysosomes (164). Silencing Rab7 expression reduces exosome secretion from MCF7 cells and causes formation of enlarged MVBs that accumulate lumenal vesicles (106). Because both Rab5 and Rab7 are critical mediators of endosomal flux, demonstrating that they affect exosomal cargo secretion is strong evidence supporting involvement of the endosomal pathway in exosome biogenesis. However, because neither Rab5 nor Rab7 seems to promote fusion with the plasma membrane, these observations highlight the challenges in pinpointing specific roles for proteins shown to perturb exosome release.

Early endosomes also generate recycling endosomes that return membrane and proteins back to the plasma membrane. Rab11 is one of several Rabs that mark recycling compartments. The human erythroleukemic cell line K562 provides an excellent system for investigating the role of Rab11 in exosome secretion. It expresses high levels of Rab11 and therefore displays enhanced Rab11-dependent processes (165, 166). Transferrin receptor is sorted to MVBs and released on exosomes after stimulating K562 cells with transferrin (167). Therefore, transferrin receptor is a marker of exosomes in this system. Overexpressing wild-type or GTP-locked Rab11

increases transferrin receptor exosome secretion, while overexpressing GDP-locked Rab11 decreases it (167, 166). Interestingly, a rise in intracellular calcium caused enlarged Rab11-labeled MVBs to form as a result of endosome fusion (166). Rab11 localizes to late recycling and post-golgi compartments suggesting that Rab11 may function in early steps of organelle maturation during exosome secretion (168). Rab11 may also play a role in tethering secretory organelles to the plasma membrane as it localizes there and interacts with the Sec15 subunit of the exocyst complex, known to play a role in plasma membrane docking (167, 169). It is currently not known if the Rab11-exocyst pathway generally contributes to exosome secretion.

Rab35 is also involved in recycling pathways and was shown to be involved in exosomal secretion of proteolipid protein from oligodendroglia (170, 171). Silencing or deactivation of Rab35 decreases exosome secretion. Overexpressing its GAPs, TBC1D10A-C, has the opposite effect. Patch-clamp experiments revealed that overexpressing GDP-locked Rab35 reduces fusion of vesicles with the plasma membrane (171). It is still unclear whether these fusion defects are direct or a consequence of fewer vesicles delivered to the plasma membrane.

Rab27a and Rab27b were identified in an RNAi screen for defective exosome secretion from HeLa cells (32). Rab27 function in secretion is well studied in several specialized cell types. In some cells, Rab27 localizes to and regulates secretion of late endosome/lysosome related organelles such as melanosomes, platelet dense granules and lysosomes in cytotoxic T lymphocytes (172-175). Constitutive secretion from polarized epithelia also involves Rab27 suggesting that these small G proteins are common components in multiple secretory pathways (176). Rab27a and Rab27b have been suggested to act at different steps in exosome secretion through different effector proteins. Knockdown of Rab27a and its effector Slp4a knockdown increased MVB size and decreased the number of immobile (plasma membrane-docked) MVBs

as observed by TIRF microscopy (32). In contrast, knockdown of Rab27b or its effector Slac2b redistributed MVBs to the perinuclear region, decreased MVB size and increased rapid movement along microtubules. These results were interpreted to suggest that Rab27b is involved in delivering secretory MVBs to the cell periphery while Rab27a is involved in docking to the plasma membrane. These functions are in line with those characterized for other secretory events since Slp4a regulates docking of secretory granules (177). Depleting Rab27a and/or Rab27b has since been shown to affect exosome secretion in other model systems (55, 178).

Other small G-proteins—Arf GTPases act together with diverse effector proteins to regulate trafficking in both the secretory and endocytic pathways. Of these, Arf6 has been implicated in secretion of exosomes from MCF-7 cells, acting upstream of syntenin-1 (141). This function involves at least one GEF protein, ARNO, and PLD2. Interestingly, depleting Arf6 also interferes with EGFR degradation demonstrating a broad function in MVB biogenesis. It is possible that Arf6 and PLD2 act upstream of a sorting mechanism that traffics MVB membranes away from the degradative pathway.

The Ral family of GTPases is comprised of two proteins, RalA and RalB, which function in secretion of platelet dense granules, Weibel-Palade bodies and cytotoxic T lymphocyte lysosomes (179). A Ral homologue in *C. elegans,* Ral-1, is involved in MVB formation since *ral-1* gene deletion alters MVB morphology and reduces the number of lumenal vesicles (180). Silencing RalA or RalB expression in mouse 4T1 cells impairs secretion of several exosome markers indicating that Ral function in MVB biogenesis and exosome secretion extends to mammals. In contrast to gene knockout, decreasing Ral-1 levels with RNAi causes an increase in the number of MVBs in close proximity to the plasma membrane leading to the interpretation that Ral-1 acts on both MVB formation and fusion with the plasma membrane (180). The major

Ral effector protein in many secretion processes is the Sec5 subunit of the exocyst complex (179). Potential involvement of the exocyst in exosome secretion has yet to be directly tested. Interestingly, oncogenic Ras activates Ral proteins providing a possible explanation for increased exosome secretion by tumor cells (179).

SNAREs—VAMP7 is a SNARE protein involved in fusion of vesicles derived from Golgi and late endosomes with the plasma membrane (181, 182). VAMP7 is localized to endosomes through interaction with Varp, a Rab32 GEF. Varp directly interacts with the VPS29 subunit of the retromer complex linking it and VAMP7 to late endosome trafficking to the plasma membrane (182). Inhibition of VAMP7 by overexpressing its inhibitory longin domain causes enlarged MVBs decorated with both Rab11 and VAMP7 to accumulate close to the plasma membrane suggesting a defect in plasma membrane fusion (183). Accordingly, exosome secretion from K562 cells is dampened by VAMP7 inhibition.

Ykt6 is a SNARE protein best characterized for its functions at the ER and Golgi. In addition, this SNARE functions in endosome to Golgi trafficking (184, 185). Depleting Ykt6 causes accumulation of CD63 and Wnt in *D. melanogaster* and human cells and decreases secretion of these proteins on exosomes from human cells (8). Interestingly, Ykt6 depletion did not affect delivery of transmembrane proteins to the cell surface arguing against effects on the general secretory pathway, which would deprive the endocytic pathway of cargo. These data suggest that sorting and flux from the MVB to Golgi is important for maintaining MVB homeostasis.

Calcium—As mentioned above, a rise in intracellular calcium triggers exosome secretion in several systems (149, 171, 186-188). Responsivity to calcium is a common feature of many

secretory processes. This is most extensively characterized for synaptic vesicle secretion from neurons. In these cells, vesicles are delivered and docked to the plasma membrane where SNARE complexes become primed or locked prior to a localized increase in calcium that triggers fusion. Synaptotagmins interact with SNARE proteins and constitute the primary calcium sensors for rapid calcium-evoked release (189). To date, no synaptotagmin protein has been directly implicated in exosome release. Synaptotagmin-VII mediates the calcium-dependent fusion of lysosomes with the plasma membrane in cytotoxic T lymphocytes, fibroblasts, osteoclasts and during plasma membrane repair (190-193). VAMP7, the only SNARE thus far implicated in fusion of secretory MVBs with the plasma membrane, forms complexes with synaptotagmin-VII during calcium-dependent lysosome exocytosis (194). It remains to be seen if synaptotagmin-VII functions extend to other endosomal compartments including MVBs. Secretion of platelet dense granules is also triggered by increased cytosolic calcium. Rab27 and its calcium-binding effector Munc13-4 in concert with Ral proteins and the exocyst complex mediate this process (175, 179, 195). Recently, Munc13-4 was shown to interact with Rab11 to mediate docking of vesicles at the plasma membrane (196). While calcium is clearly involved in different types of exosome secretion, we know very little about the kinetics of this process. Sensitive real-time assays of exosome secretion will be required to understand this response to calcium. Such studies could reveal whether different cell types produce readily releasable pools of MVBs similar to those of synaptic vesicles.

1.4 Aims of the thesis

Develop and optimize methods for monitoring EV release from cultured cell lines—Tools for polymer-based precipitation of EVs have been developed commercially as well as in independent laboratories to concentrate EVs from a variety of source fluids. Commercial kits

utilize a proprietary synthetic polymer at a defined salt concentration to "cage" EVs and promote precipitation (197). Polyethylene glycol (PEG) precipitates EVs by a comparable mechanism. PEG is hygroscopic and thus shields EVs from water molecules causing them to fall out of solution. The precipitated material is then pelleted by relatively low centrifugal force. Polymer-based precipitation is not a selective method; therefore, it is best suited for broad analysis of EV populations. Most studies of EVs use inefficient, low throughput methodologies to collect vesicles. Furthermore, because of the typically slow but still poorly characterized rate at which EVs are released, most studies analyze EVs collected over extended (hrs to days) time periods. To screen for changes in EVs using small sample volumes (~1 ml culture media) as well as over short (≥1hr) time frames, I developed a particle concentration protocol using polyethylene glycol (MW 3350) precipitation followed by binding to ConA sepharose, washing, and elution with a-D-methylmannoside, based on earlier studies of viruses (198, 199). I refer to this protocol as PEG/ConA EV isolation and found it to be comparable to standard EV collection procedures in its relative recovery of typical EV components. Since EVs could be collected from culture medium exposed to cells for short times, I was able to assess the effects of brief pharmacological treatments on EV release. The PEG/ConA procedure therefore became a key resource during the course of my thesis work.

Test the role of VPS4 and ESCRT-III in EV biogenesis—The idea that ESCRT machinery and VPS4 might be involved in EV biogenesis is not new, but a clear understanding of exactly how and when they participate has remained elusive. Reports of ESCRT-independent ILV formation, exosome biogenesis, and microvesicle shedding have led to a working consensus that there must be other ways of controlling these events in mammalian cells. For ILV and exosome formation proposed alternate models center on the involvement of particular lipids and lipid raft-

like domains, while microvesicle release is attributed to the activity of cytoskeletal machinery. While it is certainly clear that lipid- and protein-based segregation into budding-prone domains must be a part of the ILV and EV-forming process, many of the experiments testing involvement of the ESCRT machinery have focused on components of the initiating ESCRT-0 or –I complexes (104, 110, 200) with only a few attempts to assess involvement of ESCRT-III and Vps4 (29, 106, 111). In the case of ESCRT-III, the fact that filaments assemble from a mixture of as many as 12 subunits (some of which may be functionally redundant while others might have other functions altogether) complicate interpretation of gene depletion experiments. Removing a single ESCRT-III protein as in a widely cited study of ESCRT function in multivesicular endosome biogenesis (201) does not address the overall contribution of ESCRT-III to pathway function. Therefore, I globally blocked ESCRT-III polymer disassembly by expressing a dominant negative mutant of VPS4 (VPS4EQ). Inducibly expressing VPS4EQ caused a marked decrease in release of canonical EV tetraspanins, CD63 and CD9. Furthermore, VPS4 inhibition changed the protein profile of EVs residually secreted from cells. Notably, the concentration of ESCRT-III subunits in EVs was elevated despite a clear reduction in the number of EVs. These findings implicate VPS4 and ESCRT-III disassembly in the biogenesis of different EV types.

Characterize EV heterogeneity based on differential protein content—CD63 and CD9 are among the most abundant and frequently identified proteins on EVs (16, 202). CD63 is primarily localized to membranes inside of MVBs while CD9 and most other tetraspanins reside primarily on the cell surface (203). Specific functions for individual tetraspanins have been difficult to pinpoint, but all function as membrane protein scaffolds and mediate important interactions with integrins, kinases, and other cell surface receptors (203). Both CD63 and CD9

have been implicated in formation of specific EVs (54, 105) but neither has emerged as a universally required factor, and overexpression has not been shown to significantly change EV release. CD9 is implicated in processes such as proliferation, migration and cell surface contraction (204). Work described in this thesis and from others suggests that release of these proteins onto EVs may be separable (22, 23, 205). Immunostaining reveals different distributions for both endogenous and overexpressed proteins in cells. I demonstrate, using continuous sucrose density floatation, that CD63 and CD9 are enriched on physically separate EV populations. I also find that serum is a robust stimulator of EV release from the cell surface. In order to more deeply investigate the extent to which these proteins segregate on different EVs, I developed cell lines expressing different combinations of fluorescent tetraspanin fusion proteins. This work paves the way for sensitive assessment of EV heterogeneity based on CD63 and CD9 as putative markers of exosomes and ectosomes, respectively.

Investigate the exocytic MVB—With specific regard to exosome release, an important question is what distinguishes MVBs destined for exocytosis from those destined for degradation. Currently, the most well characterized factors involved in the actual trafficking and release of exocytic MVBs are Rab27a and Rab27b. I have identified Rab27b as a factor likely to distinguish exocytic from non-exocytic MVBs in U87 cells. Rab27b localizes to a subset of late endosomes that also contain the exosomal protein CD63. I found that this subset of MVBs are less acidic than remaining (Rab27b negative) MVBs. Furthermore, endosome pH appears to play a direct role in recruiting Rab27b since chloroquine neutralization increases both Rab27b endosomes and CD63 release. These findings have exciting implications regarding the identity of MVBs and how their exocytosis is regulated.

References

1. Korkut, C., B. Ataman, P. Ramachandran, J. Ashley, R. Barria, N. Gherbesi, and V. Budnik. 2009. Trans-synaptic transmission of vesicular Wnt signals through Evi/Wntless. *Cell* 139: 393-404.

2. Liegeois, S., A. Benedetto, J. M. Garnier, Y. Schwab, and M. Labouesse. 2006. The V0-ATPase mediates apical secretion of exosomes containing Hedgehog-related proteins in Caenorhabditis elegans. *J Cell Biol* 173: 949-961.

3. Ellen, A. F., S. V. Albers, W. Huibers, A. Pitcher, C. F. Hobel, H. Schwarz, M. Folea, S. Schouten, E. J. Boekema, B. Poolman, and A. J. Driessen. 2009. Proteomic analysis of secreted membrane vesicles of archaeal Sulfolobus species reveals the presence of endosome sorting complex components. *Extremophiles* 13: 67-79.

4. Makarova, K. S., N. Yutin, S. D. Bell, and E. V. Koonin. 2010. Evolution of diverse cell division and vesicle formation systems in Archaea. *Nat Rev Microbiol* 8: 731-741.

5. Oliveira, D. L., E. S. Nakayasu, L. S. Joffe, A. J. Guimaraes, T. J. Sobreira, J. D. Nosanchuk, R. J. Cordero, S. Frases, A. Casadevall, I. C. Almeida, L. Nimrichter, and M. L. Rodrigues. 2010. Characterization of yeast extracellular vesicles: evidence for the participation of different pathways of cellular traffic in vesicle biogenesis. *PLoS One* 5: e11113.

6. Wehman, A. M., C. Poggioli, P. Schweinsberg, B. D. Grant, and J. Nance. 2011. The P4-ATPase TAT-5 inhibits the budding of extracellular vesicles in C. elegans embryos. *Curr Biol* 21: 1951-1959.

7. Matusek, T., F. Wendler, S. Poles, S. Pizette, G. D'Angelo, M. Furthauer, and P. P. Therond. 2014. The ESCRT machinery regulates the secretion and long-range activity of Hedgehog. *Nature* 516: 99-103.

8. Gross, J. C., V. Chaudhary, K. Bartscherer, and M. Boutros. 2012. Active Wnt proteins are secreted on exosomes. *Nat Cell Biol* 14: 1036-1045.

9. Echevarria, J., F. Royo, R. Pazos, L. Salazar, J. M. Falcon-Perez, and N. C. Reichardt. 2014. Microarray-based identification of lectins for the purification of human urinary extracellular vesicles directly from urine samples. *Chembiochem* 15: 1621-1626.

10. Rak, J. 2013. Extracellular vesicles - biomarkers and effectors of the cellular interactome in cancer. *Front Pharmacol* 4: 21.

11. Street, J. M., P. E. Barran, C. L. Mackay, S. Weidt, C. Balmforth, T. S. Walsh, R. T. Chalmers, D. J. Webb, and J. W. Dear. 2012. Identification and proteomic profiling of exosomes in human cerebrospinal fluid. *J Transl Med* 10: 5.

12. Wolf, P. 1967. The nature and significance of platelet products in human plasma. *Br J Haematol* 13: 269-288.

13. Ronquist, G., and I. Brody. 1985. The prostasome: its secretion and function in man. *Biochim Biophys Acta* 822: 203-218.

14. Al-Nedawi, K., B. Meehan, J. Micallef, V. Lhotak, L. May, A. Guha, and J. Rak. 2008. Intercellular transfer of the oncogenic receptor EGFRvIII by microvesicles derived from tumour cells. *Nat Cell Biol* 10: 619-624.

15. Mathivanan, S., H. Ji, and R. J. Simpson. 2010. Exosomes: extracellular organelles important in intercellular communication. *J Proteomics* 73: 1907-1920.

16. Raposo, G., and W. Stoorvogel. 2013. Extracellular vesicles: exosomes, microvesicles, and friends. *J Cell Biol* 200: 373-383.

17. Vader, P., X. O. Breakefield, and M. J. Wood. 2014. Extracellular vesicles: emerging targets for cancer therapy. *Trends Mol Med* 20: 385-393.

18. Lotvall, J., A. F. Hill, F. Hochberg, E. I. Buzas, D. Di Vizio, C. Gardiner, Y. S. Gho, I. V. Kurochkin, S. Mathivanan, P. Quesenberry, S. Sahoo, H. Tahara, M. H. Wauben, K. W. Witwer, and C. Thery. 2014. Minimal experimental requirements for definition of extracellular vesicles and their functions: a position statement from the International Society for Extracellular Vesicles. *J Extracell Vesicles* 3: 26913.

19. Thery, C., A. Clayton, A. Amigorena, and G. Raposo. 2006. Isolation and characterization of exosomes from cell culture supernatants and biological fluids. *Curr Protoc Cell Biol* 3.22: 1-29.

20. Baranyai, T., K. Herczeg, Z. Onodi, I. Voszka, K. Modos, N. Marton, G. Nagy, I. Mager, M. J. Wood, S. El Andaloussi, Z. Palinkas, V. Kumar, P. Nagy, A. Kittel, E. I. Buzas, P. Ferdinandy, and Z. Giricz. 2015. Isolation of Exosomes from Blood Plasma: Qualitative and Quantitative Comparison of Ultracentrifugation and Size Exclusion Chromatography Methods. *PLoS One* 10: e0145686.

21. Murk, J. L., B. M. Humbel, U. Ziese, J. M. Griffith, G. Posthuma, J. W. Slot, A. J. Koster, A. J. Verkleij, H. J. Geuze, and M. J. Kleijmeer. 2003. Endosomal compartmentalization in

three dimensions: implications for membrane fusion. *Proc Natl Acad Sci U S A* 100: 13332-13337.

22. Bobrie, A., M. Colombo, S. Krumeich, G. Raposo, and C. Thery. 2012. Diverse subpopulations of vesicles secreted by different intracellular mechanisms are present in exosome preparations obtained by differential ultracentrifugation. *J Extracell Vesicles* 1:10.3402/jev.v1i0.18397. doi:10.3402/jev.v1i0.18397.

23. Kowal, J., G. Arras, M. Colombo, M. Jouve, J. P. Morath, B. Primdal-Bengtson, F. Dingli, D. Loew, M. Tkach, and C. Thery. 2016. Proteomic comparison defines novel markers to characterize heterogeneous populations of extracellular vesicle subtypes. *Proc Natl Acad Sci U S A* 113: E968-77.

24. Tauro, B. J., D. W. Greening, R. A. Mathias, H. Ji, S. Mathivanan, A. M. Scott, and R. J. Simpson. 2012. Comparison of ultracentrifugation, density gradient separation, and immunoaffinity capture methods for isolating human colon cancer cell line LIM1863-derived exosomes. *Methods* 56: 293-304.

25. Tauro, B. J., D. W. Greening, R. A. Mathias, S. Mathivanan, H. Ji, and R. J. Simpson. 2013. Two distinct populations of exosomes are released from LIM1863 colon carcinoma cell-derived organoids. *Mol Cell Proteomics* 12: 587-598.

26. Xu, R., D. W. Greening, A. Rai, H. Ji, and R. J. Simpson. 2015. Highly-purified exosomes and shed microvesicles isolated from the human colon cancer cell line LIM1863 by sequential centrifugal ultrafiltration are biochemically and functionally distinct. *Methods* 87: 11-25.

27. Hong, C. S., S. Funk, L. Muller, M. Boyiadzis, and T. L. Whiteside. 2016. Isolation of biologically active and morphologically intact exosomes from plasma of patients with cancer. *J Extracell Vesicles* 5: 29289.

28. Welton, J. L., J. P. Webber, L. A. Botos, M. Jones, and A. Clayton. 2015. Ready-made chromatography columns for extracellular vesicle isolation from plasma. *J Extracell Vesicles* 4: 27269.

29. Colombo, M., C. Moita, G. van Niel, J. Kowal, J. Vigneron, P. Benaroch, N. Manel, L. F. Moita, C. Thery, and G. Raposo. 2013. Analysis of ESCRT functions in exosome biogenesis, composition and secretion highlights the heterogeneity of extracellular vesicles. *J Cell Sci* 126: 5553-5565.

30. Medina, M. A., and P. Schwille. 2002. Fluorescence correlation spectroscopy for the detection and study of single molecules in biology. *Bioessays* 24: 758-764.

31. Wang, J., R. Guo, Y. Yang, B. Jacobs, S. Chen, I. Iwuchukwu, K. J. Gaines, Y. Chen, R. Simman, G. Lv, K. Wu, and J. C. Bihl. 2016. The Novel Methods for Analysis of Exosomes Released from Endothelial Cells and Endothelial Progenitor Cells. *Stem Cells Int* 2016: 2639728.

32. Ostrowski, M., N. B. Carmo, S. Krumeich, I. Fanget, G. Raposo, A. Savina, C. F. Moita, K. Schauer, A. N. Hume, R. P. Freitas, B. Goud, P. Benaroch, N. Hacohen, M. Fukuda, C. Desnos, M. C. Seabra, F. Darchen, S. Amigorena, L. F. Moita, and C. Thery. 2010. Rab27a and Rab27b control different steps of the exosome secretion pathway. *Nat Cell Biol* 12: 19-30; sup pp 1-13.

33. Pospichalova, V., J. Svoboda, Z. Dave, A. Kotrbova, K. Kaiser, D. Klemova, L. Ilkovics, A. Hampl, I. Crha, E. Jandakova, L. Minar, V. Weinberger, and V. Bryja. 2015. Simplified protocol for flow cytometry analysis of fluorescently labeled exosomes and microvesicles using dedicated flow cytometer. *J Extracell Vesicles* 4: 25530.

34. van der Pol, E., F. A. Coumans, A. E. Grootemaat, C. Gardiner, I. L. Sargent, P. Harrison, A. Sturk, T. G. van Leeuwen, and R. Nieuwland. 2014. Particle size distribution of exosomes and microvesicles determined by transmission electron microscopy, flow cytometry, nanoparticle tracking analysis, and resistive pulse sensing. *J Thromb Haemost* 12: 1182-1192.

35. Coumans, F. A., E. van der Pol, A. N. Boing, N. Hajji, G. Sturk, T. G. van Leeuwen, and R. Nieuwland. 2014. Reproducible extracellular vesicle size and concentration determination with tunable resistive pulse sensing. *J Extracell Vesicles* 3: 25922.

36. Anderson, W., R. Lane, D. Korbie, and M. Trau. 2015. Observations of Tunable Resistive Pulse Sensing for Exosome Analysis: Improving System Sensitivity and Stability. *Langmuir* 31: 6577-6587.

37. Jouvenet, N., P. D. Bieniasz, and S. M. Simon. 2008. Imaging the biogenesis of individual HIV-1 virions in live cells. *Nature* 454: 236-240.

38. Ivanchenko, S., W. J. Godinez, M. Lampe, H. G. Krausslich, R. Eils, K. Rohr, C. Brauchle, B. Muller, and D. C. Lamb. 2009. Dynamics of HIV-1 assembly and release. *PLoS Pathog* 5: e1000652.

39. Greening, D. W., S. K. Gopal, R. A. Mathias, L. Liu, J. Sheng, H. J. Zhu, and R. J. Simpson. 2015. Emerging roles of exosomes during epithelial-mesenchymal transition and cancer progression. *Semin Cell Dev Biol* 40: 60-71.

40. Luga, V., L. Zhang, A. M. Viloria-Petit, A. A. Ogunjimi, M. R. Inanlou, E. Chiu, M. Buchanan, A. N. Hosein, M. Basik, and J. L. Wrana. 2012. Exosomes mediate stromal mobilization of autocrine Wnt-PCP signaling in breast cancer cell migration. *Cell* 151: 1542-1556.

41. Lesnik, J., T. Antes, J. Kim, E. Griner, and L. Pedro. 2016. Registered report: Melanoma exosomes educate bone marrow progenitor cells toward a pro-metastatic phenotype through MET. *Elife* 5: e07383.

42. Zhang, H. G., and W. E. Grizzle. 2014. Exosomes: a novel pathway of local and distant intercellular communication that facilitates the growth and metastasis of neoplastic lesions. *Am J Pathol* 184: 28-41.

43. Guo, B. B., S. A. Bellingham, and A. F. Hill. 2016. Stimulating the Release of Exosomes Increases the Intercellular Transfer of Prions. *J Biol Chem* 291: 5128-5137.

44. Budnik, V., C. Ruiz-Canada, and F. Wendler. 2016. Extracellular vesicles round off communication in the nervous system. *Nat Rev Neurosci* 17: 160-172.

45. Tan, L., H. Wu, Y. Liu, M. Zhao, D. Li, and Q. Lu. 2016. Recent advances of exosomes in immune modulation and autoimmune diseases. *Autoimmunity* 1-9.

46. Boelens, M. C., T. J. Wu, B. Y. Nabet, B. Xu, Y. Qiu, T. Yoon, D. J. Azzam, C. Twyman-Saint Victor, B. Z. Wiemann, H. Ishwaran, P. J. Ter Brugge, J. Jonkers, J. Slingerland, and

A. J. Minn. 2014. Exosome transfer from stromal to breast cancer cells regulates therapy resistance pathways. *Cell* 159: 499-513.

47. Lopez-Verrilli, M. A., and F. A. Court. 2012. Transfer of vesicles from schwann cells to axons: a novel mechanism of communication in the peripheral nervous system. *Front Physiol* 3: 205.

48. Strauss, K., C. Goebel, H. Runz, W. Moebius, S. Weiss, I. Feussner, M. Simons, and A. Schneider. 2010. Exosome secretion ameliorates lysosomal storage of cholesterol in Niemann-Pick type C disease. *J Biol Chem* 285: 26279-26288

49. Pan, B. T., and R. M. Johnstone. 1983. Fate of the transferrin receptor during maturation of sheep reticulocytes in vitro: selective externalization of the receptor. *Cell* 33: 967-978.

50. Harding, C., J. Heuser, and P. Stahl. 1983. Receptor-mediated endocytosis of transferrin and recycling of the transferrin receptor in rat reticulocytes. *J Cell Biol* 97: 329-339.

51. Lespagnol, A., D. Duflaut, C. Beekman, L. Blanc, G. Fiucci, J. C. Marine, M. Vidal, R. Amson, and A. Telerman. 2008. Exosome secretion, including the DNA damage-induced p53-dependent secretory pathway, is severely compromised in TSAP6/Steap3-null mice. *Cell Death Differ* 15: 1723-1733.

52. Rieu, S., C. Geminard, H. Rabesandratana, J. Sainte-Marie, and M. Vidal. 2000. Exosomes released during reticulocyte maturation bind to fibronectin via integrin alpha4beta1. *Eur J Biochem* 267: 583-590.

53. Ayre, D. C., M. Elstner, N. C. Smith, E. S. Moores, A. M. Hogan, and S. L. Christian. 2015. Dynamic regulation of CD24 expression and release of CD24-containing

microvesicles in immature B cells in response to CD24 engagement. *Immunology* 146: 217-233.

54. Chairoungdua, A., D. L. Smith, P. Pochard, M. Hull, and M. J. Caplan. 2010. Exosome release of beta-catenin: a novel mechanism that antagonizes Wnt signaling. *J Cell Biol* 190: 1079-1091.

55. Hoshino, D., K. C. Kirkbride, K. Costello, E. S. Clark, S. Sinha, N. Grega-Larson, M. J. Tyska, and A. M. Weaver. 2013. Exosome secretion is enhanced by invadopodia and drives invasive behavior. *Cell Rep* 5: 1159-1168.

56. Han, K. Y., J. Dugas-Ford, M. Seiki, J. H. Chang, and D. T. Azar. 2015. Evidence for the Involvement of MMP14 in MMP2 Processing and Recruitment in Exosomes of Corneal Fibroblasts. *Invest Ophthalmol Vis Sci* 56: 5323-5329.

57. Sung, B. H., T. Ketova, D. Hoshino, A. Zijlstra, and A. M. Weaver. 2015. Directional cell movement through tissues is controlled by exosome secretion. *Nat Commun* 6: 7164.

58. Pitt, J. M., F. Andre, S. Amigorena, J. C. Soria, A. Eggermont, G. Kroemer, and L. Zitvogel. 2016. Dendritic cell-derived exosomes for cancer therapy. *J Clin Invest* 126: 1224-1232.

59. Raposo, G., H. W. Nijman, W. Stoorvogel, R. Liejendekker, C. V. Harding, C. J. Melief, and H. J. Geuze. 1996. B lymphocytes secrete antigen-presenting vesicles. *J Exp Med* 183: 1161-1172.

60. Thery, C., A. Regnault, J. Garin, J. Wolfers, L. Zitvogel, P. Ricciardi-Castagnoli, G. Raposo, and S. Amigorena. 1999. Molecular characterization of dendritic cell-derived

exosomes. Selective accumulation of the heat shock protein hsc73. *J Cell Biol* 147: 599-610.

61. Giri, P. K., and J. S. Schorey. 2008. Exosomes derived from M. Bovis BCG infected macrophages activate antigen-specific CD4+ and CD8+ T cells in vitro and in vivo. *PLoS One* 3: e2461.

62. Thery, C., L. Duban, E. Segura, P. Veron, O. Lantz, and S. Amigorena. 2002. Indirect activation of naive CD4+ T cells by dendritic cell-derived exosomes. *Nat Immunol* 3: 1156-1162.

63. Qazi, K. R., U. Gehrmann, E. Domange Jordo, M. C. Karlsson, and S. Gabrielsson. 2009. Antigen-loaded exosomes alone induce Th1-type memory through a B-cell-dependent mechanism. *Blood* 113: 2673-2683.

64. Martin, R. K., K. B. Brooks, F. Henningsson, B. Heyman, and D. H. Conrad. 2014. Antigen transfer from exosomes to dendritic cells as an explanation for the immune enhancement seen by IgE immune complexes. *PLoS One* 9: e110609.

65. Van, N., Guillaume, G. Raposo, C. Candalh, M. Boussac, R. Hershberg, N. Cerf-Bensussan, and M. Heyman. 2001. Intestinal Epithelial Cells Secrete Exosome-like Vesicles. *Gastroenterology* 121: 337-349.

66. Mallegol, J., G. Van Niel, C. Lebreton, Y. Lepelletier, C. Candalh, C. Dugave, J. K. Heath, G. Raposo, N. Cerf-Bensussan, and M. Heyman. 2007. T84-intestinal epithelial exosomes bear MHC class II/peptide complexes potentiating antigen presentation by dendritic cells. *Gastroenterology* 132: 1866-1876.

67. Stenqvist, A. C., O. Nagaeva, V. Baranov, and L. Mincheva-Nilsson. 2013. Exosomes secreted by human placenta carry functional Fas ligand and TRAIL molecules and convey apoptosis in activated immune cells, suggesting exosome-mediated immune privilege of the fetus. *J Immunol* 191: 5515-5523.

68. Robbins, P. D., and A. E. Morelli. 2014. Regulation of immune responses by extracellular vesicles. *Nat Rev Immunol* 14: 195-208.

69. Yanez-Mo, M., P. R. Siljander, Z. Andreu, A. B. Zavec, F. E. Borras, E. I. Buzas, K. Buzas, E. Casal, F. Cappello, J. Carvalho, E. Colas, A. Cordeiro-da Silva, S. Fais, J. M. Falcon-Perez, I. M. Ghobrial, B. Giebel, M. Gimona, M. Graner, I. Gursel, M. Gursel, N. H. Heegaard, A. Hendrix, P. Kierulf, K. Kokubun, M. Kosanovic, V. Kralj-Iglic, E. M. Kramer-Albers, S. Laitinen, C. Lasser, T. Lener, E. Ligeti, A. Line, G. Lipps, A. Llorente, J. Lotvall, M. Mancek-Keber, A. Marcilla, M. Mittelbrunn, I. Nazarenko, E. N. Nolte-'t Hoen, T. A. Nyman, L. O'Driscoll, M. Olivan, C. Oliveira, E. Pallinger, H. A. Del Portillo, J. Reventos, M. Rigau, E. Rohde, M. Sammar, F. Sanchez-Madrid, N. Santarem, K. Schallmoser, M. S. Ostenfeld, W. Stoorvogel, R. Stukelj, S. G. Van der Grein, M. H. Vasconcelos, M. H. Wauben, and O. De Wever. 2015. Biological properties of extracellular vesicles and their physiological functions. *J Extracell Vesicles* 4: 27066.

70. Hedlund, M., A. C. Stenqvist, O. Nagaeva, L. Kjellberg, M. Wulff, V. Baranov, and L. Mincheva-Nilsson. 2009. Human placenta expresses and secretes NKG2D ligands via exosomes that down-modulate the cognate receptor expression: evidence for immunosuppressive function. *J Immunol* 183: 340-351.

71. Ashiru, O., P. Boutet, L. Fernandez-Messina, S. Aguera-Gonzalez, J. N. Skepper, M. Vales-Gomez, and H. T. Reyburn. 2010. Natural killer cell cytotoxicity is suppressed by exposure to the human NKG2D ligand MICA*008 that is shed by tumor cells in exosomes. *Cancer Res* 70: 481-489.

72. Huber, V., S. Fais, M. Iero, L. Lugini, P. Canese, P. Squarcina, A. Zaccheddu, M. Colone, G. Arancia, M. Gentile, E. Seregni, R. Valenti, G. Ballabio, F. Belli, E. Leo, G. Parmiani, and L. Rivoltini. 2005. Human colorectal cancer cells induce T-cell death through release of proapoptotic microvesicles: role in immune escape. *Gastroenterology* 128: 1796-1804.

73. Holder, B., T. Jones, V. Sancho Shimizu, T. F. Rice, B. Donaldson, M. Bouqueau, K. Forbes, and B. Kampmann. 2016. Macrophage Exosomes Induce Placental Inflammatory Cytokines: A Novel Mode of Maternal-Placental Messaging. *Traffic* 17: 168-178.

74. Singh, P. P., V. L. Smith, P. C. Karakousis, and J. S. Schorey. 2012. Exosomes isolated from mycobacteria-infected mice or cultured macrophages can recruit and activate immune cells in vitro and in vivo. *J Immunol* 189: 777-785.

75. Walker, J. D., C. L. Maier, and J. S. Pober. 2009. Cytomegalovirus-infected human endothelial cells can stimulate allogeneic CD4+ memory T cells by releasing antigenic exosomes. *J Immunol* 182: 1548-1559.

76. Lenassi, M., G. Cagney, M. Liao, T. Vaupotic, K. Bartholomeeusen, Y. Cheng, N. J. Krogan, A. Plemenitas, and B. M. Peterlin. 2010. HIV Nef is secreted in exosomes and triggers apoptosis in bystander CD4+ T cells. *Traffic* 11: 110-122.

77. Ramakrishnaiah, V., C. Thumann, I. Fofana, F. Habersetzer, Q. Pan, P. E. de Ruiter, R. Willemsen, J. A. Demmers, V. Stalin Raj, G. Jenster, J. Kwekkeboom, H. W. Tilanus, B. L. Haagmans, T. F. Baumert, and L. J. van der Laan. 2013. Exosome-mediated transmission of hepatitis C virus between human hepatoma Huh7.5 cells. *Proc Natl Acad Sci U S A* 110: 13109-13113.

78. Pegtel, D. M., K. Cosmopoulos, D. A. Thorley-Lawson, M. A. van Eijndhoven, E. S. Hopmans, J. L. Lindenberg, T. D. de Gruijl, T. Wurdinger, and J. M. Middeldorp. 2010. Functional delivery of viral miRNAs via exosomes. *Proc Natl Acad Sci U S A* 107: 6328-6333.

79. Longatti, A., B. Boyd, and F. V. Chisari. 2015. Virion-independent transfer of replication-competent hepatitis C virus RNA between permissive cells. *J Virol* 89: 2956-2961.

80. Hurley, J. H., and P. I. Hanson. 2010. Membrane budding and scission by the ESCRT machinery: it's all in the neck. *Nat Rev Mol Cell Biol* 11: 556-566.

81. McCullough, J., L. A. Colf, and W. I. Sundquist. 2013. Membrane fission reactions of the mammalian ESCRT pathway. *Annu Rev Biochem* 82: 663-692.

82. Hanson, P. I., and A. Cashikar. 2012. Multivesicular body morphogenesis. *Annu Rev Cell Dev Biol* 28: 337-362.

83. Henne, W. M., H. Stenmark, and S. D. Emr. 2013. Molecular mechanisms of the membrane sculpting ESCRT pathway. *Cold Spring Harb Perspect Biol* 5:

84. Hurley, J. H. 2010. The ESCRT complexes. *Crit Rev Biochem Mol Biol* 45: 463-487.

85. Henne, W. M., N. J. Buchkovich, and S. D. Emr. 2011. The ESCRT pathway. *Dev Cell* 21: 77-91.

86. Wollert, T., D. Yang, X. Ren, H. H. Lee, Y. J. Im, and J. H. Hurley. 2009. The ESCRT machinery at a glance. *J Cell Sci* 122: 2163-2166.

87. Katoh, K., H. Shibata, H. Suzuki, A. Nara, K. Ishidoh, E. Kominami, T. Yoshimori, and M. Maki. 2003. The ALG-2-interacting protein Alix associates with CHMP4b, a human homologue of yeast Snf7 that is involved in multivesicular body sorting. *J Biol Chem* 278: 39104-39113.

88. Dowlatshahi, D. P., V. Sandrin, S. Vivona, T. A. Shaler, S. E. Kaiser, F. Melandri, W. I. Sundquist, and R. R. Kopito. 2012. ALIX is a Lys63-specific polyubiquitin binding protein that functions in retrovirus budding. *Dev Cell* 23: 1247-1254.

89. Pashkova, N., L. Gakhar, S. C. Winistorfer, A. B. Sunshine, M. Rich, M. J. Dunham, L. Yu, and R. C. Piper. 2013. The yeast Alix homolog Bro1 functions as a ubiquitin receptor for protein sorting into multivesicular endosomes. *Dev Cell* 25: 520-533.

90. Muziol, T., E. Pineda-Molina, R. B. Ravelli, A. Zamborlini, Y. Usami, H. Gottlinger, and W. Weissenhorn. 2006. Structural basis for budding by the ESCRT-III factor CHMP3. *Dev Cell* 10: 821-830.

91. Bajorek, M., H. L. Schubert, J. McCullough, C. Langelier, D. M. Eckert, W. M. Stubblefield, N. T. Uter, D. G. Myszka, C. P. Hill, and W. I. Sundquist. 2009. Structural basis for ESCRT-III protein autoinhibition. *Nat Struct Mol Biol* 16: 754-762.

92. Xiao, J., X. W. Chen, B. Davies, A. R. Saltiel, D. Katzmann, and Z. Xu. 2009. Structural basis of Ist1 function and Ist1-Did2 interaction in the multivesicular body pathway and cytokinesis. *Molecular biology of the cell* 20: 3514-3524.

93. Cashikar, A. G., S. Shim, R. Roth, M. R. Maldazys, J. E. Heuser, and P. I. Hanson. 2014. Structure of cellular ESCRT-III spirals and their relationship to HIV budding. *Elife* 3: 10.7554/eLife.02184

94. Henne, W. M., N. J. Buchkovich, Y. Zhao, and S. D. Emr. 2012. The endosomal sorting complex ESCRT-II mediates the assembly and architecture of ESCRT-III helices. *Cell* 151: 356-371.

95. Lin, Y., L. A. Kimpler, T. V. Naismith, J. M. Lauer, and P. I. Hanson. 2005. Interaction of the mammalian endosomal sorting complex required for transport (ESCRT) III protein hSnf7-1 with itself, membranes, and the AAA+ ATPase SKD1. *J Biol Chem* 280: 12799-12809.

96. Zamborlini, A., Y. Usami, S. R. Radoshitzky, E. Popova, G. Palu, and H. Gottlinger. 2006. Release of autoinhibition converts ESCRT-III components into potent inhibitors of HIV-1 budding. *Proc Natl Acad Sci U S A* 103: 19140-19145.

97. Shim, S., L. A. Kimpler, and P. I. Hanson. 2007. Structure/function analysis of four core ESCRT-III proteins reveals common regulatory role for extreme C-terminal domain. *Traffic* 8: 1068-1079.

98. Babst, M., D. J. Katzmann, E. J. Estepa-Sabal, T. Meerloo, and S. D. Emr. 2002. Escrt-III: an endosome-associated heterooligomeric protein complex required for mvb sorting. *Dev Cell* 3: 271-282.

99. Hanson, P. I., S. Shim, and S. A. Merrill. 2009. Cell biology of the ESCRT machinery. *Curr Opin Cell Biol* 21: 568-574.

100. Peel, S., P. Macheboeuf, N. Martinelli, and W. Weissenhorn. 2011. Divergent pathways lead to ESCRT-III-catalyzed membrane fission. *Trends Biochem Sci* 36: 199-210.

101. Simpson, R. J., J. W. Lim, R. L. Moritz, and S. Mathivanan. 2009. Exosomes: proteomic insights and diagnostic potential. *Expert Rev Proteomics* 6: 267-283.

102. Choi, D. S., D. K. Kim, Y. K. Kim, and Y. S. Gho. 2013. Proteomics, transcriptomics and lipidomics of exosomes and ectosomes. *Proteomics* 13: 1554-1571.

103. Kowal, J., M. Tkach, and C. Thery. 2014. Biogenesis and secretion of exosomes. *Curr Opin Cell Biol* 29C: 116-125.

104. Trajkovic, K., C. Hsu, S. Chiantia, L. Rajendran, D. Wenzel, F. Wieland, P. Schwille, B. Brugger, and M. Simons. 2008. Ceramide triggers budding of exosome vesicles into multivesicular endosomes. *Science* 319: 1244-1247.

105. van Niel, G., S. Charrin, S. Simoes, M. Romao, L. Rochin, P. Saftig, M. S. Marks, E. Rubinstein, and G. Raposo. 2011. The Tetraspanin CD63 Regulates ESCRT-Independent and -Dependent Endosomal Sorting during Melanogenesis. *Dev Cell* 21: 708-721.

106. Baietti, M. F., Z. Zhang, E. Mortier, A. Melchior, G. Degeest, A. Geeraerts, Y. Ivarsson, F. Depoortere, C. Coomans, E. Vermeiren, P. Zimmermann, and G. David. 2012. Syndecan-syntenin-ALIX regulates the biogenesis of exosomes. *Nat Cell Biol* 14: 677-685.

107. Babst, M. 2011. MVB vesicle formation: ESCRT-dependent, ESCRT-independent and everything in between. *Curr Opin Cell Biol* 23: 452-457.

108. Buschow, S. I., E. N. Nolte-'t Hoen, G. van Niel, M. S. Pols, T. ten Broeke, M. Lauwen, F. Ossendorp, C. J. Melief, G. Raposo, R. Wubbolts, M. H. Wauben, and W. Stoorvogel. 2009. MHC II in dendritic cells is targeted to lysosomes or T cell-induced exosomes via distinct multivesicular body pathways. *Traffic* 10: 1528-1542.

109. Hurley, J. H., and G. Odorizzi. 2012. Get on the exosome bus with ALIX. *Nat Cell Biol* 14: 654-655.

110. Nabhan, J. F., R. Hu, R. S. Oh, S. N. Cohen, and Q. Lu. 2012. Formation and release of arrestin domain-containing protein 1-mediated microvesicles (ARMMs) at plasma membrane by recruitment of TSG101 protein. *Proc Natl Acad Sci U S A* 109: 4146-4151.

111. Choudhuri, K., J. Llodra, E. W. Roth, J. Tsai, S. Gordo, K. W. Wucherpfennig, L. C. Kam, D. L. Stokes, and M. L. Dustin. 2014. Polarized release of T-cell-receptor-enriched microvesicles at the immunological synapse. *Nature* 507: 118-123.

112. Charrin, S., S. Jouannet, C. Boucheix, and E. Rubinstein. 2014. Tetraspanins at a glance. *J Cell Sci* 127: 3641-3648.

113. Hemler, M. E. 2005. Tetraspanin functions and associated microdomains. *Nat Rev Mol Cell Biol* 6: 801-811.

114. Keerthikumar, S., D. Chisanga, D. Ariyaratne, H. Al Saffar, S. Anand, K. Zhao, M. Samuel, M. Pathan, M. Jois, N. Chilamkurti, L. Gangoda, and S. Mathivanan. 2015. ExoCarta: A Web-Based Compendium of Exosomal Cargo. *J Mol Biol* 428: 688-692.

115. Mazurov, D., L. Barbashova, and A. Filatov. 2013. Tetraspanin protein CD9 interacts with metalloprotease CD10 and enhances its release via exosomes. *FEBS J* 280: 1200-1213.

116. Perez-Hernandez, D., C. Gutierrez-Vazquez, I. Jorge, S. Lopez-Martin, A. Ursa, F. Sanchez-Madrid, J. Vazquez, and M. Yanez-Mo. 2013. The intracellular interactome of tetraspanin-enriched microdomains reveals their function as sorting machineries toward exosomes. *J Biol Chem* 288: 11649-11661.

117. van Niel, G., P. Bergam, A. Di Cicco, I. Hurbain, A. Lo Cicero, F. Dingli, R. Palmulli, C. Fort, M. C. Potier, L. J. Schurgers, D. Loew, D. Levy, and G. Raposo. 2015. Apolipoprotein E Regulates Amyloid Formation within Endosomes of Pigment Cells. *Cell Rep* 13: 43-51.

118. Charrin, S., S. Manie, M. Oualid, M. Billard, C. Boucheix, and E. Rubinstein. 2002. Differential stability of tetraspanin/tetraspanin interactions: role of palmitoylation. *FEBS Lett* 516: 139-144.

119. Yang, X., C. Claas, S. K. Kraeft, L. B. Chen, Z. Wang, J. A. Kreidberg, and M. E. Hemler. 2002. Palmitoylation of tetraspanin proteins: modulation of CD151 lateral interactions, subcellular distribution, and integrin-dependent cell morphology. *Mol Biol Cell* 13: 767-781.

120. Yang, X. H., O. V. Kovalenko, T. V. Kolesnikova, M. M. Andzelm, E. Rubinstein, J. L. Strominger, and M. E. Hemler. 2006. Contrasting effects of EWI proteins, integrins, and protein palmitoylation on cell surface CD9 organization. *J Biol Chem* 281: 12976-12985.

121. Cherukuri, A., R. H. Carter, S. Brooks, W. Bornmann, R. Finn, C. S. Dowd, and S. K. Pierce. 2004. B cell signaling is regulated by induced palmitoylation of CD81. *J Biol Chem* 279: 31973-31982.

122. Berditchevski, F., E. Odintsova, S. Sawada, and E. Gilbert. 2002. Expression of the palmitoylation-deficient CD151 weakens the association of alpha 3 beta 1 integrin with the tetraspanin-enriched microdomains and affects integrin-dependent signaling. *J Biol Chem* 277: 36991-37000.

123. Sharma, C., X. H. Yang, and M. E. Hemler. 2008. DHHC2 affects palmitoylation, stability, and functions of tetraspanins CD9 and CD151. *Mol Biol Cell* 19: 3415-3425.

124. Espenel, C., E. Margeat, P. Dosset, C. Arduise, C. Le Grimellec, C. A. Royer, C. Boucheix, E. Rubinstein, and P. E. Milhiet. 2008. Single-molecule analysis of CD9 dynamics and partitioning reveals multiple modes of interaction in the tetraspanin web. *J Cell Biol* 182: 765-776.

125. Charrin, S., S. Manie, M. Billard, L. Ashman, D. Gerlier, C. Boucheix, and E. Rubinstein. 2003. Multiple levels of interactions within the tetraspanin web. *Biochem Biophys Res Commun* 304: 107-112.

126. Charrin, S., F. le Naour, O. Silvie, P. E. Milhiet, C. Boucheix, and E. Rubinstein. 2009. Lateral organization of membrane proteins: tetraspanins spin their web. *Biochem J* 420: 133-154.

127. Min, G., H. Wang, T. T. Sun, and X. P. Kong. 2006. Structural basis for tetraspanin functions as revealed by the cryo-EM structure of uroplakin complexes at 6-A resolution. *J Cell Biol* 173: 975-983.

128. Zuidscherwoude, M., F. Gottfert, V. M. Dunlock, C. G. Figdor, G. van den Bogaart, and A. B. van Spriel. 2015. The tetraspanin web revisited by super-resolution microscopy. *Sci Rep* 5: 12201.

129. Heberle, F. A., and G. W. Feigenson. 2011. Phase separation in lipid membranes. *Cold Spring Harb Perspect Biol* 3.

130. Baumgart, T., A. T. Ammond, P. Sengupta, S. T. Hess, D. A. Holowka, B. A. Baird, and W. W. Webb. 2007. Large-scale fluid/fluid phase separation of proteins and lipids in giant plasma membrane vesicles. *Proc Natl Acad Sci U S A* 104: 3165-3170.

131. Morales-Penningston, N. F., J. Wu, E. R. Farkas, S. L. Goh, T. M. Konyakhina, J. Y. Zheng, W. W. Webb, and G. W. Feigenson. 2010. GUV preparation and imaging: minimizing artifacts. *Biochim Biophys Acta* 1798: 1324-1332.

132. Wubbolts, R., R. S. Leckie, P. T. Veenhuizen, G. Schwarzmann, W. Mobius, J. Hoernschemeyer, J. W. Slot, H. J. Geuze, and W. Stoorvogel. 2003. Proteomic and biochemical analyses of human B cell-derived exosomes. Potential implications for their function and multivesicular body formation. *J Biol Chem* 278: 10963-10972.

133. Laulagnier, K., C. Motta, S. Hamdi, S. Roy, F. Fauvelle, J. F. Pageaux, T. Kobayashi, J. P. Salles, B. Perret, C. Bonnerot, and M. Record. 2004. Mast cell- and dendritic cell-derived exosomes display a specific lipid composition and an unusual membrane organization. *Biochem J* 380: 161-171.

134. Llorente, A., T. Skotland, T. Sylvanne, D. Kauhanen, T. Rog, A. Orlowski, I. Vattulainen, K. Ekroos, and K. Sandvig. 2013. Molecular lipidomics of exosomes released by PC-3 prostate cancer cells. *Biochim Biophys Acta* 1831: 1302-1309.

135. Carayon, K., K. Chaoui, E. Ronzier, I. Lazar, J. Bertrand-Michel, V. Roques, S. Balor, F. Terce, A. Lopez, L. Salome, and E. Joly. 2011. Proteolipidic composition of exosomes changes during reticulocyte maturation. *J Biol Chem* 286: 34426-34439.

136. Silvie, O., S. Charrin, M. Billard, J. F. Franetich, K. L. Clark, G. J. van Gemert, R. W. Sauerwein, F. Dautry, C. Boucheix, D. Mazier, and E. Rubinstein. 2006. Cholesterol contributes to the organization of tetraspanin-enriched microdomains and to CD81-dependent infection by malaria sporozoites. *J Cell Sci* 119: 1992-2002.

137. Hogue, I. B., J. R. Grover, F. Soheilian, K. Nagashima, and A. Ono. 2011. Gag induces the coalescence of clustered lipid rafts and tetraspanin-enriched microdomains at HIV-1 assembly sites on the plasma membrane. *J Virol* 85: 9749-9766.

138. Dachary-Prigent, J., J. M. Freyssinet, J. M. Pasquet, J. C. Carron, and A. T. Nurden. 1993. Annexin V as a probe of aminophospholipid exposure and platelet membrane vesiculation: a flow cytometry study showing a role for free sulfhydryl groups. *Blood* 81: 2554-2565.

139. Kajimoto, T., T. Okada, S. Miya, L. Zhang, and S. Nakamura. 2013. Ongoing activation of sphingosine 1-phosphate receptors mediates maturation of exosomal multivesicular endosomes. *Nat Commun* 4: 2712.

140. Laulagnier, K., D. Grand, A. Dujardin, S. Hamdi, H. Vincent-Schneider, D. Lankar, J. P. Salles, C. Bonnerot, B. Perret, and M. Record. 2004. PLD2 is enriched on exosomes and its activity is correlated to the release of exosomes. *FEBS Lett* 572: 11-14.

141. Ghossoub, R., F. Lembo, A. Rubio, C. B. Gaillard, J. Bouchet, N. Vitale, J. Slavik, M. Machala, and P. Zimmermann. 2014. Syntenin-ALIX exosome biogenesis and budding into multivesicular bodies are controlled by ARF6 and PLD2. *Nat Commun* 5: 3477.

142. Lai, R. C., S. S. Tan, R. W. Yeo, A. B. Choo, A. T. Reiner, Y. Su, Y. Shen, Z. Fu, L. Alexander, S. K. Sze, and S. K. Lim. 2016. MSC secretes at least 3 EV types each with a unique permutation of membrane lipid, protein and RNA. *J Extracell Vesicles* 5: 29828.

143. Connolly, K. D., I. A. Guschina, V. Yeung, A. Clayton, M. S. Draman, C. Von Ruhland, M. Ludgate, P. E. James, and D. A. Rees. 2015. Characterisation of adipocyte-derived extracellular vesicles released pre- and post-adipogenesis. *J Extracell Vesicles* 4: 29159.

144. Piper, R. C., I. Dikic, and G. L. Lukacs. 2014. Ubiquitin-dependent sorting in endocytosis. *Cold Spring Harb Perspect Biol* 6.

145. Sette, P., K. Nagashima, R. C. Piper, and F. Bouamr. 2013. Ubiquitin conjugation to Gag is essential for ESCRT-mediated HIV-1 budding. *Retrovirology* 10: 79.

146. Burke, M. C., M. S. Oei, N. J. Edwards, S. Ostrand-Rosenberg, and C. Fenselau. 2014. Ubiquitinated proteins in exosomes secreted by myeloid-derived suppressor cells. *J Proteome Res* 13: 5965-5972.

147. Buschow, S. I., J. M. Liefhebber, R. Wubbolts, and W. Stoorvogel. 2005. Exosomes contain ubiquitinated proteins. *Blood Cells Mol Dis* 35: 398-403.

148. Smith, V. L., L. Jackson, and J. S. Schorey. 2015. Ubiquitination as a Mechanism To Transport Soluble Mycobacterial and Eukaryotic Proteins to Exosomes. *J Immunol* 195: 2722-2730.

149. Tamai, K., N. Tanaka, T. Nakano, E. Kakazu, Y. Kondo, J. Inoue, M. Shiina, K. Fukushima, T. Hoshino, K. Sano, Y. Ueno, T. Shimosegawa, and K. Sugamura. 2010. Exosome secretion of dendritic cells is regulated by Hrs, an ESCRT-0 protein. *Biochem Biophys Res Commun* 399: 384-390.

150. Gauvreau, M. E., M. H. Cote, M. C. Bourgeois-Daigneault, L. D. Rivard, F. Xiu, A. Brunet, A. Shaw, V. Steimle, and J. Thibodeau. 2009. Sorting of MHC class II molecules into exosomes through a ubiquitin-independent pathway. *Traffic* 10: 1518-1527.

151. Buschow, S. I., B. W. van Balkom, M. Aalberts, A. J. Heck, M. Wauben, and W. Stoorvogel. 2010. MHC class II-associated proteins in B-cell exosomes and potential functional implications for exosome biogenesis. *Immunol Cell Biol* 88: 851-856.

152. MacDonald, C., J. A. Payne, M. Aboian, W. Smith, D. J. Katzmann, and R. C. Piper. 2015. A family of tetraspans organizes cargo for sorting into multivesicular bodies. *Dev Cell* 33: 328-342.

153. MacDonald, C., M. A. Stamnes, D. J. Katzmann, and R. C. Piper. 2015. Tetraspan cargo adaptors usher GPI-anchored proteins into multivesicular bodies. *Cell Cycle* 0.

154. Lineberry, N., L. Su, L. Soares, and C. G. Fathman. 2008. The single subunit transmembrane E3 ligase gene related to anergy in lymphocytes (GRAIL) captures and then ubiquitinates transmembrane proteins across the cell membrane. *J Biol Chem* 283: 28497-28505.

155. Latysheva, N., G. Muratov, S. Rajesh, M. Padgett, N. A. Hotchin, M. Overduin, and F. Berditchevski. 2006. Syntenin-1 is a new component of tetraspanin-enriched microdomains: mechanisms and consequences of the interaction of syntenin-1 with CD63. *Mol Cell Biol* 26: 7707-7718.

156. Rajesh, S., R. Bago, E. Odintsova, G. Muratov, G. Baldwin, P. Sridhar, S. Rajesh, M. Overduin, and F. Berditchevski. 2011. Binding to syntenin-1 protein defines a new mode of ubiquitin-based interactions regulated by phosphorylation. *J Biol Chem* 286: 39606-39614.

157. Bezanilla, M., A. S. Gladfelter, D. R. Kovar, and W. L. Lee. 2015. Cytoskeletal dynamics: a view from the membrane. *J Cell Biol* 209: 329-337.

158. de Curtis, I., and J. Meldolesi. 2012. Cell surface dynamics - how Rho GTPases orchestrate the interplay between the plasma membrane and the cortical cytoskeleton. *J Cell Sci* 125: 4435-4444.

159. Li, B., M. A. Antonyak, J. Zhang, and R. A. Cerione. 2012. RhoA triggers a specific signaling pathway that generates transforming microvesicles in cancer cells. *Oncogene* 31: 4740-4749.

160. Fackler, O. T., and R. Grosse. 2008. Cell motility through plasma membrane blebbing. *J Cell Biol* 181: 879-884.

161. Charras, G., and E. Paluch. 2008. Blebs lead the way: how to migrate without lamellipodia. *Nat Rev Mol Cell Biol* 9: 730-736.

162. Ridley, A. J. 2015. Rho GTPase signalling in cell migration. *Curr Opin Cell Biol* 36: 103-112.

163. Stenmark, H., R. G. Parton, O. Steele-Mortimer, A. Lutcke, J. Gruenberg, and M. Zerial. 1994. Inhibition of rab5 GTPase activity stimulates membrane fusion in endocytosis. *EMBO J* 13: 1287-1296.

164. Rink, J., E. Ghigo, Y. Kalaidzidis, and M. Zerial. 2005. Rab conversion as a mechanism of progression from early to late endosomes. *Cell* 122: 735-749.

165. Green, E. G., E. Ramm, N. M. Riley, D. J. Spiro, J. R. Goldenring, and M. Wessling-Resnick. 1997. Rab11 is associated with transferrin-containing recycling compartments in K562 cells. *Biochem Biophys Res Commun* 239: 612-616.

166. Savina, A., C. M. Fader, M. T. Damiani, and M. I. Colombo. 2005. Rab11 promotes docking and fusion of multivesicular bodies in a calcium-dependent manner. *Traffic* 6: 131-143.

167. Savina, A., M. Vidal, and M. I. Colombo. 2002. The exosome pathway in K562 cells is regulated by Rab11. *J Cell Sci* 115: 2505-2515.

168. Welz, T., J. Wellbourne-Wood, and E. Kerkhoff. 2014. Orchestration of cell surface proteins by Rab11. *Trends Cell Biol* 24: 407-415.

169. Zhang, X. M., S. Ellis, A. Sriratana, C. A. Mitchell, and T. Rowe. 2004. Sec15 is an effector for the Rab11 GTPase in mammalian cells. *J Biol Chem* 279: 43027-43034.

170. Chaineau, M., M. S. Ioannou, and P. S. McPherson. 2013. Rab35: GEFs, GAPs and effectors. *Traffic* 14: 1109-1117.

171. Hsu, C., Y. Morohashi, S. Yoshimura, N. Manrique-Hoyos, S. Jung, M. A. Lauterbach, M. Bakhti, M. Gronborg, W. Mobius, J. Rhee, F. A. Barr, and M. Simons. 2010. Regulation of exosome secretion by Rab35 and its GTPase-activating proteins TBC1D10A-C. *J Cell Biol* 189: 223-232.

172. Figueiredo, A. C., C. Wasmeier, A. K. Tarafder, J. S. Ramalho, R. A. Baron, and M. C. Seabra. 2008. Rab3GEP is the non-redundant guanine nucleotide exchange factor for Rab27a in melanocytes. *J Biol Chem* 283: 23209-23216.

173. Tarafder, A. K., C. Wasmeier, A. C. Figueiredo, A. E. Booth, A. Orihara, J. S. Ramalho, A. N. Hume, and M. C. Seabra. 2011. Rab27a targeting to melanosomes requires nucleotide exchange but not effector binding. *Traffic* 12: 1056-1066.

174. Kondo, H., R. Shirakawa, T. Higashi, M. Kawato, M. Fukuda, T. Kita, and H. Horiuchi. 2006. Constitutive GDP/GTP exchange and secretion-dependent GTP hydrolysis activity for Rab27 in platelets. *J Biol Chem* 281: 28657-28665.

175. Elstak, E. D., M. Neeft, N. T. Nehme, J. Voortman, M. Cheung, M. Goodarzifard, H. C. Gerritsen, P. M. van Bergen En Henegouwen, I. Callebaut, G. de Saint Basile, and P. van der Sluijs. 2011. The munc13-4-rab27 complex is specifically required for tethering secretory lysosomes at the plasma membrane. *Blood* 118: 1570-1578.

176. Chiang, L., J. Ngo, J. E. Schechter, S. Karvar, T. Tolmachova, M. C. Seabra, A. N. Hume, and S. F. Hamm-Alvarez. 2011. Rab27b regulates exocytosis of secretory vesicles in acinar epithelial cells from the lacrimal gland. *Am J Physiol Cell Physiol* 301: C507-21.

177. Lam, A. D., S. Ismail, R. Wu, O. Yizhar, D. R. Passmore, S. A. Ernst, and E. L. Stuenkel. 2010. Mapping dynamic protein interactions to insulin secretory granule behavior with TIRF-FRET. *Biophys J* 99: 1311-1320.

178. Ostenfeld, M. S., D. K. Jeppesen, J. R. Laurberg, A. T. Boysen, J. B. Bramsen, B. Primdal-Bengtson, A. Hendrix, P. Lamy, F. Dagnaes-Hansen, M. H. Rasmussen, K. H. Bui, N. Fristrup, E. I. Christensen, I. Nordentoft, J. P. Morth, J. B. Jensen, J. S. Pedersen, M. Beck, D. Theodorescu, M. Borre, K. A. Howard, L. Dyrskjot, and T. F. Orntoft. 2014. Cellular disposal of miR23b by RAB27-dependent exosome release is linked to acquisition of metastatic properties. *Cancer Res* 74: 5758-5771.

179. Shirakawa, R., and H. Horiuchi. 2015. Ral GTPases: crucial mediators of exocytosis and tumourigenesis. *J Biochem* 157: 285-299.

180. Hyenne, V., A. Apaydin, D. Rodriguez, C. Spiegelhalter, S. Hoff-Yoessle, M. Diem, S. Tak, O. Lefebvre, Y. Schwab, J. G. Goetz, and M. Labouesse. 2015. RAL-1 controls multivesicular body biogenesis and exosome secretion. *J Cell Biol* 211: 27-37.

181. Chaineau, M., L. Danglot, and T. Galli. 2009. Multiple roles of the vesicular-SNARE TI-VAMP in post-Golgi and endosomal trafficking. *FEBS Lett* 583: 3817-3826.

182. Hesketh, G. G., I. Perez-Dorado, L. P. Jackson, L. Wartosch, I. B. Schafer, S. R. Gray, A. J. McCoy, O. B. Zeldin, E. F. Garman, M. E. Harbour, P. R. Evans, M. N. Seaman, J. P.

Luzio, and D. J. Owen. 2014. VARP is recruited on to endosomes by direct interaction with retromer, where together they function in export to the cell surface. *Dev Cell* 29: 591-606.

183. Fader, C. M., D. G. Sanchez, M. B. Mestre, and M. I. Colombo. 2009. TI-VAMP/VAMP7 and VAMP3/cellubrevin: two v-SNARE proteins involved in specific steps of the autophagy/multivesicular body pathways. *Biochim Biophys Acta* 1793: 1901-1916.

184. Kweon, Y., A. Rothe, E. Conibear, and T. H. Stevens. 2003. Ykt6p is a multifunctional yeast R-SNARE that is required for multiple membrane transport pathways to the vacuole. *Mol Biol Cell* 14: 1868-1881.

185. Tai, G., L. Lu, T. L. Wang, B. L. Tang, B. Goud, L. Johannes, and W. Hong. 2004. Participation of the syntaxin 5/Ykt6/GS28/GS15 SNARE complex in transport from the early/recycling endosome to the trans-Golgi network. *Mol Biol Cell* 15: 4011-4022.

186. Savina, A., M. Furlan, M. Vidal, and M. I. Colombo. 2003. Exosome release is regulated by a calcium-dependent mechanism in K562 cells. *J Biol Chem* 278: 20083-20090.

187. Emmanouilidou, E., K. Melachroinou, T. Roumeliotis, S. D. Garbis, M. Ntzouni, L. H. Margaritis, L. Stefanis, and K. Vekrellis. 2010. Cell-produced alpha-synuclein is secreted in a calcium-dependent manner by exosomes and impacts neuronal survival. *J Neurosci* 30: 6838-6851.

188. Kapustin, A. N., M. L. Chatrou, I. Drozdov, Y. Zheng, S. M. Davidson, D. Soong, M. Furmanik, P. Sanchis, R. T. De Rosales, D. Alvarez-Hernandez, R. Shroff, X. Yin, K. Muller, J. N. Skepper, M. Mayr, C. P. Reutelingsperger, A. Chester, S. Bertazzo, L. J.

Schurgers, and C. M. Shanahan. 2015. Vascular smooth muscle cell calcification is mediated by regulated exosome secretion. *Circ Res* 116: 1312-1323.

189. Rizo, J., and J. Xu. 2015. The Synaptic Vesicle Release Machinery. *Annu Rev Biophys* 44: 339-367.

190. Fowler, K. T., N. W. Andrews, and J. W. Huleatt. 2007. Expression and function of synaptotagmin VII in CTLs. *J Immunol* 178: 1498-1504.

191. Martinez, I., S. Chakrabarti, T. Hellevik, J. Morehead, K. Fowler, and N. W. Andrews. 2000. Synaptotagmin VII regulates Ca(2+)-dependent exocytosis of lysosomes in fibroblasts. *J Cell Biol* 148: 1141-1149.

192. Zhao, H., Y. Ito, J. Chappel, N. W. Andrews, S. L. Teitelbaum, and F. P. Ross. 2008. Synaptotagmin VII regulates bone remodeling by modulating osteoclast and osteoblast secretion. *Dev Cell* 14: 914-925.

193. Andrews, N. W. 2005. Membrane resealing: synaptotagmin VII keeps running the show. *Sci STKE* 2005: pe19.

194. Rao, S. K., C. Huynh, V. Proux-Gillardeaux, T. Galli, and N. W. Andrews. 2004. Identification of SNAREs involved in synaptotagmin VII-regulated lysosomal exocytosis. *J Biol Chem* 279: 20471-20479.

195. Chicka, M. C., Q. Ren, D. Richards, L. M. Hellman, J. Zhang, M. G. Fried, and S. W. Whiteheart. 2016. Role of Munc13-4 as a Ca2+-dependent tether during platelet secretion. *Biochem J* 473: 627-639.

196. Johnson, J. L., J. He, M. Ramadass, K. Pestonjamasp, W. B. Kiosses, J. Zhang, and S. D. Catz. 2016. Munc13-4 Is a Rab11-binding Protein That Regulates Rab11-positive Vesicle Trafficking and Docking at the Plasma Membrane. *J Biol Chem* 291: 3423-3438.

197. Peterson, M. F., N. Otoc, J. K. Sethi, A. Gupta, and T. J. Antes. 2015. Integrated systems for exosome investigation. *Methods* 87: 31-45.

198. Adams, A. 1973. Concentration of Epstein-Barr virus from cell culture fluids with polyethylene glycol. *J Gen Virol* 20: 391-394.

199. Kohno, T., S. Mohan, T. Goto, C. Morita, T. Nakano, W. Hong, J. C. Sangco, S. Morimatsu, and K. Sano. 2002. A new improved method for the concentration of HIV-1 infective particles. *J Virol Methods* 106: 167-173.

200. van Niel, G., R. Wubbolts, and W. Stoorvogel. 2008. Endosomal sorting of MHC class II determines antigen presentation by dendritic cells. *Curr Opin Cell Biol* 20: 437-444.

201. Stuffers, S., C. Sem Wegner, H. Stenmark, and A. Brech. 2009. Multivesicular endosome biogenesis in the absence of ESCRTs. *Traffic* 10: 925-937.

202. Choi, D. S., D. K. Kim, Y. K. Kim, and Y. S. Gho. 2015. Proteomics of extracellular vesicles: Exosomes and ectosomes. *Mass Spectrom Rev* 34: 474-490.

203. Pols, M. S., and J. Klumperman. 2009. Trafficking and function of the tetraspanin CD63. *Exp Cell Res* 315: 1584-1592.

204. Wang, H. X., T. V. Kolesnikova, C. Denison, S. P. Gygi, and M. E. Hemler. 2011. The C-terminal tail of tetraspanin protein CD9 contributes to its function and molecular organization. *J Cell Sci* 124: 2702-2710.

205. Roucourt, B., S. Meeussen, J. Bao, P. Zimmermann, and G. David. 2015. Heparanase activates the syndecan-syntenin-ALIX exosome pathway. *Cell Res* 25: 412-428.

Chapter 1 Figures

A.

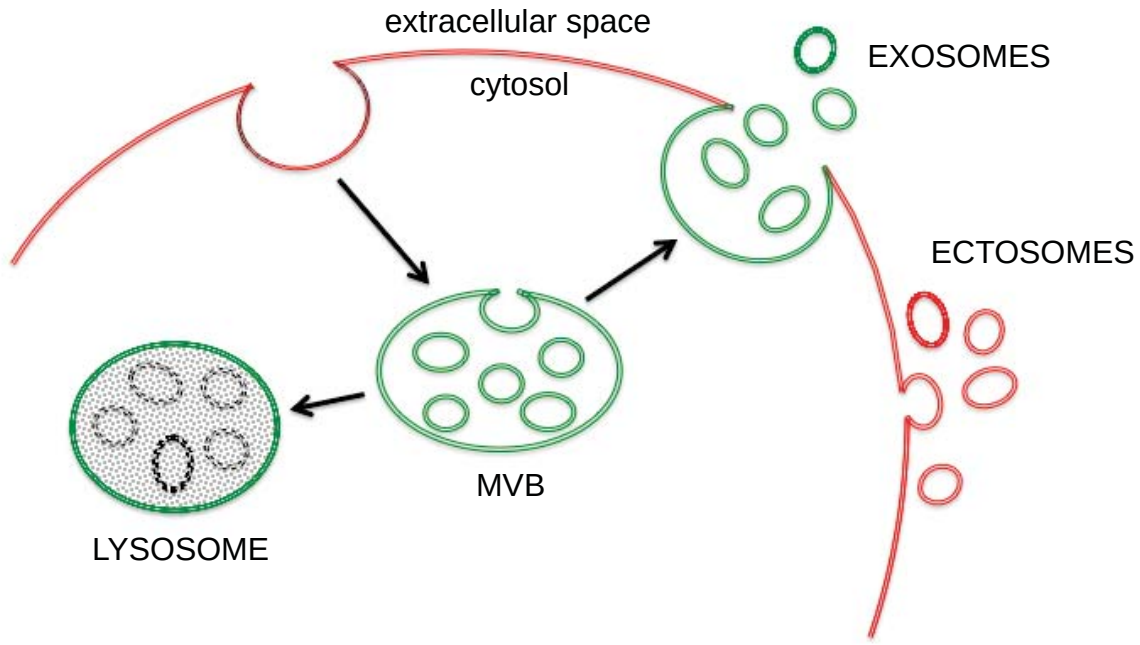

B.

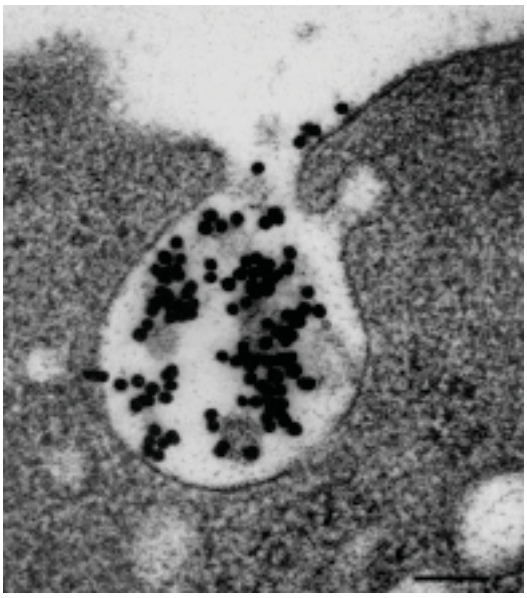

C.

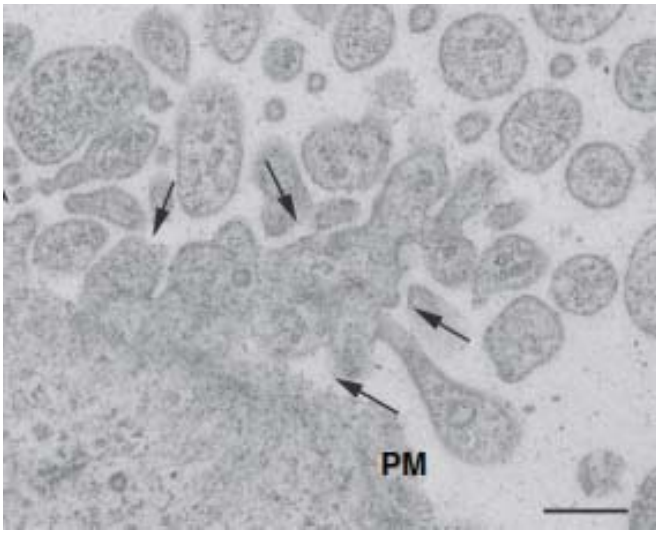

FIGURE1-1. Cells release different types of extracellular vesicles. *A*, Schematic of the different membranes from which EVs arise. *B*, EM image of a MVB containing immunogold-labeled transferrin fusing with the plasma membrane to release transferrin receptor-bearing exosomes. Scale bar = 200nm.[2] *C*, EM image of ectosome release. Arrows show sites of budding from the plasma membrane (PM) of breast cancer cells. Scale bar = 500nm.[3]

[2] Harding, C., P. Stahl. 1983. Transferrin recycling in reticulocytes: pH and iron are important determinants of ligand binding and processing. Biochem. Biophys. Res. Commun. 113:650–658.

[3] LoCicero, A., P. Stahl, G. Raposo. 2015. Extracellular vesicles shuffling intercellular messages: for good or for bad. Curr Opin Cell Biol 35: 69-77.

Chapter 2

Inhibiting VPS4 impairs extracellular vesicle biogenesis and demonstrates a broad role for ESCRTs in exosome and ectosome release

Abstract

Extracellular vesicles (EVs) play important roles in intercellular communication. Two broad classes of EVs can be distinguished by their intracellular origin. Exosomes are generated within endosomes and released when these fuse with the plasma membrane, while ectosomes bud directly from the plasma membrane. Topologically equivalent processes including intralumenal vesicle formation for degradation in the endosomal pathway and virus budding from the plasma membrane depend on Endosomal Sorting Complex Required for Transport (ESCRT)-III and the ATPase VPS4 for membrane fission and release. Whether this machinery is generally required for EV biogenesis has, however, been the subject of debate. Here, we use two complementary methods for isolating EVs from cultured cells and demonstrate that inhibiting VPS4 stabilizes ESCRT-III polymers and correspondingly reduces constitutive release of both protein and miRNA in EVs. Notably, we find that tetraspanins that preferentially reside on different membranes are enriched on distinct populations of EVs, both of which depend on VPS4 activity for their release. Stimulating cells with serum increases EV release primarily from the plasma membrane and is again VPS4-dependent. All together, our data indicate that inhibiting

VPS4 blocks both exosome and ectosome release thereby generally implicating ESCRT-III in EV biogenesis.

Introduction

Extracellular vesicles (EVs) are released by virtually all cells and are present both in tissues and in a variety of body fluids (1). Early observations revealed roles for EVs in discarding membrane proteins during reticulocyte maturation (2, 3) and in eliciting immune responses (4, 5). Since then it has become clear that EVs modulate cell behavior in numerous ways and function broadly in intercellular communication (6). EVs can be classified based on their tissue of origin, e.g. prostasomes derive from prostate cells, oncosomes from tumor cells, etc. However, each cell can also release EVs from different membranes. Exosomes are released when endosomal multivesicular bodies (MVBs) fuse with the plasma membrane (7). Ectosomes or shedding microvesicles are released directly from the plasma membrane (8, 9). Differentiating among these by standard techniques is difficult, and it is likely that most EV preparations include both types of vesicles (10, 11).

EVs contain proteins, lipids, and RNA. If EVs indeed represent specific signaling entities then mechanisms are needed to selectively package cargo molecules into them. Our understanding of this sorting is still incomplete, but numerous molecules are known to be overrepresented in EVs. These include the widely expressed tetraspanins CD63, CD81, and CD9. Tetraspanins are four-pass transmembrane glycoproteins known for their propensity to assemble into tetraspanin enriched microdomains (12) that may play roles in defining EV content. Exosomes from CD81 deficient T lymphocytes are selectively missing proteins that interact with CD81 (13). CD9 directs release of the membrane endopeptidase CD10 on EVs (14). CD63 interacts with premelanosomal protein and mediates its sorting to ILVs released from

melanocytes (15). Similar proteins in yeast have recently been identified as organizers of non-ubiquitinated MVB cargo (16). Other proteins frequently detected in EVs include adaptor-type molecules such as ALIX and syntenin-1 that may help to recruit soluble cargo (17). A few factors specifically implicated in concentrating RNA in EVs include sumoylated heterogeneous nuclear ribonuclear protein A2B1 (18) and annexin a2 (19), Overall, however, much remains to be understood about mechanisms responsible for sorting specific cargo to EVs.

In addition to selecting cargo, producing EVs requires machinery to deform the membrane and release vesicles. Polymers of ESCRT-III drive membrane fission in topologically comparable events including virus budding and intralumenal vesicle formation, acting as spiral coils to constrict vesicle necks (20, 21). The AAA+ ATPase VPS4 remodels and disassembles ESCRT-III filaments, and is essential for ongoing ESCRT-III function. Because of these roles, ESCRT-III and VPS4 have long been considered likely to play central roles in EV biogenesis. However, specific attempts to test their involvement have provided contradictory results. These contradictions may result at least in part from the modularity of the ESCRT machinery. If ESCRT-III function is indeed generally employed for EV membrane fission, we expect inhibiting it to have a general effect on EV release. Here we use stable cell lines in which expression of an inhibitory VPS4 mutant is tightly regulated and inducible to test the effects of uniformly inhibiting ESCRT-III remodeling on EV release. We also develop and characterize an efficient, small-scale method for collecting EVs. Our results demonstrate that inhibiting VPS4 blocks both exosome and ectosome release thereby generally implicating ESCRT-III in EV biogenesis.

Methods

Antibodies, Plasmids and reagents—Antibodies used include mouse monoclonal antibodies against CD63 (Dev Biostudies (H5C6) or Ancell (46-4-5)), CD9 (Serotec MCA496GA), mCherry (Novus Biologicals (96752)) and rabbit polycolonal antibodies against CHMP4A (22), calnexin (Cell Signaling Technologies (2433)), and syntenin-1 (ProteinTech (22399)). Secondary antibodies were conjugated to horseradish peroxidase for immunoblotting (ThermoFisher), IRdye800CW for infrared-based cell quantitation (LiCor) and Alexa Fluor 488 immunofluorescence (ThermoFisher).

pEGFP-CD63 (kind gift from Paul Roche, NIH) was used to generate pmCherry-CD63 using BamHI and XhoI sites. GFP-CD9 was generated by transferring CD9 from pcDNA3.1 FLAG-CD9 (kind gift from Michael Caplan, Yale School of Medicine) into pEGFP-C2 between BamHI and XhoI sites. GPI-mCherry was a kind gift from Gerald Baron (Rocky Mountain Laboratories, NIAID, NIH).

HEK293TREx cells with tetracycline inducible $VPS4A_{E228Q}$ or $VPS4B_{E235Q}$ described in (22, 23) were maintained in 5µg/ml blasticidin and 100µg/ml zeocin. PANC-1 cells were from ATCC. U87 cells were from Joshua Rubin (Washington University School of Medicine). All cell lines were maintained in Dulbecco's modified Eagle's medium supplemented with 10% tetracycline-tested fetal bovine serum and 1mM L-Glutamine. Cell lines stably expressing the indicated exogenous constructs were generated by transfecting with Lipofectamine 2000 (Invitrogen) followed by selection with 500µg/ml G418.

Chemicals were from Sigma Aldrich (St. Louis, MO) unless otherwise noted. Protein concentrations were determined with Bio-Rad protein assay reagent using bovine serum albumin as a standard.

EV collection by differential centrifugation—EVs were collected into culture medium containing fetal bovine serum depleted of exosomes by overnight centrifugation at 100,000 × g. To concentrate EVs, EV containing medium was cleared of larger membranes by spinning at 1,500 × g for 10 min followed by 10,000 × g for 30 min or passage through a 0.2μm PVDF low protein binding syringe filter (Millipore). EVs were then pelleted from this supernatant at 100,000 × g for 2 hr, resuspended in 1ml phosphate buffered saline (PBS), and pelleted again at 100,000 × g for 1 hr. Unless otherwise indicated in figure legend, final EV pellets were suspended in PBS in a volume normalized to the total protein content of the cells from which they were derived and used for immunoblotting.

Sucrose gradients—EV pellets obtained by differential centrifugation were suspended in 2 ml of 20 mM HEPES pH7.4, 2.5 M sucrose and placed in the bottom of a SW41 centrifuge tube. A 10ml linear sucrose gradient (2M-0.25M sucrose, 20mM HEPES pH7.4) was layered over this and then centrifuged at 210,000 × g for ≥14 hr. 1ml fractions were collected, diluted with 3ml TBS (20mM Tris pH7.5, 100mM NaCl) and bound to nitrocellulose by passage through a slot blot apparatus (Minifold I (Midwest Scientific)). The membrane was dried and subjected to immunoblotting for EV proteins.

EV collection by polyethylene glycol precipitation and concanavalin A binding—Culture media was cleared of larger membranes as described for differential centrifugation and then combined with an equal volume of 40% polyethylene glycol (PEG, 3350 average molecular weight) in PBS. After 1 hr on ice, precipitates were pelleted at 17,000 × g for 20 min and resuspended in ConA binding buffer (20mM Tris-Cl pH7.4, 150mM NaCl, 2mM $MnCl_2$, 2mM $CaCl_2$). Samples were incubated overnight with conconavalinA sepharose (GE Healthcare). Beads were washed and either boiled in SDS-PAGE sample buffer or eluted with 1M α-D-

methylmannoside in binding buffer. All EV isolates were normalized to the total protein present in the cell cultures from which they were isolated.

SDS-PAGE and immunoblotting—Samples were boiled in SDS-PAGE sample buffer (2% SDS, 60mM Tris pH 6.8, 0.01% bromophenol blue, 10% glycerol) with or without 1% β-mercaptoethanol for 5 min and spun for 2 min at 21,000 × g. CD63 and CD9 immunoblotting required non-reducing conditions. Proteins were separated on 10% gels followed by transfer to nitrocellulose. Membranes were blocked and probed in TBS, 0.05% Tween and 5% nonfat dry milk. Blots were imaged on a ChemiDoc MP imaging system (Bio-Rad) and quantitated with Bio-Rad Image Studio software.

Quantitative RT-PCR analysis of miRNA—EVs collected by differential centrifugation were suspended in PBS and RNA was isolated using TRIzol LS (Invitrogen). Samples were spiked with 100nM *C. elegans* synthetic miRNA as a control (cel-miR-39, 5'-UCACCGGGUGUAAACAGCUUG-3'). cDNA synthesis was primed with hairpin stem-loop oligonucleotides as previously described (24) (miR-92a, 5'-GCGTGGTCCCGACCACCACAGCCGCCACGACCACGCACAGGC-3'; miR-150, 5'-GCGTGGTCCCGACCACCACAGCCGCCACGACCACGCCACTGG-3'; cel-miR-39, 5'-GCGTGGTCCCGACCACCACAGCCGCCACGACCACGCCAAGCT-3'). cDNA was amplified in an ABI Prism 7500 Fast real-time PCR machine for 40 PCR cycles using SYBR green PCR master mixture (Applied Biosystems), 100 nM template specific (miR-92a, 5'-GTGACGATCTATTGCACTTGTCCCG-3'; miR-150, 5'-GTGACGATCTCTCCCAACCCTTGTA-3'; cel-miR-39, 5'-CAGTGACGATCTCACCGGGTGTAAATC-3'), and a 100 nM universal reverse primer (5'-

TCCCGACCACCACAGCC-3'). Relative quantification of miRNA expression was performed using the comparative threshold method with normalization to cel-miR-39.

Fluorescent EV particle counts—EVs collected by differential centrifugation were resuspended in PBS in a volume normalized to the total protein content of the cells from which they were collected. 1µl was placed on a glass slide, overlaid with a 12 mm diameter glass coverslip pre-coated with poly-L-lysine, and imaged by widefield fluorescence microscopy as described below. Counting of thresholded images was done using the particle counting plug-in in ImageJ.

Immunofluorescence—Cells on poly-L-lysine coated #1.5 glass were fixed in 2% paraformaldehyde in PBS, permeabilized with 0.1% saponin, and blocked and stained with antibodies diluted in PBS containing 5% goat serum and 0.01% saponin.

Microscopy—Imaging was performed with an Olympus IX81 microscope equipped with a 60×/1.42 NA oil objective. Confocal images were obtained with a Yokogawa CSU-10 spinning disc confocal and a Cascade 512B camera. Widefield images for particle counting were acquired with a Hamamatsu Flash 2.8 camera.

Infrared (IR) immune-labeling and quantitation—Cells plated in poly-L-Lysine coated 24-well plates at varying densities were fixed and stained as for immunofluorescence using IRdye secondary antibodies. Staining was detected on an Odyssey infrared imager (Li-Cor).

Results

CD63 and CD9 reside on separable populations of EVs—The tetraspanins CD63 and CD9 are among the proteins most commonly recovered in EVs (25). Interestingly, these two

proteins do not typically share the same subcellular distribution: CD63 is enriched on intralumenal vesicles within MVBs (26) while CD9 localizes primarily to the plasma membrane (27). We confirmed this contrasting localization in HEK293 cells stably co-expressing mCherry-CD63 and GFP-CD9 (Figure 1A). Quantitative comparison of surface and total tetraspanin immunostaining revealed a similar distribution for the endogenous proteins in untransfected HEK293 cells (Figure 1, B and C).

Based on their differential localization, we wondered if CD63 and CD9 might be enriched in distinct EVs that separately derive from their primary membrane of occupancy, the MVB and the plasma membrane. To assess this, we isolated EVs by differential centrifugation using a typical protocol (28, 29) (Figure 1D). We refer to the resulting EV pellet as the "100k EV fraction." As a general rule, we attempted to maintain comparable culture conditions across all EV collection experiments (e.g. cell density and time in culture before beginning EV collection) to avoid significant losses and variation due to elusive factors such as EV adherence to culture dishes or re-uptake by cells. To determine how homogenous the EVs bearing CD63 and CD9 are, we floated the 100k EV pellet to equilibrium in linear sucrose gradients (Figure 1D). Immunoblot quantitation demonstrated that membranes containing CD63 peak at 1.13 g/ml (Figure 1E). This is similar to the previously reported density of exosomes (4, 26). In contrast, membranes containing CD9 were most concentrated at 1.2-1.24 g/ml. These results indicate that CD63 and CD9 are differentially enriched on separable extracellular membranes, potentially corresponding to exosomes and ectosomes.

Collecting EVs by polyethylene glycol precipitation and binding to concanavalin A— Isolating EVs by ultracentrifugation requires large numbers of cells and long collection times to obtain a manageable pellet. This limits the resolution of experiments designed to study EV

release. We therefore developed an enrichment protocol to improve sample handling when collecting EVs from fewer cells and/or after shorter incubations (Figure 2A). Polyethylene glycol (PEG) has been used for decades to concentrate viral particles (30-32). Based on its hygroscopic properties, PEG displaces water from solutes and causes them to precipitate. Since viruses and EVs are similar in size, we used PEG to precipitate EVs from culture media. Among PEG formulations, and in line with virus precipitation protocols, we found that 6000g/mol and 3350g/mol PEG polymers consistently precipitated the most EV-associated tetraspanin proteins. To compare PEG precipitated EVs with those 100k EVs we repeated our sucrose gradient analysis on PEG precipitated EV pellets. CD63 membranes peaked at 1.16 g/ml, and CD9 membranes at 1.25 g/ml demonstrating that both methods yield comparably separable EV membranes. Serum protein coprecipitation with the EVs was lowest with 3350g/mol PEG (data not shown). However even in pellets induced by 3350g/mol PEG we found that serum proteins – particularly serum albumin – interfered with immunoblots when the amount of EVs was limiting, i.e. after short collection times. To further enrich for EVs, we took advantage of the fact that glycoproteins on the EV surface specifically bind lectins while albumin, which is not glycosylated, does not (33). EVs contain high mannose glycans (34, 35), and we found that conconavalin A (ConA) sepharose bound the majority of both CD63 and CD9 present in PEG precipitates (Figure 2B). Importantly, albumin did not bind. EVs were eluted with methyl-alpha-D-mannopyranoside, which binds with high affinity to ConA (36), confirming that EV glycans were specifically bound to ConA. Using this two-step protocol of PEG precipitation followed by ConA enrichment, we were able to reduce the number of cells and the collection times necessary to detect CD63 and CD9 by immunoblotting.

To compare the material recovered using this protocol (PEG/ConA) to that isolated by differential centrifugation, we prepared EVs using each of the two methods in parallel. We compared EVs from two cancer cell lines (PANC1 and U87) expected to release high numbers of EVs (37) as well as from HEK293 cells. Culture media collected after 24 hr on cells was split and EVs isolated using PEG/ConA collection or traditional differential centrifugation (Figure 2C). Immunoblotting showed that both methods produced the same relative recovery of exosome associated tetraspanins (Figure 2C). Both methods also revealed enrichment of syntenin-1 – a cytoplasmic adaptor protein that binds CD63 and is implicated in EV biogenesis – in EVs (17, 38) (Figure 2C). Interestingly, there was more variation in the amount of CD63 released by different cell lines than in the amount of CD9. This trend was also previously noted in a comparison of tumor cell EVs (39) and could be because CD63 and CD9 are, at least in part, released on separable membranes (Figure 1E above).

Dominant-negative VPS4 reduces CD63 and CD9 release in EVs—Expressing ATPase defective VPS4 inhibits ESCRT-III disassembly and has a dominant negative effect on ESCRT-dependent processes by co-assembling with endogenous enzyme (22, 23, 40, 41). To ask how this mutant affects EV production we turned to previously characterized cell lines that inducibly express ATPase deficient VPS4A E228Q or VPS4B E235Q (22, 23). These cell lines allow for rapid and uniform expression of the mutant VPS4, and have previously been used to resolve controversies surrounding the role of the ESCRT machinery in viral budding events (23). We tested cell lines expressing mutant forms of VPS4A or VPS4B and observed similar effects; individual figures indicate the isoform used and the notation “VPS4EQ” refers to figures and experiments that show data obtained with both isoforms. Treating cells with tetracycline for 2 hr initiated expression of VPS4EQ, which then accumulated over the ensuing 16-24 hr of

incubation (Figure 3A). Since VPS4EQ blocks disassembly of ESCRT-III polymers, we monitored sedimentation of endogenous ESCRT-III proteins as a read-out of VPS4 inhibition (22, 42). Polymerization of a representative ESCRT-III protein, CHMP4A, demonstrated that ESCRT-III cycling was inhibited within 2 hr of initiating mutant VPS4 expression (Figure 3A).

To monitor the effect of inhibiting VPS4 on production and/or release of EVs, we added EV collection media 2 hrs after initiating VPS4 expression and collected the media 24 hr later. We prepared both 100k EVs and PEG/ConA EVs from these cells and assessed their protein content by immunoblotting. We found that expressing VPS4EQ decreased the amount of both CD63 and CD9 in EVs by ~50% or more (Figure 3, B-E). Notably, cellular levels of CD63 and CD9 were strikingly stabilized (~2-fold increase) in VPS4EQ expressing cells. Firstly, this observation clearly shows that the decrease in tetraspanin release on EVs was not simply due to decreased protein levels. Secondly, this observation indicates that the increased cellular CD63 and CD9 is at least partly due to inhibition of their expulsion. Of course, decreased lysosomal degradation is a likely contributing factor. Nonetheless, the fact that the amount of CD63 and CD9 recovered in EVs was decreased despite their increased cellular expression strongly supports our hypothesis that VPS4 is important for generating EVs bearing these proteins. While ESCRT function has been connected to biogenesis of EVs containing syntenin-1, the effect of VPS4 inhibition has been unclear. In line with the well-characterized role of VPS4 in regulating ESCRT-III function, our inducible system clearly shows that VPS4EQ inhibits synteni-1 release on EVs (Figure 3, C and E). Importantly, we did not detect the endoplasmic reticulum protein, calnexin, in the 100k EV fractions confirming the absence of non-EV membranes even in VPS4EQ expressing cells (Figure 3B). These results confirm that inhibiting VPS4 reduces

release of EVs bearing both MVB and plasma membrane associated tetraspanins and an associated adaptor protein.

Dominant-negative VPS4 decreases release of miRNA in EVs—We wondered how broadly VPS4EQ expression affects the composition of the 100k EV fraction. To look at effects on potential EV cargo, we tested for the presence of two representative miRNAs. We selected miR150, which is released by HEK293 cells (43) and miR92a, which is important for cell proliferation during development of both normal and tumor tissues (44). Both miRNAs have been identified extracellularly in humans, likely in EVs (45). qRT-PCR analysis of the 100k EV fraction revealed that less miR-92a and miR-150 was released from VPS4EQ expressing cells than from controls (Figure 4A). This demonstrates that VPS4 activity is important for release of physiologically important miRNA cargo.

Dominant-negative VPS4 decreases membrane particle release—Reduced release of specific membrane proteins or EV-associated cargo does not necessarily indicate that the number of EVs released is decreased and could instead reflect a change in cargo composition. We therefore sought to independently measure the number of released EVs using fluorescence microscopy-based particle counting (46). Glycophosphatidylinositol (GPI)-anchored proteins are present in EVs (47), but lack cytoplasmic sorting determinants. We stably transfected VPS4EQ inducible HEK293 cells with a plasmid encoding GPI-anchored mCherry, and confirmed that GPI-mCherry was present at both the cell surface and on internal membranes (Figure 4B). We therefore reasoned that GPI-mCherry is likely to be present in both exosomes and ectosomes. We collected and prepared 100k EVs from these cells. As expected, expressing VPS4EQ reduced the amount of GPI-mCherry detected by immunoblotting 100k EV fractions (Figure 4, C and D). In order to count EVs, we resuspended 100k EV pellets in a defined volume, spotted them onto

poly-lysine coated glass and counted discrete particles by widefield fluorescence microscopy. Expressing VPS4EQ decreased the number of particles released by ~5-fold, supporting the idea that VPS4 function is important in the overall release of EVs from the cell (Figure 4E).

Serum triggers VPS4-dependent CD9 and CD63 release—EV production is increasingly thought to be a physiological response enabling intercellular communication. Stimuli such as calcium ionophores and phorbol esters, which mimic and exaggerate specific effects of receptor activation, robustly increase EV release (48, 49). In more physiologic settings, growth factors enhance release of EVs that promote endothelial cell proliferation (50), or tumor cell migration (51). To assess physiologically triggered EV release and determine whether it too requires ESCRT function, we starved and then stimulated cells with serum and monitored EV release over the ensuing 4-5 hr. Immunoblot analysis of EVs collected during this time revealed that serum increased release of both CD63 and CD9. Interestingly, CD9 release was typically a fold greater than CD63 release (Figure 5, A and B). For insight into the time course of this response we analyzed EVs collected at 1 hr intervals after adding serum. Most CD63 and CD9 was released during the first hr, demonstrating that serum triggered a rapid and transient increase in EV release (Figure 5C). To test whether serum-stimulated EV release depended on VPS4 activity we induced expression of VPS4EQ 4 hr prior to serum stimulation and EV collection, as above. Immunoblotting demonstrated that VPS4EQ decreased the serum-triggered release of CD63 and CD9 to ~25% of controls (Figure 5, D and E). These results demonstrate that serum-triggered EV release also depends on VPS4 function and by extension on normal cycling of ESCRT-III.

Release of CD63 but not CD9 is reduced by depolymerizing microtubules—Growth factors such as epidermal growth factor are known to stimulate release of bleb-like plasma membrane bulges as EVs (52, 53). MVB exocytosis and exosome release is, however, also

triggered by activating PKC or elevating calcium (54, 55). EVs recovered after serum stimulation could therefore derive from either MVBs or the plasma membrane. We wondered where the VPS4-sensitive EVs released after serum stimulation originate. Endosome trafficking to the plasma membrane for exocytosis requires transport along microtubules (56), and we therefore asked how depolymerizing microtubules with nocodazole affects CD63 and CD9 release. We reasoned that perturbing MVB trafficking would not affect ectosome release while exosome release should be blocked. Cells were treated with nocodazole for 30 minutes prior to EV collection. Immunostaining cells for α-tubulin clearly show that microtubules were depolymerized after 30 minutes of nocodazole treatment (Figure 7, A and B). When these cells were stimulated with serum, the amount of CD63 released was reduced by ~60% (Figure 7, C and D). Consistent with the idea that CD9 EVs originate primarily at the plasma membrane, CD9 release was largely unchanged (Figure 7, C and D).

CD63 retargeted to the plasma membrane is released comparably to CD9 in EVs—While the majority of CD63 resides on intracellular membranes, a proportion is present together with CD9 at the plasma membrane (Figure 1B). We noticed that the amount of CD63 still released after nocodazole treatment correlated with the proportion of CD63 normally detected at the plasma membrane (~40%). We therefore wondered if CD63 on the plasma membrane is, like CD9, released directly in EVs. To further explore this question, we asked how relocalizing CD63 from endosomes to the plasma membrane affects its release on EVs. Subsets of tetraspanins, including CD63 but not CD9, possess a C-terminal YXXΦ motif important for targeting to late endosomes and/or lysosomes via an interaction with clathrin adaptor protein complexes (57). We stably transfected HEK293 cells with inducible VPS4AEQ with plasmids encoding mCherry fusions of wild-type CD63 or CD63 Y236A (CD63YA). As expected (58), mCherry-CD63YA

was visibly redistributed onto the plasma membrane compared to wild-type CD63 (Figure 7, A and B). Quantitative immunocytochemistry revealed that the distribution of CD63YA between the plasma membrane and internal membranes was comparable to that of CD9 (Figure 7, C and D).

Stimulating cells expressing mCherry-CD63 with serum approximately doubled the amount of CD63 released (Figure 7, E and F), as seen above for endogenous CD63 (Figure 5B). Stimulating cells expressing mCherry-CD63YA with serum increased the amount of CD63 released by almost 10-fold (Figure 7, E and F). Given that the only difference between wild-type and mutant CD63 is subcellular localization, these results support the idea that stimulating cells with serum preferentially releases tetraspanin-containing EVs from the plasma membrane. Importantly, we found that expressing VPSEQ reduced mCherry-CD63YA release (Figure 7, G and H) to a similar extent as seen with CD9, further confirming a role for VPS4 and its substrates in the release of EVs from the plasma membrane.

Discussion

Cells release a variety of EVs that differ in cargo composition, membrane of origin, and function. This heterogeneity has complicated investigations of the mechanisms responsible for EV biogenesis. The ESCRT machinery is frequently suggested to play an important role in this process based both on topology and on the consistent recovery of ESCRT and ESCRT-associated proteins in EVs. Specific roles for ESCRTs in the formation of EVs have, however, remained unclear as different systems suggest different requirements/involvement of ESCRT and ESCRT-associated proteins. Here we provide evidence that VPS4 activity is important for the biogenesis of two separable EV populations, implicating it and, more generally, its ESCRT-III substrates in formation of both exosomes and ectosomes.

VPS4 is responsible for ESCRT-III polymer disassembly, and connectivity between VPS4 and ESCRT-III function in MVB formation, cytokinesis and virus budding is well established (59-61). Previous attempts to characterize VPS4's role in EV biogenesis using dominant-negative mutant VPS4 expression have come to varying conclusions. These include finding no effect on release of exogenously overexpressed proteolipid protein or CD63 (62) or of endogenous CD63 (17). Other studies reveal that expressing mutant VPS4 affects release of specific types of EVs including T-cell ectosomes (63), arrestin domain-containing protein 1 mediated microvesicles (64) and hedgehog-containing EVs – likely ectosomes – released by epithelial cells in *Drosophila melanogaster* wing imaginal discs (65). RNAi based depletion of VPS4 affects EV release in various settings albeit to varying degrees and with limited temporal resolution (raposo, wehman, baietti). Our findings extend and generalize these previous studies by demonstrating that acutely inhibiting VPS4 decreases release of both endosome- and plasma membrane-derived EVs from the widely used HEK293 cultured cell line.

Expressing mutant VPS4 efficiently traps all ESCRT-III proteins in their polymerized or filamentous state (Figure 3 and (66)), suggesting a likely role for ESCRT-III in EV production. Only a few previous studies have addressed the contribution of ESCRT-III proteins to this process, and have come to varying conclusions (67). The presence of 12 non-equivalent ESCRT-III proteins in humans complicates this type of analysis (68). Definitive experiments await a better understanding of which are actually involved in different ESCRT-dependent cellular processes.

In order to assess the generality of VPS4 function in EV biogenesis we studied two tetraspanins, CD63 and CD9, and found that their subcellular distribution is completely different and that they are generally released on exosomes and ectosomes, respectively. Earlier studies of

these two “exosome markers” are, in fact, consistent with our observations. Release of CD63, but not CD9, depends on Rab27 (10, 69). Interestingly, treating cells with heparinase selectively stimulated CD63 but not CD9 release indicating mechanistic differences in their release (70). Importantly, however, our finding that inhibiting VPS4 impairs release of both CD63 and CD9 implicates ESCRT-III in both exosome and ectosome biogenesis. In the future, separating these vesicle populations will be an important step toward characterizing the specific requirements for ESCRT proteins in each type of release.

An important aspect of this study was the development of a facile method for concentrating EVs in a form amenable for subsequent immunoblot analysis. Our direct comparison to traditional differential centrifugation showed that comparable EV profiles were obtained. Despite these similarities, we cannot rule out some loss of EVs during PEG precipitation or affinity binding. Several approaches for collecting and measuring EVs outside of ultracentrifugation have been characterized, and each has associated benefits and caveats. Both antibody-based immobilization coupled with fluorescence activated cell scanning and microfluidics approaches provide sensitive detection (69, 71), but these methods are biased toward EVs expressing specific surface antigens. Polymer based methods have been described in the literature and are also commercially available (e.g. ExoQuick®, System Biosciences) (72, 73). These methods non-selectively collect all EVs, but method characterization has focused on biofluids with high EV content (e.g. serum or culture medium on cells over days) and not been used for quantitative analyses of EV release from cultured cells amenable to genetic and/or pharmacologic manipulation. Our method of separating EVs from other precipitated protein using lectin affinity facilitated detection of EVs released over relatively short time periods, which is beneficial to assessing transient changes in EV release and the effects of brief

pharmacological treatments. Given these features, we think this assay will have broad applicability in the study of EV biogenesis.

References

1. Lo Cicero, A., P. D. Stahl, and G. Raposo. 2015. Extracellular vesicles shuffling intercellular messages: for good or for bad. *Curr Opin Cell Biol* 35: 69-77.

2. Pan, B. T., and R. M. Johnstone. 1983. Fate of the transferrin receptor during maturation of sheep reticulocytes in vitro: selective externalization of the receptor. *Cell* 33: 967-978.

3. Harding, C., J. Heuser, and P. Stahl. 1983. Receptor-mediated endocytosis of transferrin and recycling of the transferrin receptor in rat reticulocytes. *J Cell Biol* 97: 329-339.

4. Raposo, G., H. W. Nijman, W. Stoorvogel, R. Liejendekker, C. V. Harding, C. J. Melief, and H. J. Geuze. 1996. B lymphocytes secrete antigen-presenting vesicles. *J Exp Med* 183: 1161-1172.

5. Zitvogel, L., A. Regnault, A. Lozier, J. Wolfers, C. Flament, D. Tenza, P. Ricciardi-Castagnoli, G. Raposo, and S. Amigorena. 1998. Eradication of established murine tumors using a novel cell-free vaccine: dendritic cell-derived exosomes. *Nat Med* 4: 594-600.

6. Antonyak, M. A., and R. A. Cerione. 2014. Microvesicles as mediators of intercellular communication in cancer. *Methods Mol Biol* 1165: 147-173.

7. Kowal, J., M. Tkach, and C. Thery. 2014. Biogenesis and secretion of exosomes. *Curr Opin Cell Biol* 29C: 116-125.

8. Raposo, G., and W. Stoorvogel. 2013. Extracellular vesicles: exosomes, microvesicles, and friends. *J Cell Biol* 200: 373-383.

9. Cocucci, E., and J. Meldolesi. 2015. Ectosomes and exosomes: shedding the confusion between extracellular vesicles. *Trends Cell Biol* 25: 364-372.

10. Bobrie, A., M. Colombo, S. Krumeich, G. Raposo, and C. Thery. 2012. Diverse subpopulations of vesicles secreted by different intracellular mechanisms are present in exosome preparations obtained by differential ultracentrifugation. *J Extracell Vesicles* 1: 10.3402/jev.v1i0.18397

11. Colombo, M., C. Moita, G. van Niel, J. Kowal, J. Vigneron, P. Benaroch, N. Manel, L. F. Moita, C. Thery, and G. Raposo. 2013. Analysis of ESCRT functions in exosome biogenesis, composition and secretion highlights the heterogeneity of extracellular vesicles. *J Cell Sci* 126: 5553-5565.

12. Hemler, M. E. 2005. Tetraspanin functions and associated microdomains. *Nat Rev Mol Cell Biol* 6: 801-811.

13. Perez-Hernandez, D., C. Gutierrez-Vazquez, I. Jorge, S. Lopez-Martin, A. Ursa, F. Sanchez-Madrid, J. Vazquez, and M. Yanez-Mo. 2013. The intracellular interactome of tetraspanin-enriched microdomains reveals their function as sorting machineries toward exosomes. *J Biol Chem* 288: 11649-11661.

14. Mazurov, D., L. Barbashova, and A. Filatov. 2013. Tetraspanin protein CD9 interacts with metalloprotease CD10 and enhances its release via exosomes. *FEBS J* 280: 1200-1213.

15. van Niel, G., S. Charrin, S. Simoes, M. Romao, L. Rochin, P. Saftig, M. S. Marks, E. Rubinstein, and G. Raposo. 2011. The Tetraspanin CD63 Regulates ESCRT-Independent and -Dependent Endosomal Sorting during Melanogenesis. *Dev Cell* 21: 708-721.

16. MacDonald, C., M. A. Stamnes, D. J. Katzmann, and R. C. Piper. 2015. Tetraspan cargo adaptors usher GPI-anchored proteins into multivesicular bodies. *Cell Cycle* 0.

17. Baietti, M. F., Z. Zhang, E. Mortier, A. Melchior, G. Degeest, A. Geeraerts, Y. Ivarsson, F. Depoortere, C. Coomans, E. Vermeiren, P. Zimmermann, and G. David. 2012. Syndecan-syntenin-ALIX regulates the biogenesis of exosomes. *Nat Cell Biol* 14: 677-685.

18. Villarroya-Beltri, C., C. Gutierrez-Vazquez, F. Sanchez-Cabo, D. Perez-Hernandez, J. Vazquez, N. Martin-Cofreces, D. J. Martinez-Herrera, A. Pascual-Montano, M. Mittelbrunn, and F. Sanchez-Madrid. 2013. Sumoylated hnRNPA2B1 controls the sorting of miRNAs into exosomes through binding to specific motifs. *Nat Commun* 4: 2980.

19. Hagiwara, K., T. Katsuda, L. Gailhouste, N. Kosaka, and T. Ochiya. 2015. Commitment of Annexin A2 in recruitment of microRNAs into extracellular vesicles. *FEBS Lett* 589: 4071-4078.

20. Odorizzi, G. 2015. Membrane manipulations by the ESCRT machinery. *F1000Res* 4: 516.

21. Carlson, L. A., Q. T. Shen, M. R. Pavlin, and J. H. Hurley. 2015. ESCRT Filaments as Spiral Springs. *Dev Cell* 35: 397-398.

22. Lin, Y., L. A. Kimpler, T. V. Naismith, J. M. Lauer, and P. I. Hanson. 2005. Interaction of the mammalian endosomal sorting complex required for transport (ESCRT) III protein hSnf7-1 with itself, membranes, and the AAA+ ATPase SKD1. *J Biol Chem* 280: 12799-12809.

23. Taylor, G. M., P. I. Hanson, and M. Kielian. 2007. Ubiquitin depletion and dominant-negative VPS4 inhibit rhabdovirus budding without affecting alphavirus budding. *J Virol* 81: 13631-13639.

24. Michel, C. I., C. L. Holley, B. S. Scruggs, R. Sidhu, R. T. Brookheart, L. L. Listenberger, M. A. Behlke, D. S. Ory, and J. E. Schaffer. 2011. Small nucleolar RNAs U32a, U33, and U35a are critical mediators of metabolic stress. *Cell Metab* 14: 33-44.

25. Keerthikumar, S., D. Chisanga, D. Ariyaratne, H. Al Saffar, S. Anand, K. Zhao, M. Samuel, M. Pathan, M. Jois, N. Chilamkurti, L. Gangoda, and S. Mathivanan. 2015. ExoCarta: A Web-Based Compendium of Exosomal Cargo. *J Mol Biol* 428: 688-692.

26. Escola, J. M., M. Kleijmeer, W. Stoorvogel, J. M. Griffith, O. Yoshie, and H. J. Geuze. 1998. Selective enrichment of tetraspan proteins on the internal vesicles of multivesicular endosomes and on exosomes secreted by human B-lymphocytes. *J Biol Chem* 273: 20121-20127.

27. Israels, S. J., E. M. McMillan-Ward, J. Easton, C. Robertson, and A. McNicol. 2001. CD63 associates with the alphaIIb beta3 integrin-CD9 complex on the surface of activated platelets. *Thromb Haemost* 85: 134-141.

28. Tauro, B. J., D. W. Greening, R. A. Mathias, H. Ji, S. Mathivanan, A. M. Scott, and R. J. Simpson. 2012. Comparison of ultracentrifugation, density gradient separation, and immunoaffinity capture methods for isolating human colon cancer cell line LIM1863-derived exosomes. *Methods* 10: e0145686.

29. Thery, C., A. Clayton, A. Amigorena, and G. Raposo. 2006. Isolation and characterization of exosomes from cell culture supernatants and biological fluids. *Curr Protoc Cell Biol* 3.22: 1-29.

30. Yamamoto, K. R., B. M. Alberts, R. Benzinger, L. Lawhorne, and G. Treiber. 1970. Rapid bacteriophage sedimentation in the presence of polyethylene glycol and its application to large-scale virus purification. *Virology* 40: 734-744.

31. Adams, A. 1973. Concentration of Epstein-Barr virus from cell culture fluids with polyethylene glycol. *J Gen Virol* 20: 391-394.

32. Asenjo, J. A., and B. A. Andrews. 2011. Aqueous two-phase systems for protein separation: A perspective. *J Chromatogr A* 1218: 8826-8835.

33. Cao, J., C. Shen, H. Wang, H. Shen, Y. Chen, A. Nie, G. Yan, H. Lu, Y. Liu, and P. Yang. 2009. Identification of N-glycosylation sites on secreted proteins of human hepatocellular carcinoma cells with a complementary proteomics approach. *J Proteome Res* 8: 662-672.

34. Krishnamoorthy, L., J. W. J. Bess, A. B. Preston, K. Nagashima, and L. K. Mahal. 2009. HIV-1 and microvesicles from T cells share a common glycome, arguing for a common origin. *Nat Chem Biol* 5: 244-250.

35. Batista, B. S., W. S. Eng, K. T. Pilobello, K. Hendricks-Munoz, and L. K. Mahal. 2011. Identification of a Conserved Glycan Signature for Microvesicles. *J Proteome Res* 10: 4624-4633.

36. Novogrodsky, A., and E. Katchalski. 1971. Lymphocyte transformation induced by concanavalin A and its reversion by methyl-alpha-D-mannopyranoside. *Biochim Biophys Acta* 228: 579-583.

37. Vader, P., X. O. Breakefield, and M. J. Wood. 2014. Extracellular vesicles: emerging targets for cancer therapy. *Trends Mol Med* 20: 385-393.

38. Latysheva, N., G. Muratov, S. Rajesh, M. Padgett, N. A. Hotchin, M. Overduin, and F. Berditchevski. 2006. Syntenin-1 is a new component of tetraspanin-enriched microdomains: mechanisms and consequences of the interaction of syntenin-1 with CD63. *Mol Cell Biol* 26: 7707-7718.

39. Yoshioka, Y., Y. Konishi, N. Kosaka, T. Katsuda, T. Kato, and T. Ochiya. 2013. Comparative marker analysis of extracellular vesicles in different human cancer types. *J Extracell Vesicles* 2: 10.3402/jev.v2i0.20424

40. Yoshimori, T., F. Yamagata, A. Yamamoto, N. Mizushima, Y. Kabeya, A. Nara, I. Miwako, M. Ohashi, M. Ohsumi, and Y. Ohsumi. 2000. The mouse SKD1, a homologue of yeast Vps4p, is required for normal endosomal trafficking and morphology in mammalian cells. *Mol Biol Cell* 11: 747-763.

41. Dukes, J. D., J. D. Richardson, R. Simmons, and P. Whitley. 2008. A dominant-negative ESCRT-III protein perturbs cytokinesis and trafficking to lysosomes. *Biochem J* 411: 233-239.

42. Shim, S., L. A. Kimpler, and P. I. Hanson. 2007. Structure/function analysis of four core ESCRT-III proteins reveals common regulatory role for extreme C-terminal domain. *Traffic* 8: 1068-1079.

43. Guduric-Fuchs, J., A. O'Connor, B. Camp, C. L. O'Neill, R. J. Medina, and D. A. Simpson. 2012. Selective extracellular vesicle-mediated export of an overlapping set of microRNAs from multiple cell types. *BMC Genomics* 13: 357.

44. Li, M., X. Guan, Y. Sun, J. Mi, X. Shu, F. Liu, and C. Li. 2014. miR-92a family and their target genes in tumorigenesis and metastasis. *Exp Cell Res* 323: 1-6.

45. Zhang, J., S. Li, L. Li, M. Li, C. Guo, J. Yao, and S. Mi. 2015. Exosome and exosomal microRNA: trafficking, sorting, and function. *Genomics Proteomics Bioinformatics* 13: 17-24.

46. Higginbotham, J. N., M. Demory Beckler, J. D. Gephart, J. L. Franklin, G. Bogatcheva, G. J. Kremers, D. W. Piston, G. D. Ayers, R. E. McConnell, M. J. Tyska, and R. J. Coffey. 2011. Amphiregulin exosomes increase cancer cell invasion. *Curr Biol* 21: 779-786.

47. Tan, S. S., Y. Yin, T. Lee, R. C. Lai, R. W. Yeo, B. Zhang, A. Choo, and S. K. Lim. 2013. Therapeutic MSC exosomes are derived from lipid raft microdomains in the plasma membrane. *J Extracell Vesicles* 2: 10.3402/jev.v2i0.22614

48. Aatonen, M. T., T. Ohman, T. A. Nyman, S. Laitinen, M. Gronholm, and P. R. Siljander. 2014. Isolation and characterization of platelet-derived extracellular vesicles. *J Extracell Vesicles* 3: 10.3402/jev.v3.24692

49. Soo, C. Y., Y. Song, Y. Zheng, E. C. Campbell, A. C. Riches, F. Gunn-Moore, and S. J. Powis. 2012. Nanoparticle tracking analysis monitors microvesicle and exosome secretion from immune cells. *Immunology* 136: 192-197.

50. Lopatina, T., S. Bruno, C. Tetta, N. Kalinina, M. Porta, and G. Camussi. 2014. Platelet-derived growth factor regulates the secretion of extracellular vesicles by adipose mesenchymal stem cells and enhances their angiogenic potential. *Cell Commun Signal* 12: 26.

51. Hoshino, D., K. C. Kirkbride, K. Costello, E. S. Clark, S. Sinha, N. Grega-Larson, M. J. Tyska, and A. M. Weaver. 2013. Exosome secretion is enhanced by invadopodia and drives invasive behavior. *Cell Rep* 5: 1159-1168.

52. Li, B., M. A. Antonyak, J. Zhang, and R. A. Cerione. 2012. RhoA triggers a specific signaling pathway that generates transforming microvesicles in cancer cells. *Oncogene* 31: 4740-4749.

53. Muralidharan-Chari, V., J. Clancy, C. Plou, M. Romao, P. Chavrier, G. Raposo, and C. D'Souza-Schorey. 2009. ARF6-regulated shedding of tumor cell-derived plasma membrane microvesicles. *Curr Biol* 19: 1875-1885.

54. Abache, T., F. Le Naour, S. Planchon, F. Harper, C. Boucheix, and E. Rubinstein. 2007. The transferrin receptor and the tetraspanin web molecules CD9, CD81, and CD9P-1 are differentially sorted into exosomes after TPA treatment of K562 cells. *J Cell Biochem* 102: 650-664.

55. Savina, A., M. Furlan, M. Vidal, and M. I. Colombo. 2003. Exosome release is regulated by a calcium-dependent mechanism in K562 cells. *J Biol Chem* 278: 20083-20090.

56. Akhmanova, A., and J. A. r. Hammer. 2010. Linking molecular motors to membrane cargo. *Curr Opin Cell Biol* 22: 479-487.

57. Rous, B. A., B. J. Reaves, G. Ihrke, J. A. G. Briggs, S. R. Gray, D. J. Stephens, G. Banting, and J. P. Luzio. 2002. Role of adaptor complex AP-3 in targeting wild-type and mutated CD63 to lysosomes. *Molecular biology of the cell* 13: 1071-1082.

58. Flannery, A. R., C. Czibener, and N. W. Andrews. 2010. Palmitoylation-dependent association with CD63 targets the Ca2+ sensor synaptotagmin VII to lysosomes. *J Cell Biol* 191: 599-613.

59. Teis, D., S. Saksena, and S. D. Emr. 2008. Ordered assembly of the ESCRT-III complex on endosomes is required to sequester cargo during MVB formation. *Dev Cell* 15: 578-589.

60. Elia, N., R. Sougrat, T. A. Spurlin, J. H. Hurley, and J. Lippincott-Schwartz. 2011. Dynamics of endosomal sorting complex required for transport (ESCRT) machinery during cytokinesis and its role in abscission. *Proc Natl Acad Sci U S A* 108: 4846-4851.

61. Cashikar, A. G., S. Shim, R. Roth, M. R. Maldazys, J. E. Heuser, and P. I. Hanson. 2014. Structure of cellular ESCRT-III spirals and their relationship to HIV budding. *Elife* 3: 10.7554/eLife.02184

62. Trajkovic, K., C. Hsu, S. Chiantia, L. Rajendran, D. Wenzel, F. Wieland, P. Schwille, B. Brugger, and M. Simons. 2008. Ceramide triggers budding of exosome vesicles into multivesicular endosomes. *Science* 319: 1244-1247.

63. Choudhuri, K., J. Llodra, E. W. Roth, J. Tsai, S. Gordo, K. W. Wucherpfennig, L. C. Kam, D. L. Stokes, and M. L. Dustin. 2014. Polarized release of T-cell-receptor-enriched microvesicles at the immunological synapse. *Nature* 507: 118-123.

64. Nabhan, J. F., R. Hu, R. S. Oh, S. N. Cohen, and Q. Lu. 2012. Formation and release of arrestin domain-containing protein 1-mediated microvesicles (ARMMs) at plasma membrane by recruitment of TSG101 protein. *Proc Natl Acad Sci U S A* 109: 4146-4151.

65. Matusek, T., F. Wendler, S. Poles, S. Pizette, G. D'Angelo, M. Furthauer, and P. P. Therond. 2014. The ESCRT machinery regulates the secretion and long-range activity of Hedgehog. *Nature* 516: 99-103.

66. Hanson, P. I., R. Roth, Y. Lin, and J. E. Heuser. 2008. Plasma membrane deformation by circular arrays of ESCRT-III protein filaments. *J Cell Biol* 180: 389-402.

67. Hierro, A., A. L. Rojas, R. Rojas, N. Murthy, G. Effantin, A. V. Kajava, A. C. Steven, J. S. Bonifacino, and J. H. Hurley. 2007. Functional architecture of the retromer cargo-recognition complex. *Nature* 449: 1063-1067.

68. Hanson, P. I., and A. Cashikar. 2012. Multivesicular body morphogenesis. *Annu Rev Cell Dev Biol* 28: 337-362.

69. Ostrowski, M., N. B. Carmo, S. Krumeich, I. Fanget, G. Raposo, A. Savina, C. F. Moita, K. Schauer, A. N. Hume, R. P. Freitas, B. Goud, P. Benaroch, N. Hacohen, M. Fukuda, C. Desnos, M. C. Seabra, F. Darchen, S. Amigorena, L. F. Moita, and C. Thery. 2010. Rab27a and Rab27b control different steps of the exosome secretion pathway. *Nat Cell Biol* 12: 19-30; sup pp 1-13.

70. Roucourt, B., S. Meeussen, J. Bao, P. Zimmermann, and G. David. 2015. Heparanase activates the syndecan-syntenin-ALIX exosome pathway. *Cell Res* 25: 412-428.

71. Son, K. J., A. Rahimian, D. S. Shin, C. Siltanen, T. Patel, and A. Revzin. 2015. Microfluidic compartments with sensing microbeads for dynamic monitoring of cytokine and exosome release from single cells. *Analyst* 141: 679-688.

72. Alvarez, M. L., M. Khosroheidari, R. Kanchi Ravi, and J. K. DiStefano. 2012. Comparison of protein, microRNA, and mRNA yields using different methods of urinary exosome isolation for the discovery of kidney disease biomarkers. *Kidney Int* 82: 1024-1032.

73. Shin, H., C. Han, J. M. Labuz, J. Kim, J. Kim, S. Cho, Y. S. Gho, S. Takayama, and J. Park. 2015. High-yield isolation of extracellular vesicles using aqueous two-phase system. *Sci Rep* 5: 13103.

Chapter 2 Figures

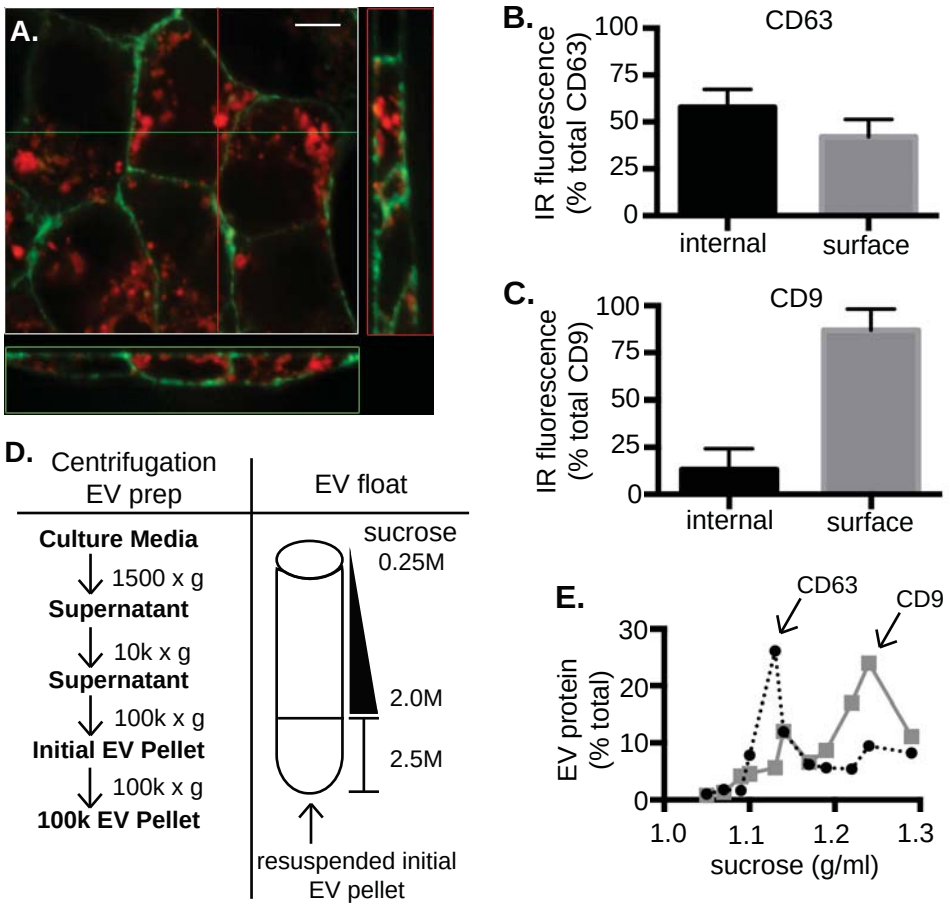

FIGURE 2-1. CD63 and CD9 are released on distinct EVs. *A*, Confocal z-stacks in orthogonal view of HEK293 cells stably transfected with constructs expressing GFP-CD9 and mCherry-CD63. Scale bar = 10µm. *B, C* Untransfected HEK293 cells were immunolabeled for endogenous CD63 (B) or CD9 (C) in the absence or presence of detergent to measure surface and total protein, respectively. Fluorescence inside the cell or at the cell surface is shown as percent of total fluorescence. The values are mean and standard deviation of three independent experiments. *D*, Flow chart of EV isolation and sucrose flotation procedures. *E*, 100k EVs from HEK293 cells were floated in linear sucrose gradients. The x-axis indicates the density of each fraction as determined by refractometry. Fractions were immunoblotted for CD63 (black line) and CD9 (gray line), quantitated and the values plotted as percent of total signal from all fractions combined. Data show a representative experiment out of four biological replicates.

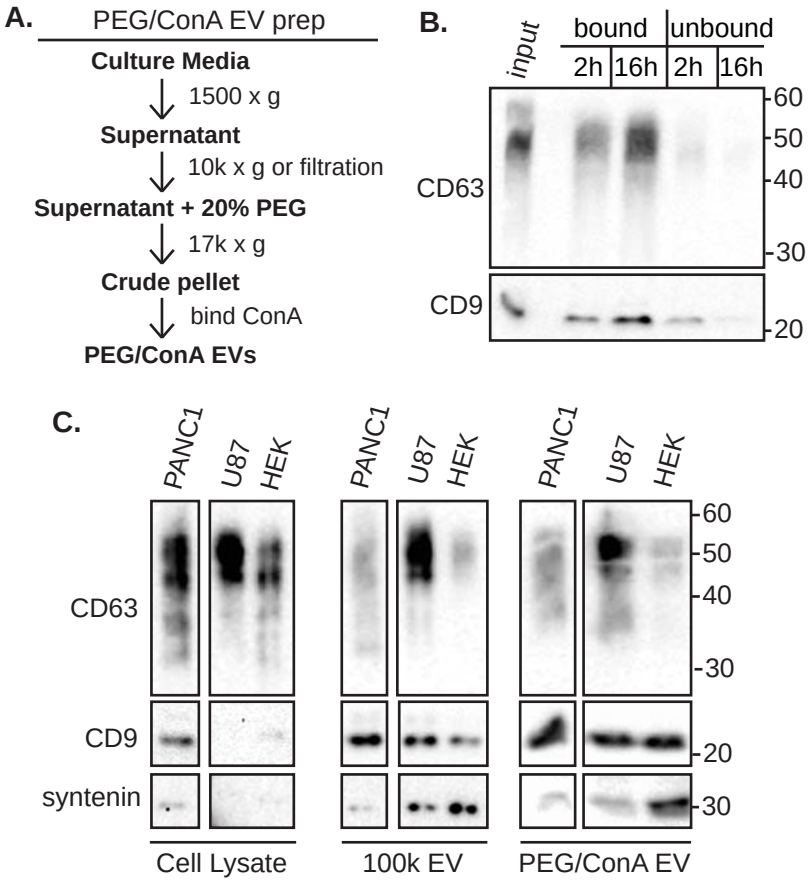

FIGURE 2-2. Comparison of PEG/ConA and ultracentrifugation EV collection methods. *A,* Flow chart of PEG/ConA EV collection procedure. *B*, EVs released from HEK293 cells over 24hr were precipitated with PEG and bound to ConA sepharose for 2hr or overnight. EV protein was released from the beads by boiling in SDS-PAGE loading buffer. *C*, EVs released by the indicated cell lines over 24hr were harvested from culture media by PEG/ConA (PEG/ConA EV) using 1/5th of the total culture supernatant or by ultracentrifugation (100k EV) using the remaining culture supernatant. EVs released by 10% of the total cell culture were separated by SDS-PAGE then immunoblotted for CD63, CD9 and syntenin. Cell lysates were prepared by solubilizing in 1% Triton X-100, and 10µg of whole cell protein from each cell type was loaded. All lanes of an indicated protein are from the same gel. Gel slicing removed an irrelevant lane.

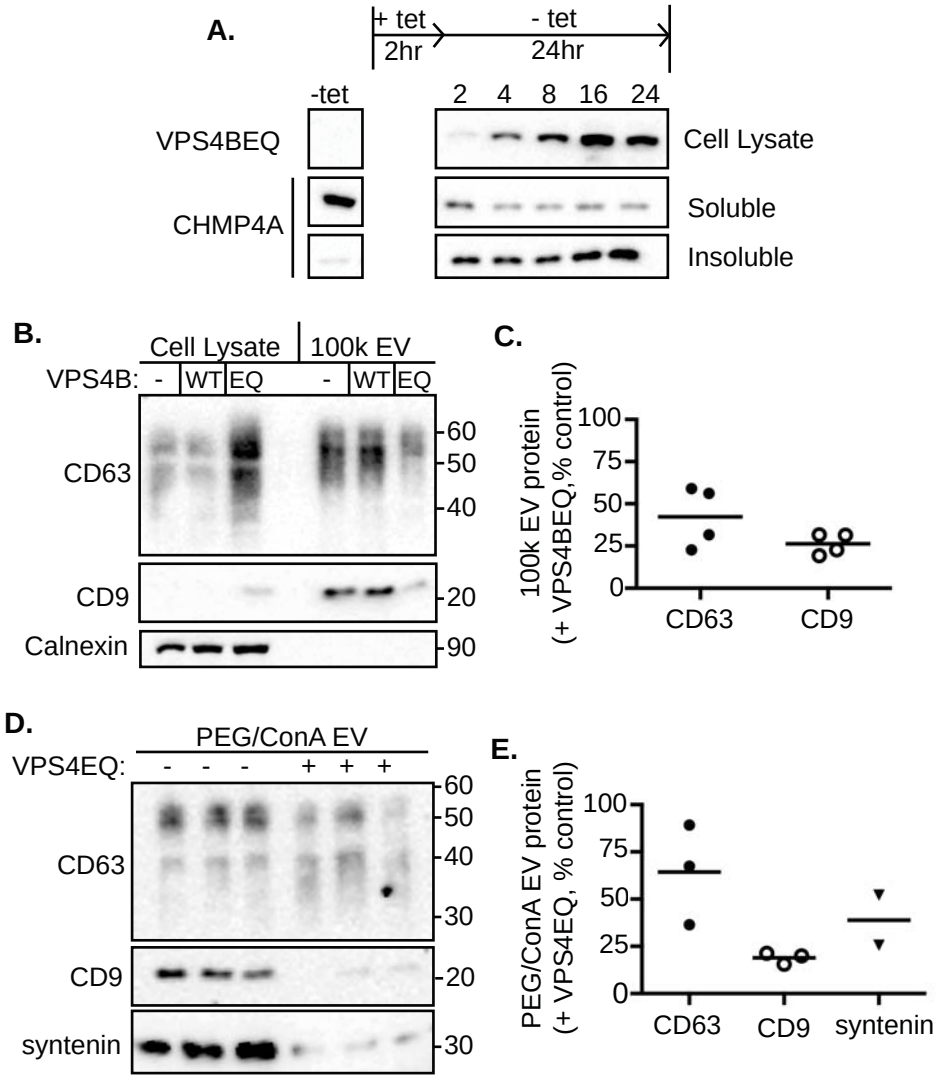

Figure 2-3. CD63 and CD9 EVs depend on VPS4. *A*, Immunoblot of whole cell protein (top panel) at the indicated time points after induction of GFP-VPS4EQ with 0.5µg/ml tetracycline for 2 hr. Middle and bottom panels, immunoblot of soluble supernatants and insoluble pellets separated by centrifugation at 17,000 × g. Pellets were resuspended in the same volume as supernatants, and equal volumes of each were loaded. *B*, Total cellular protein from 0.05 × 106 cells (Cell Lysate) and 100k EVs from 10 × 106 cells (100k EV) were immunoblotted for CD63 and CD9. *C*, Immunoblot quantitation: line indicates the average of four independent experiments and values are displayed as percent of no VPS4 overexpression. *D*, EVs from VPS4EQ-expressing HEK293 cells were collected by PEG/ConA then immunoblotted for CD63, CD9 and syntenin. Each lane in the experiment shown represents a technical replicate prepared from 1/3rd of the total culture supernatant. *E*, Immunoblot quantitation: line indicates the average of three independent experiments, and values are displayed as percent of no VPS4EQ expression. For experiments with technical replicates the average of the three replicates was treated as a single independent experiment.

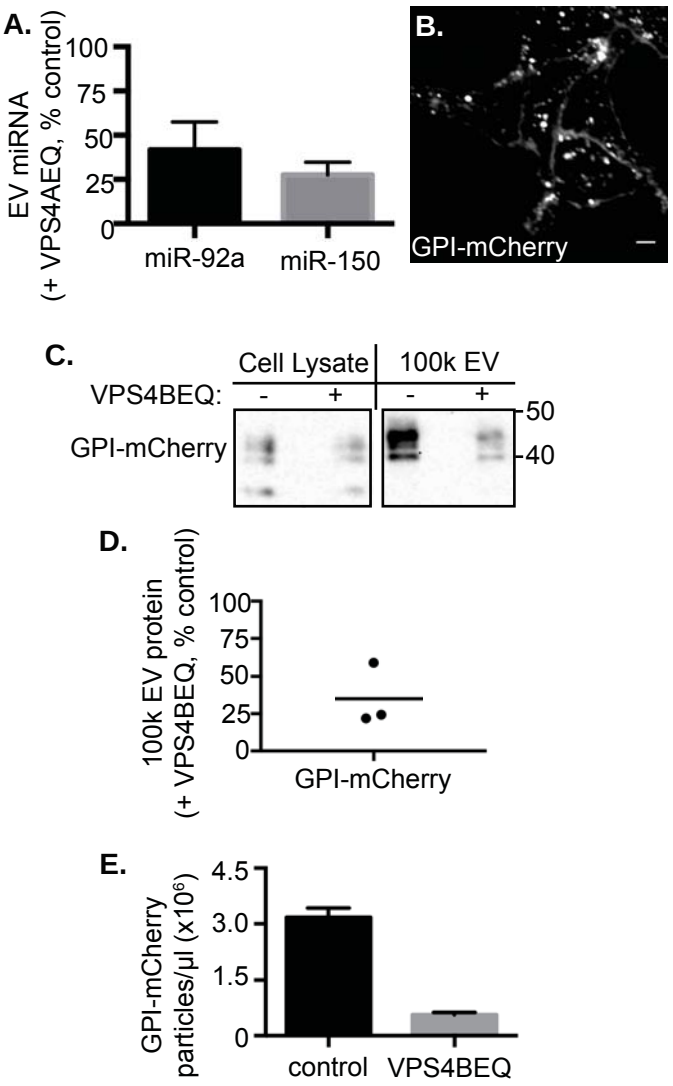

FIGURE 2-4. VPS4-dependent release of miRNAs and membrane vesicles. *A*, qRT-PCR analysis of 100k EVs from cells expressing VPS4EQ. Values were normalized to spike-in cel-miR39 RNA and are presented as the percent of no VPS4EQ expression. *B*, Single confocal section of HEK293 cells stably expressing GPI-mCherry (scale bar = 10µm). *C*, Immunoblot of whole cell protein (Cell Lysate) and 100k EVs from HEK293 cells expressing GPI-mCherry. *D*, mCherry immunoblot quantitation of 100k EVs is shown as percent of no VPS4EQ expression. *E*, GPI-mCherry particle counts. Values are average particle counts from 5 images. Error bars indicate standard deviation. Data show one of two biological replicates.

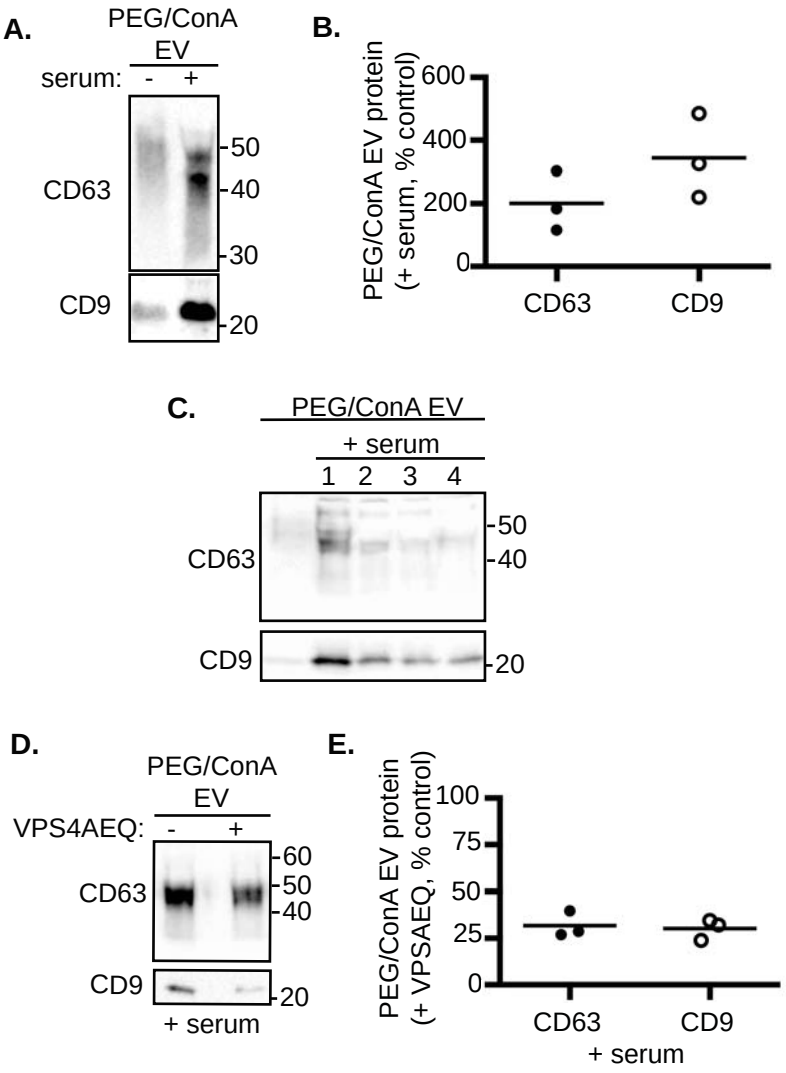

FIGURE 2-5. Characteristics of serum-triggered EV release. *A,B,* HEK293 cells were grown for 16 hr without serum then culture medium was replaced with fresh serum-free medium (-) or medium containing 10% serum (+) for 4 hr. EVs harvested by PEG/ConA were immunoblotted for CD63 and CD9 (A) with immunoblot quantitation (B): line indicates the average of three experiments, and values are displayed as the percent of no serum. *C*, HEK293 cells were grown 16 hr without serum before incubating in fresh serum-free medium for 1 hr. The medium was then collected and cells were incubated with fresh medium containing 10% serum every hr for 4 hr. EVs were harvested by PEG/ConA and immunoblotted for CD63 and CD9. *D, E,* Serum-triggered EVs from control and VPS4EQ-expressing cells were harvested by PEG/ConA and immunobloted for CD63 and CD9 (D) with immunoblot quantitation (E): line indicates the average of three experiments, and values are displayed as the percent of no VPS4EQ expression.

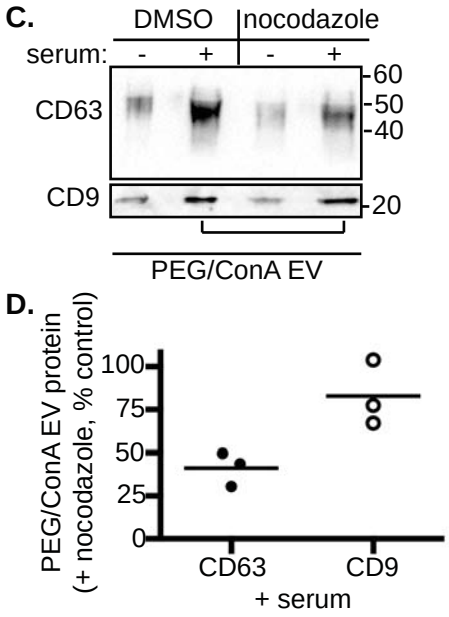

FIGURE 2-6. CD63 EV release depends on polymerized microtubules. *A, B,* HEK293 cells were treated with 12μM nocodazole or DMSO and immunostained for α-tubulin. *C, D,* Serum-triggered EVs released from nocodazole or DMSO-treated cells were harvested by PEG/ConA and immunoblotted for CD63 and CD9 (C) with immunoblot quantitation (D): line indicates the average of three experiments, and values are displayed as the percent of DMSO treatment.

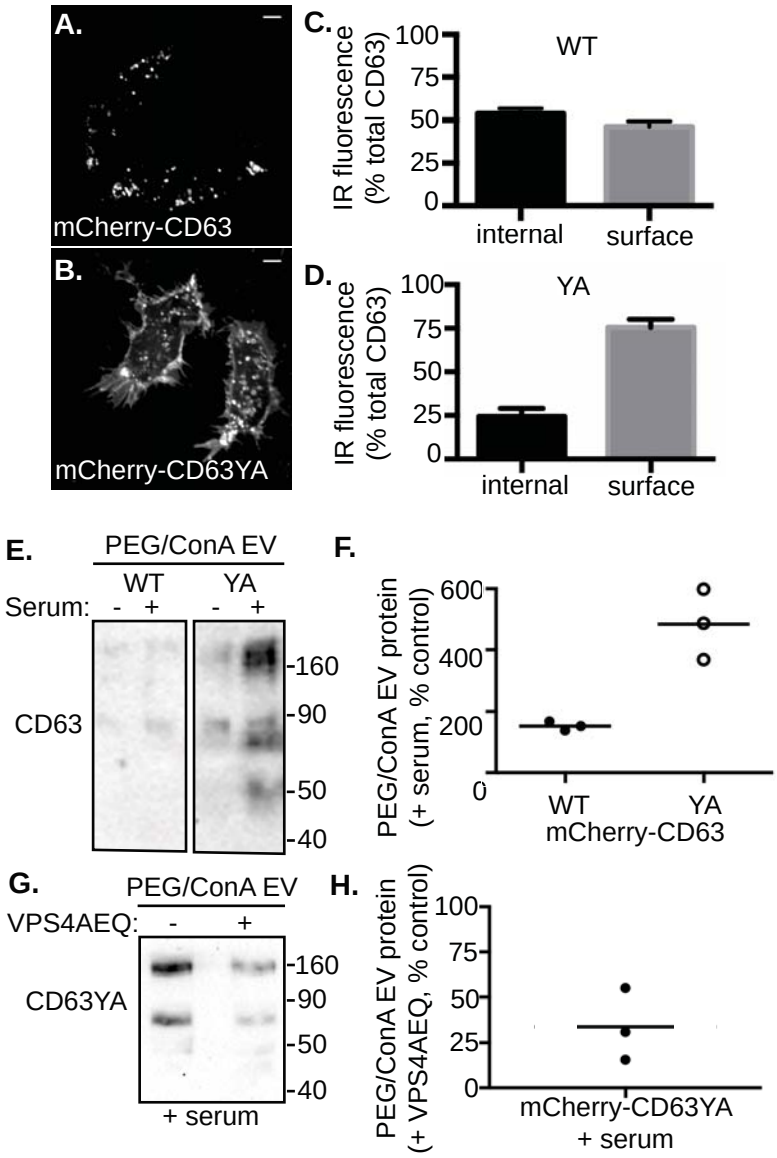

FIGURE 2-7. Serum-triggered release of surface-localized CD63. *A, B,* Confocal sections of HEK293 cells stably expressing mCherry-CD63 (A) or mCherry-CD63YA (B) (scale bar = 10µm). *C, D,* Cells stably expressing CD63 (C) or CD63YA (D) were immunolabeled against CD63 in the absence or presence of detergent to measure surface and total protein, respectively. Fluorescence at internal or surface localizations is shown as percent of total fluorescence. The values are mean and standard deviation of three independent experiments. *E, F,* anti-mCherry immunoblot of serum-triggered EVs released from HEK293 cells stably expressing wild-type CD63 or CD63YA (E) with immunoblot quantitation (F): line indicates the average of three experiments, and values are displayed as the percent of no serum. *G, H,* anti-mCherry immunoblot of serum-triggered EVs released from control and VPS4EQ-expressing cells (G) with immunoblot quantitation (H): line indicates the average of three experiments, and values are displayed as the percent of no VPS4EQ expression.

Chapter 3

Rab27b is a selective and pH sensitive marker of exocytic MVBs

Abstract

With specific regard to exosome release, an important question is what distinguishes MVBs destined for exocytosis from those destined for degradation. Currently, the best-characterized factors involved in the trafficking and release of exocytic MVBs are Rab27a and Rab27b. In this chapter, I identify Rab27b as a factor likely to distinguish exocytic from non-exocytic MVBs in U87 glioblastoma cells. Rab27b localizes to a subset of CD63 containing late endosomes or MVBs. I find that these MVBs are less acidic than CD63 containing MVBs that lack Rab27b. Furthermore, endosome pH appears to play a direct role in recruiting Rab27b since chloroquine neutralization strikingly increases Rab27b on endosomes. These findings have exciting implications for understanding how MVB identity and exocytosis is regulated.

Introduction

Aside from delivery to lysosomes, MVBs can also fuse with the plasma membrane to release their contents from the cell. MVBs thus have two potential fates: degradation or secretion. While degradation predominates in most situations, it is not known what controls the fate of individual MVBs. Furthermore, MVB fate may change in response to cellular or environmental cues. There are indications that heterogeneity among MVBs may correlate with their eventual fate; for example, lysobisphosphatidic acid (LBPA) is concentrated in ILVs

targeted for degradation (1) but is largely absent from exosomes (2, 3). Regulated recruitment of appropriate Rab GTPases is likely to play a key role in this decision, with recruitment of exocytosis-enabling Rab GTPases such as Rab27a (4), Rab35 (5), or Rab11 (6) shown to correlate with secretion. An important and unresolved question is how MVBs destined to undergo exocytosis differ from those that feed into the degradative pathway.

Among the Rab proteins implicated in MVB exocytosis, Rab27a and Rab27b are the best studied based on their involvement in exosome release from several cell types using numerous cargos. Rab proteins are recruited to specific cellular compartments by GEF proteins, act in their GTP-bound form to recruit effector proteins, and are inactivated or released by action of GAP proteins. One GEF and two GAPs have been identified for Rab27, and neither is specific to Rab27 alone. MADD/DENN/Rab3GEP functions as a GEF for both Rab27 and Rab3, and its activity toward Rab27 may be important for secretion of melanosomes and platelet dense granules (7, 8). TBC1D10A and TBC1D10B were identified as Rab27 GAPs *in vitro*, and are implicated in Rab27 inactivation in pancreatic acinar cells and melanocytes (9). Rab27 effectors fall into one of three categories based on their structural composition. Synaptotagmin-like proteins (Slps) are characterized by an N-terminal Rab27-binding Slp-homology domain (SHD) and C-terminal C2 domains that bind phospholipids. Slac2 proteins comprise the second group and posses a SHD but lack C2 domains. Slac2a and Slac2b possess regions that bind to myosins and actin. Munc13-4 is the sole member of the third category and possesses two C2 domains that flank the Munc domain and a unique Rab27 binding region. The Rab27 effectors are thought to function separately or in concert to regulate secretory vesicle transport, docking, and tethering to the plasma membrane. The precise coordination of this network and the specific members involved are likely to differ among cell types and secretory vesicles (10).

Despite varied tissue expression and, in some cases, apparently overlapping functions with other Rabs (e.g. Rab3) (11), Rab27 is clearly a factor recruited to different types of organelles that share a common secretory fate. In the following chapter, we show that Rab27b is expressed in a restricted subset of cell types. The glioblastoma U87 cell line contained distinct Rab27b marked organelles that corresponded to a subset of CD63 containing endosomes. Interestingly, we find that Rab27b preferentially localized to a subset of less acidic (Lysotracker negative) CD63 containing organelles. Furthermore, neutralizing endosomal pH by incubation with chloroquine increased recruitment of Rab27b to CD63 containing endosomes and enhanced CD63 release from the cell. These findings reveal unique features of secretory MVBs.

Methods

Antibodies, Plasmids and reagents—Antibodies used include a mouse monoclonal antibody against CD63 (Dev Biostudies H5C6), a polyclonal antibody against Rab27b (Synaptic Systems 168103), a monoclonal antibody against EEA1 (BD Biosciences 610456), a monoclonal antibody against LBPA (Echelon Biosciences 6C4), Secondary antibodies were conjugated to Alexa Fluor 488, Alexa Fluor 555 or Alexa Fluor 647 for immunofluorescence (ThermoFisher).

U87 cells were from Joshua Rubin (Washington University School of Medicine). MCF-7 cells were from Jason Weber (Washington University School of Medicine). Both cell lines were maintained in Dulbecco's modified Eagle's medium supplemented with 10% fetal bovine serum and 1mM L-Glutamine. Lyso Tracker Red was from Invitrogen (L7528). Chloroquine was from Sigma-Aldrich (St. Louis, MO), and 50mM (100×) stock solution was made in PBS.

Immunofluorescence—Cells on #1.5 glass were fixed in 2% paraformaldehyde in PBS, permeabilized with 0.1% saponin, and blocked and stained with antibodies diluted in PBS containing 5% goat serum and 0.01% saponin..

Microscopy—Widefield imaging was performed with an Olympus IX81 microscope equipped with a 60×/1.42 NA oil objective and a Hamamatsu Flash 2.8 camera. Confocal imaging was performed with a Nikon A-1 laser-scanning microscope equipped with a 100x/1.3 NA oil objective.

Results and Discussion

Identification of cell lines expressing Rab27b—Given the previously reported roles of Rab27a and Rab27b proteins in exosome release and the known role of Rab27a in promoting exocytosis of lysosome related organelles in pigment containing cells, we wondered whether these proteins might selectively identify MVBs destined for exocytosis. We focused our analysis on Rab27b because of the availability of a rabbit polyclonal antibody (purchased from SySy) that clearly and robustly recognizes endogenous Rab27b by immunofluorescence. We first assessed specific immunostaining in three cell lines that we previously characterized for their ability to release exosomes. Of these, two cell lines displayed distinct patterns of Rab27b staining – the breast adenocarcinoma MCF-7 and glioblastoma U87 (Figure 3-1). The osteoscarcoma-derived U2OS cell line did not display specific Rab27b immunostaining, which was expected based on previous proteomics studies in these cells (12) (data not shown).

MCF-7 and U87 cells exhibited different distribution of Rab27b which are likely attributable to the cells' specific phenotypic identity. In epithelial MCF-7 cells, Rab27b staining was most evident at the cell periphery that is not in contact with an adjacent cell (Figure 3-1, A).

In order to further define the identity of the Rab27b positive compartments, I costained MCF-7 cells for Rab27b and the late endosome/lysosome/exosome marker CD63. While the majority of CD63 is present on compartments distributed throughout the cytoplasm, a distinct subset of CD63 immunostaining overlapped with Rab27b (Figure 3-1, A). This suggests that the compartments marked by Rab27b in these cells are endosomal in nature and may represent MVBs that give rise to exosomes. The somewhat polarized distribution of Rab27b in MCF-7 cells is strikingly reminiscent of that observed in acinar lacrimal gland epithelia where it localizes to apical secretory vesicles (13). MCF-7 cells form multicellular polarized spheroids with a central lumen when grown in 3D matrix (14). In the future, MCF-7 could provide a system in which to study polarized exosome secretion.

In mesenchymal U87 cells we saw clearly distinct Rab27b positive organelles localized throughout the cell (Figure 3-1B). Intriguingly, all Rab27b marked organelles also contained CD63, while only a subset of CD63 marked organelles were positive for Rab27b (Figure 3-2, A). The consistent presence of CD63 indicated that Rab27b marked compartments were likely to represent MVBs. I further characterized the Rab27b marked organelles by immunostaining for markers of other endocytic organelles. EEA1 is a marker for early endosomes, and showed no overlap with Rab27b indicating that Rab27b does not recruit to early endosomes in these cells (Figure 3-2, B). LBPA is another marker of MVBs, but we found no overlap between LBPA and Rab27b (Figure 3-2, C). This observation is consistent with previous reports that LBPA is present on a subpopulation of MVBs targeted for degradation and is absent from exosomes (3, 15). These observations demonstrate that Rab27b marks a distinct set of organelles that these organelles may correspond to the elusive secretory MVB.

Changes in organelle pH enhance Rab27b recruitment—We wondered what might be different between CD63 labeled MVBs that are Rab27b positive versus those that are not. Given that the contents of secretory MVBs (i.e. exosomes) are not degraded, we hypothesized that pH could be a distinguishing factor. To test this question, we treated cells with Lysotracker Red, which specifically labels acidic organelles, followed by aldehyde fixation and immunostaining for Rab27b and CD63. We found that Lysotracker labeled a significant proportion of CD63 positive organelles. However, those marked by both CD63 and Rab27b did not contain Lysotracker, suggesting that Rab27b localized to non-acidic endosomes (Figure3-3). This observation led us to hypothesize that pH is a factor contributing to Rab27b recruitment. To test this idea we treated cells with the weak base chloroquine to neutralize acidic organelles and then immunostained for CD63 and Rab27b. We observed a remarkable increase in the number and size of Rab27b/CD63 positive vesicles (Figure3-4, A and B). These observations support the notion that endosomal pH contributes to regulation of Rab27b recruitment.

Enhanced Rab27b recruitment in response to increased endosomal pH has several exciting implications. First, this finding suggests that secretory MVBs in U87 cells are less acidic than those MVBs likely directed for degradation. Second, it indicates plasticity in MVB fate. Endosome neutralization perturbs degradation in lysosomes where activity of resident proteases requires low pH. Rab27b recruitment to facilitate exocytosis could be a compensatory mechanism to prevent accumulation of normally degraded material. Our results are in agreement with other studies that show upregulated exosome secretion in response to lysosome inhibitors such as bafilomycin (16). One complication in interpreting the lysotracker staining is the questionable maintenance of formaldehyde fixed lysotracker after cell permeabilization. However, the fact that Rab27b did not mark observable lysotracker positive organelles taken

with increased Rab27b recruitment/number of organelles strongly suggests that non-acidic pH is a characteristic of exocytic MVBs that could be important in regulating Rab27b recruitment.

How the cell senses endosome neutralization is an important question. To this end, a transient receptor potential (TRP) calcium channel on the lysosomal membrane was identified as a key factor in regulating secretion after lysosome neutralization by uropathogenic *E. coli* (17). Notably, Rab27 marks these secretory compartments, and the calcium sensor synaptotagmin VII is involved. Thus, it is possible that pH neutralization triggers lysosomal calcium efflux to promote exocytosis.

As discussed above, Rab recruitment to membranes is regulated by the coordinated action of GEFs and GAPs. Furthermore, Rab27 GTP cycling is important for diverse secretory processes (8, 13, 18, 19). Rab GDP dissociation inhibitor (GDI) also controls Rabs, including Rab27b, by binding the Rab in its GDP locked conformation to block nucleotide exchange (20). Each of these regulatory components is an obvious candidate for further investigation into how organelle pH signals Rab27b recruitment.

In conclusion, MVBs have long been thought of as intermediate organelles en route to lysosomal degradation. Current research has unveiled the complex nature and diverse fates of the MVB. Here we extend on these concepts by showing that a subset of MVBs in the U87 cell line may be marked for exocytosis by recruitment of Rab27b. Our discovery that Rab27b preferentially localizes to Lysotracker negative CD63 containing organelles and that neutralizing pH dramatically increases the overall level of Rab27b recruitment raises the intriguing question of which regulatory components are responsive to organelle pH. Future studies should be aimed

at discerning the regulation of Rab27b recruitment by GEFs, GAPs and GDI in response to changes in endosomal pH.

References

1. Matsuo, H., J. Chevallier, N. Mayran, I. Le Blanc, C. Ferguson, J. Faure, N. Sartori Blanc, S. Matile, J. Dubochet, R. Sadoul, R. G. Parton, F. Vilbois, and J. Gruenberg. 2004. Role of LBPA and Alix in multivesicular liposome formation and endosome organization. *Science* 303: 531-534.

2. Kowal, J., M. Tkach, and C. Thery. 2014. Biogenesis and secretion of exosomes. *Curr Opin Cell Biol* 29C: 116-125.

3. Trajkovic, K., C. Hsu, S. Chiantia, L. Rajendran, D. Wenzel, F. Wieland, P. Schwille, B. Brugger, and M. Simons. 2008. Ceramide triggers budding of exosome vesicles into multivesicular endosomes. *Science* 319: 1244-1247.

4. Ostrowski, M., N. B. Carmo, S. Krumeich, I. Fanget, G. Raposo, A. Savina, C. F. Moita, K. Schauer, A. N. Hume, R. P. Freitas, B. Goud, P. Benaroch, N. Hacohen, M. Fukuda, C. Desnos, M. C. Seabra, F. Darchen, S. Amigorena, L. F. Moita, and C. Thery. 2010. Rab27a and Rab27b control different steps of the exosome secretion pathway. *Nat Cell Biol* 12: 19-30; sup pp 1-13.

5. Hsu, C., Y. Morohashi, S. Yoshimura, N. Manrique-Hoyos, S. Jung, M. A. Lauterbach, M. Bakhti, M. Gronborg, W. Mobius, J. Rhee, F. A. Barr, and M. Simons. 2010. Regulation of exosome secretion by Rab35 and its GTPase-activating proteins TBC1D10A-C. *J Cell Biol* 189: 223-232.

6. Savina, A., M. Vidal, and M. I. Colombo. 2002. The exosome pathway in K562 cells is regulated by Rab11. *J Cell Sci* 115: 2505-2515.

7. Figueiredo, A. C., C. Wasmeier, A. K. Tarafder, J. S. Ramalho, R. A. Baron, and M. C. Seabra. 2008. Rab3GEP is the non-redundant guanine nucleotide exchange factor for Rab27a in melanocytes. *J Biol Chem* 283: 23209-23216.

8. Kondo, H., R. Shirakawa, T. Higashi, M. Kawato, M. Fukuda, T. Kita, and H. Horiuchi. 2006. Constitutive GDP/GTP exchange and secretion-dependent GTP hydrolysis activity for Rab27 in platelets. *J Biol Chem* 281: 28657-28665.

9. Itoh, T., and M. Fukuda. 2006. Identification of EPI64 as a GTPase-activating protein specific for Rab27A. *J Biol Chem* 281: 31823-31831.

10. Fukuda, M. 2013. Rab27 effectors, pleiotropic regulators in secretory pathways. *Traffic* 14: 949-963.

11. Pavlos, N. J., and R. Jahn. 2011. Distinct yet overlapping roles of Rab GTPases on synaptic vesicles. *Small GTPases* 2: 77-81.

12. Beck, M., A. Schmidt, J. Malmstroem, M. Claassen, A. Ori, A. Szymborska, F. Herzog, O. Rinner, J. Ellenberg, and R. Aebersold. 2011. The quantitative proteome of a human cell line. *Mol Syst Biol* 7: 549.

13. Chiang, L., J. Ngo, J. E. Schechter, S. Karvar, T. Tolmachova, M. C. Seabra, A. N. Hume, and S. F. Hamm-Alvarez. 2011. Rab27b regulates exocytosis of secretory vesicles in acinar epithelial cells from the lacrimal gland. *Am J Physiol Cell Physiol* 301: C507-21.

14. do Amaral, J. B., P. Rezende-Teixeira, V. M. Freitas, and G. M. Machado-Santelli. 2011. MCF-7 cells as a three-dimensional model for the study of human breast cancer. *Tissue Eng Part C Methods* 17: 1097-1107.

15. Tomas, A., S. O. Vaughan, T. Burgoyne, A. Sorkin, J. A. Hartley, D. Hochhauser, and C. E. Futter. 2015. WASH and Tsg101/ALIX-dependent diversion of stress-internalized EGFR from the canonical endocytic pathway. *Nat Commun* 6: 7324.

16. Savina, A., M. Furlan, M. Vidal, and M. I. Colombo. 2003. Exosome release is regulated by a calcium-dependent mechanism in K562 cells. *J Biol Chem* 278: 20083-20090.

17. Miao, Y., G. Li, X. Zhang, H. Xu, and S. N. Abraham. 2015. A TRP Channel Senses Lysosome Neutralization by Pathogens to Trigger Their Expulsion. *Cell* 161: 1306-1319.

18. Hou, Y., X. Chen, T. Tolmachova, S. A. Ernst, and J. A. Williams. 2013. EPI64B acts as a GTPase-activating protein for Rab27B in pancreatic acinar cells. *J Biol Chem* 288: 19548-19557.

19. Tarafder, A. K., C. Wasmeier, A. C. Figueiredo, A. E. Booth, A. Orihara, J. S. Ramalho, A. N. Hume, and M. C. Seabra. 2011. Rab27a targeting to melanosomes requires nucleotide exchange but not effector binding. *Traffic* 12: 1056-1066.

20. Imai, A., S. Yoshie, T. Nashida, M. Fukuda, and H. Shimomura. 2009. Redistribution of small GTP-binding protein, Rab27B, in rat parotid acinar cells after stimulation with isoproterenol. *Eur J Oral Sci* 117: 224-230.

Chapter 3 Figures

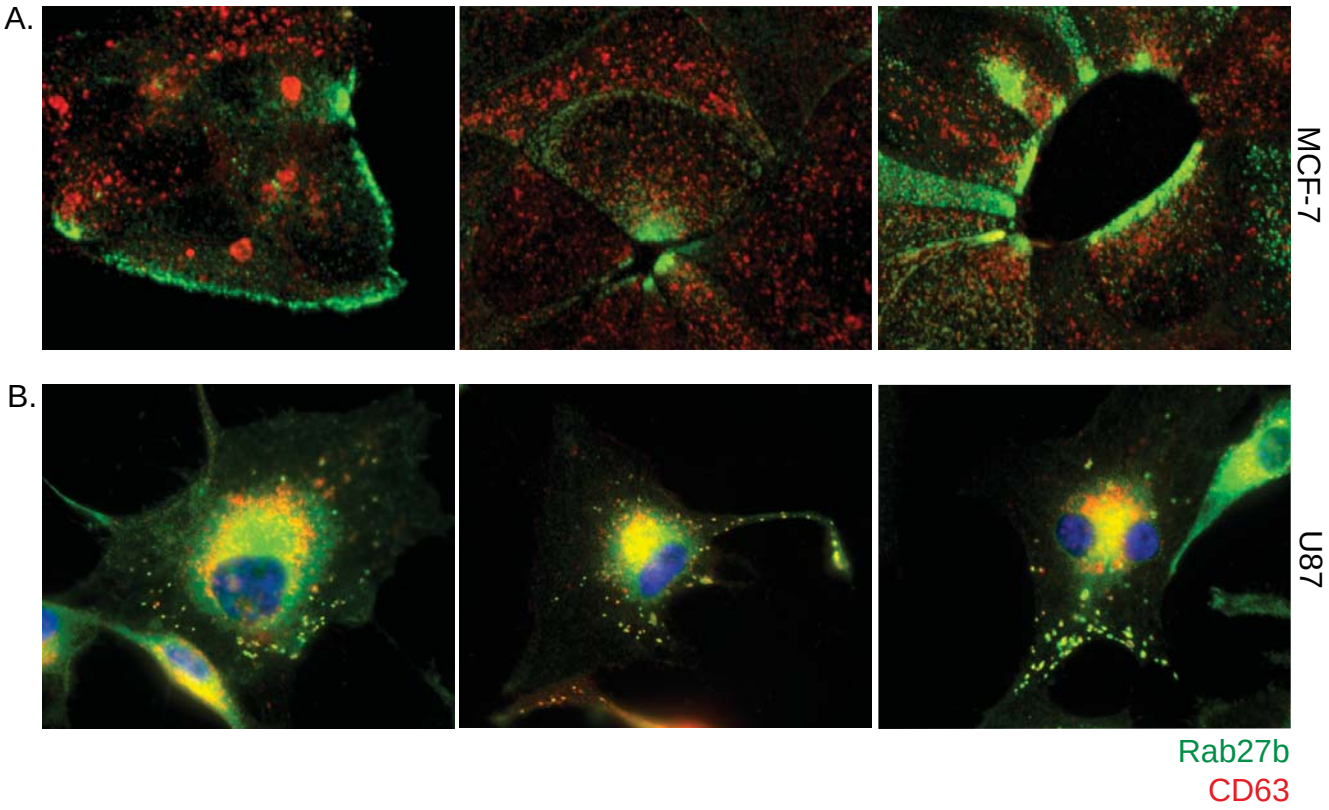

FIGURE 3-1. Rab27b localizes to endosomes in different cell types. *A, B,* Widefield fluorescence microscopy images of MCF-7 cells (A) or U87 cells (B) stained for Rab27b and CD63 as described in Methods.

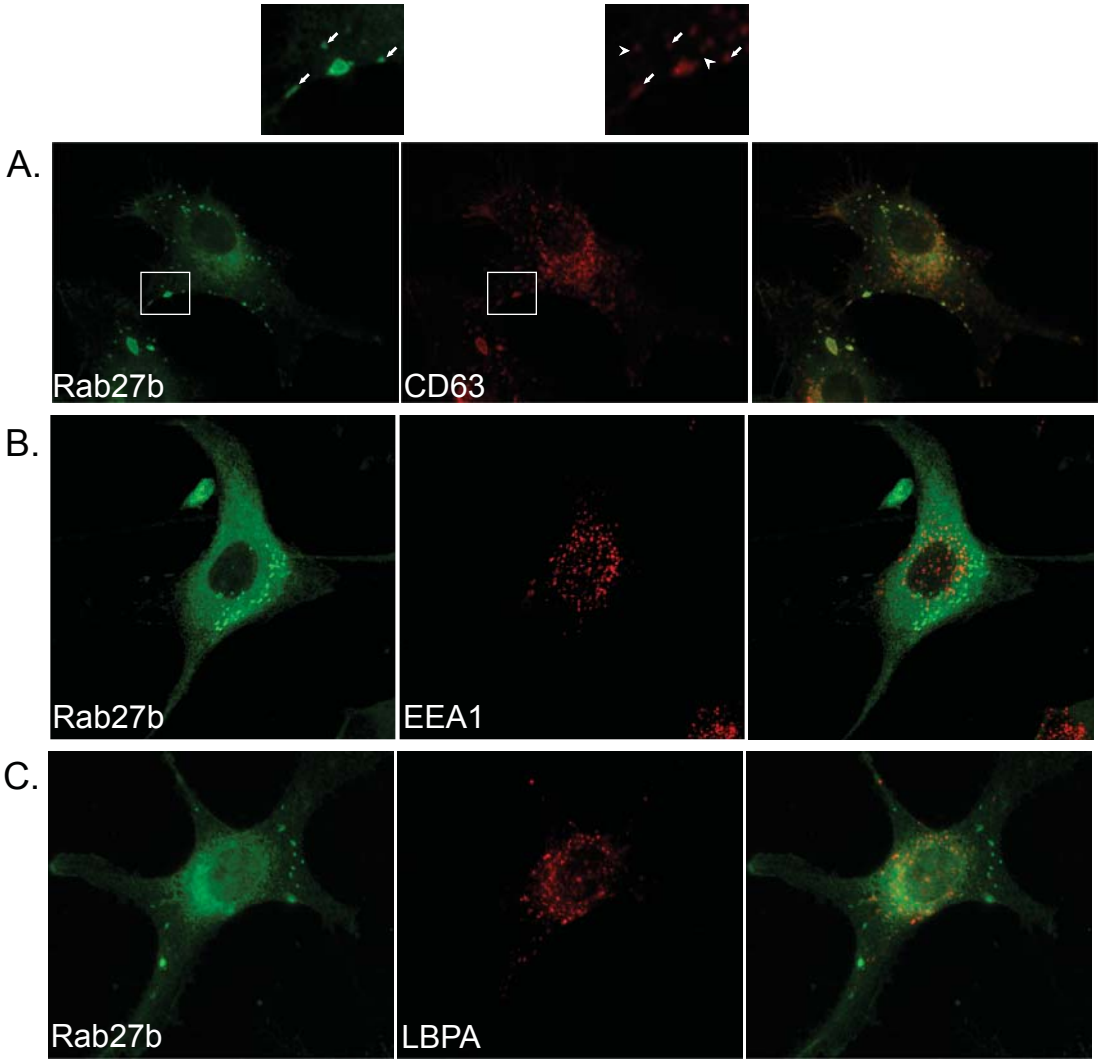

FIGURE 3-2. Rab27b localizes to a subset of CD63+ endosomes in U87 cells. Maximum intensity projections from confocal Z-series of U87 cells immunostained with the indicated antibodies as described in Methods. *A*, Rab27b and CD63 costains. White boxes show regions enlarged in insets. Structures with both Rab27b and CD63 staining are indicated by arrows. Structures with only CD63 are indicated by arrowheads. *B*, Rab27b and LBPA immunostaining shows little to no overlap. *C*, Rab27b and EEA1 immunostaining shows little to no overlap.

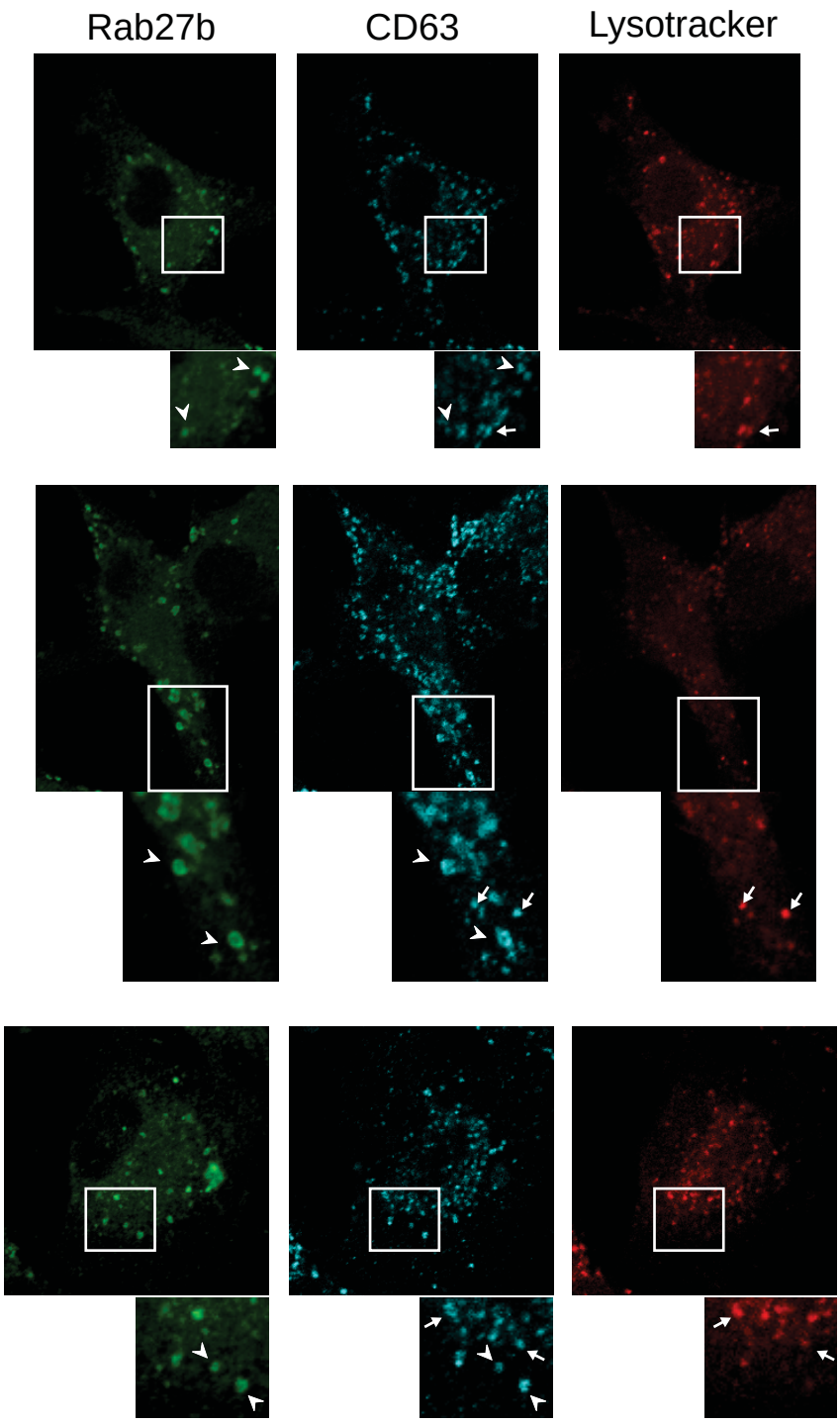

FIGURE 3-3. Rab27b markes non-acidic endosomes. Images are single confocal planes. U87 cells were treated with Lysotracker Red for 30min before aldehyde fixation and immunostaining.DMSO. White boxes indicate regions enlarged in insets. Structures with CD63+/Rab27b+/Lysotracker- staining are indicated with arrowheads. Structures with CD63+/Rab27-/Lysotracker+ staining are indicated with arrows.

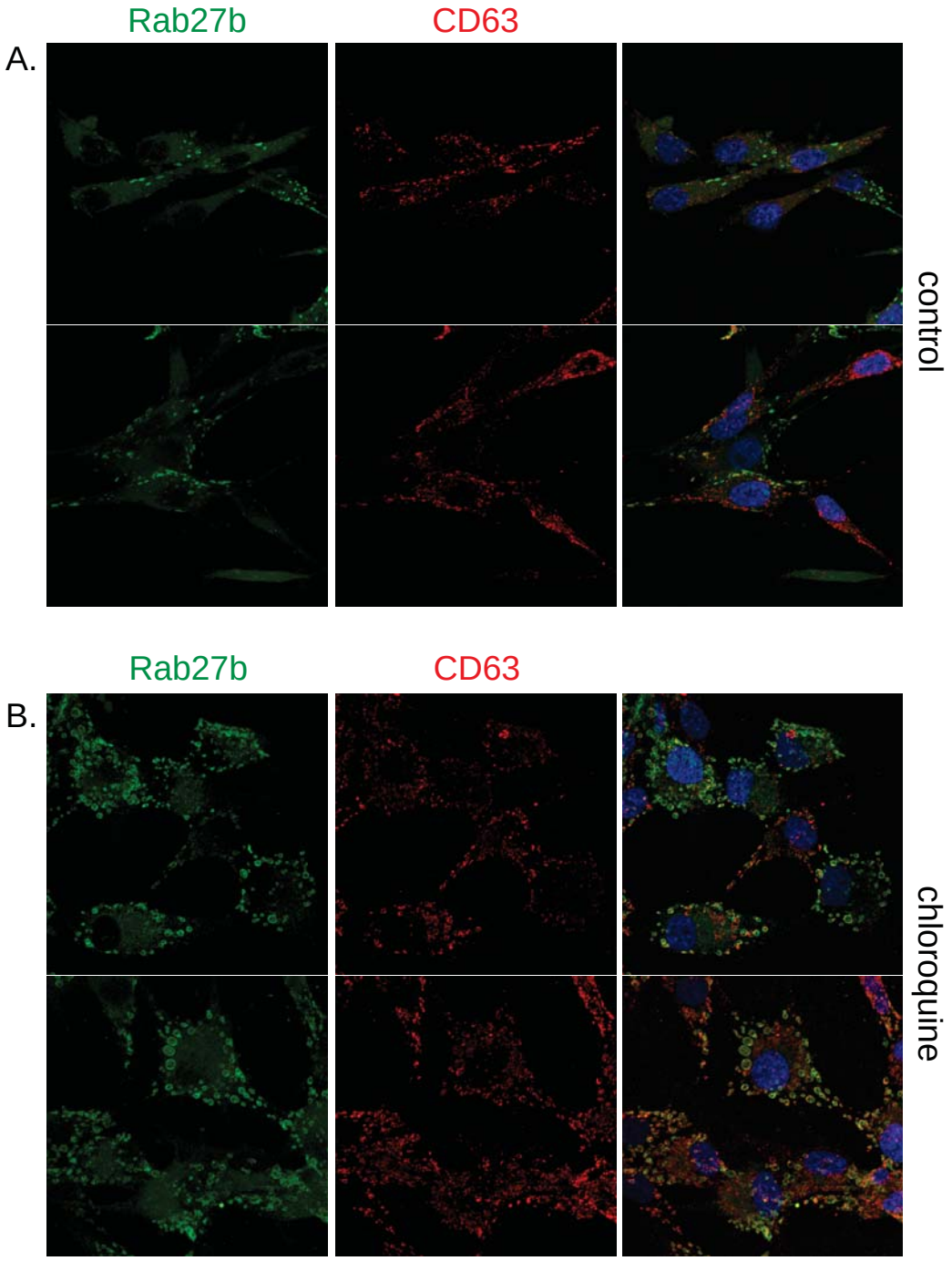

FIGURE 3-4. Neutral endosome pH enhances Rab27b recruitment. Images are maximum intensity projections of confocal Z-series. *A, B,* U87 cells where treated with PBS (A) or chloroquine (B) for 4 hrs before immunostaining for Rab27b and CD63.

Chapter 4

Preliminary data and future directions

4.1 CD63 and CD9 as markers for distinguishing exosomes versus ectosomes

EVs enriched for either CD63 or CD9 are to some extent physically separable (Figure 2-1, E). The data presented in Chapter 2 indicate that CD9 is primarily released on ectosomes. The size of plasma membrane derived vesicles is reported to range from ~150-1000 nm and thus the lower size limits overlap with that of exosomes. The methods we employed to isolate EVs include steps to clear large vesicles (i.e. centrifugation at 10,000 x g and/or filtration through 0.2μm pores). Despite these precautions we cannot exclude the possibility that larger vesicles are present in the material pelleted at 100,000 x g. We therefore analyzed 100k EVs by nanoparticle tracking. The results of this analysis indicated that the majority of EVs were <200nm with a mean size of 132±7.1nm and a mode of 100±5.5nm (Figure 4-1). Because our preparations contain a mixture of both EV types, these results imply that ectosomes bearing CD9 are not drastically different in size from exosomes bearing CD63. These data support the notion that EVs collected by size-based methods represent a mixture of exosomes and ectosomes.

It is clear that the steady state subcellular distribution of these tetraspanin proteins differs (Figure 2-1), indicating that they do not co-assemble into stable microdomains. An interesting question arising from this observation is whether tetraspanins actually co-assemble *in vivo* as

opposed to detergent solubilized membranes, in which multiple heteromeric tetraspanin-tetraspanin interactions have been reported (1).

Endocytic trafficking of CD63 is regulated by C-terminal YXXΦ motif that binds to clathrin adaptor proteins. In contrast, CD9 does not have this motif and is largely restricted to the plasma membrane. Despite their differential steady-state distributions, both proteins cycle through the endocytic system. Because of this dynamic trafficking, CD9 does end up on exosomes and CD63 on ectosomes (2, our results, Chapter 2). Both CD63 and CD9 can be tagged on their cytoplasmic N-termini without affecting trafficking or known interactions with cellular proteins and function. In order to probe the segregation and/or overlap between these markers on individual vesicles I generated HEK293 cell lines that stably express different combinations of mCherry-CD63, EGFP-CD63 and EGFP-CD9 proteins. Confocal images are shown in Figure 4-2 and demonstrate that each fusion protein mimics the localization of the endogenous protein (Figure 4-2, A-D).

The level of overexpression was determined by comparing immunoblots of each cell line to those of the parent cell line (Figure 4-3, A). In order to demonstrate that the tetraspanin fusions are released on EVs, I harvested EVs from culture media using the PEG/ConA protocol described in Chapter 2. Both total cell protein and EVs were subjected to immunoblotting with antibodies against GFP or mCherry. Importantly, the level of fluorescent protein released on EVs correlates with the relative expression level in the cells from which they derived (Figure 4-3, B).

Fluorescence Cross-correlation Spectroscopy (FCCS) is attractive as a future application utilizing these cells to directly monitor the degree of CD63 and CD9 segregation on different populations of EVs. FCS measures fluctuations in fluorescence as particles in Brownian motion

pass through a ~1 fl confocal volume. If two fluorophores are located on the same EV, fluorescence fluctuations in two colors cross-correlate enabling FCCS. In future studies, it will be interesting to use EVs collected from these cell lines to assess the degree of separation of these proteins on EVs. If we see coincidence between the signals, we can determine what percentage of EVs have one or the other label. EVs from the mCherry-CD63 and GFP-CD63 co-expressing cells will be an important control for positive cross-correlation. In addition, EVs from cells individually expressing mCherry-CD63 and GFP-CD9 would be mixed together as a control for negative correlation. Hence, the cell lines described above will be important tools for assessing the relative ratios of CD63 and CD9 in different EV populations.

4.2. Extended analysis of EV cargo proteins

In Chapter 2, our analysis of EV secretion focused primarily on tetraspanins (CD63 and CD9) as well as the adaptor protein syntenin-1, which associates with CD63. These proteins are clearly enriched in EVs relative to total cell lysates. Furthermore, they have each been implicated in different aspects of EV biology. We also assessed a sample of miRNA cargo as well as a general membrane marker (GPI-mCherry). Our results demonstrated that inhibition of VPS4 resulted in decreased EV release. Notably, however, EV release was not completely abrogated. During the course of my thesis work, I monitored the fate of several other candidate EV proteins. In contrast to the tetraspanins, I observed variable reproducibility in the effects of inhibiting VPS4 on the recovery of these proteins. Much of this may be due to challenges associated with sample handling and/or lack of robust antibodies; therefore, we could not comment on their relevance in that unit. However, these results could reflect complexities in the cohort of mechanisms at play during EV biogenesis and general membrane trafficking. A number of reproducible changes are noteworthy and merit further study. In particular, ESCRT-III proteins

were readily recovered in EVs released after VPS4 inhibition. The resulting changes in their recovery may provide evidence for the direct role of VPS4 and ESCRT-III in the membrane fission process that generates EVs. The following section describes these changes and discusses their potential implications in different aspects of EV biogenesis.

VPS4 inhibition alters EV protein composition—Hsc70 is an often-cited EV-associated protein. During the course of my thesis work I found that Hsc70 was modestly, albeit reproducibly, decreased in EVs released by cells expressing VPS4EQ (Figure 4-3, A). Preliminarily, we found that Hsc70 was not particularly enriched or de-enriched in EVs compared to cellular levels (data not shown). Hsc70 is a soluble heat shock protein that functions in proteostasis. It is implicated in regulating misfolded protein responses, autophagy and even direct sorting to exosomes (3, 4). Its presence in EVs is likely directly connected to these functions. Therefore, the mechanism by which VPS4EQ expression affects its incorporation into EVs is likely to be an interesting avenue for further investigation.

GSK3β is another soluble protein that we monitored in EVs released from various cell types. Motivation for focus on this cargo comes from the β-catenin dependent sequestration of GSK3β into MVBs following stimulation of cells by Wnt (5). In resting conditions, GSK3β was consistently de-enriched in EVs. In contrast to the EV proteins discussed thus far, we found that cells expressing VPS4EQ released greater concentrations of GSK3β compared to control cells (Figure 4-3, B).

LAMP1 and LAMP2 are single-pass transmembrane proteins primarily associated with the limiting membrane of late endosomes/lysosomes. Our preliminary inspection of EVs released by different cell types demonstrated that these proteins, while detectable in EV preparations, are

de-enriched relative to their cellular expression levels (data not shown). This finding is in agreement with those of several EV characterization studies. Similar to our findings for GSK3**β**, LAMP2 levels were increased in EVs recovered from cells expressing VPS4EQ (Figure 4-3, C). Taken together, it seems likely that while our results show that VPS4 inhibition reduced EV numbers it also altered the protein profile of EVs that were released from these cells. This effect may result from parallel inhibition of both EV biogenesis and other pathways involved in proteostasis

Altogether, the changes in EV protein content elicited by VPS4 inhibiton may reflect broader effects on membrane trafficking within the endosomal network. For example, there have been hints that regulation of lysosome homeostasis are linked to exosome secretion (6, 7). VPS4 inhibition perturbs lysosomal flux and triggers autophagy (8, 9). Inhibition of lysosomal function with the proton pump inhibitor bafilomycin has been shown to enhance exosome release (10). These results underscore the potential for plasticity in MVB fate in terms of lysosomal degradation versus extracellular release. Such observations warrant further investigation into the specific steps at which VPS4 and ESCRT-III act during trafficking of EV cargo proteins.

ESCRT proteins are incorporated into EVs—The data presented in Chapter 2 show that inhibition of VPS4, the master regulator of ESCRT-III disassembly, inhibits release of both exosomes and ectosomes. Others have similarly implicated different components of the ESCRT machinery in both exosome and ectosome biogenesis (11-15). Importantly, both vesicle types share a common physical requirement for membrane fission to separate the vesicle and the membrane from which it derived. Given this requirement, ESCRT-III and factors involved in its assembly and disassembly are the strongest candidates for this process.

Notable among studies of all EVs is that ALIX and Tsg101 are broadly cited as markers of EVs and especially exosomes. The implication is that these proteins, which are important nucleators of ESCRT-III assembly, are directly involved in EV biogenesis. However, efforts to directly connect this function to EV production have yielded variable results (12, 13, 16, 17). Nonetheless, the common presence of these proteins in EVs from various sources supports the notion that ESCRT is important for EV formation.

A concern when interpreting the content of EV preparations is the possibility of cross-contamination by large polymeric protein structures as well as protein aggregates. To confirm that extracellular ESCRT-III is indeed associated with membranes, we subjected 100k EV pellets to sucrose gradient floatation (Figure 4-5, A). This analysis clearly showed that the major ESCRT-III protein CHMP4A is membrane associated. A recent study done in collaboration with our lab employed quantitative tandem-mass-tag proteomics to compare EVs obtained by differential ultracentrifugation either directly or after Opti-prep gradient floatation in order to discern vesicle-associated proteins from other contaminants (18). In agreement with our findings using sucrose gradients, several ESCRT-III members were enriched in the Opti-prep fractions. Notably, we found elevated levels of CHMP4A (ESCRT-III) in EVs produced by cells in which VPS4 was inhibited (Figure 4-5, B). The role of VPS4 in ESCRT-III polymer disassembly is well established. Hence, this finding suggests that blocked disassembly causes ESCRT-III subunits to accumulate within EVs. Thus, more ESCRT-III was recovered despite the fact that fewer EVs were released. This finding may provide clues concerning the importance of ESCRT-III disassembly during EV biogenesis.

Methods

Antibodies, Plasmids and reagents—Antibodies used include mouse monoclonal antibodies against CD63 (Dev Biostudies (H5C6)), a monoclonal antibody against LAMP1 (Dev Biostudies H4A3), a polyclonal antibody against GSK3β (ProteinTech 22104-1-AP), a polyclonal antibody against CHMP4A (19), and a monoclonal antibody against Hsc70 (Sigma Aldrich H5147).Secondary antibodies were conjugated to horseradish peroxidase for immunoblotting (ThermoFisher), HEK293TREx cells were maintained as described in Chapter 2.

pmCherry-CD63 was described in Chapter 2 and was used to generate pCDNA4.1mCherry-CD63 using NdeI and BamHI sites. pEGFP-CD9 was described in Chapter 2. Cells were transfected using Lipofectamine 2000 followed by selection with 500μg/ml G418 and/or 100μg/ml zeocin.

EV collection and sucrose gradients—EV collection by PEG/ConA or differential centrifugation was performed as described in Chapter 2. EV pellets collected by differential centrifugation were suspended in 1.25 ml of 73% sucrose buffer in 20mM HEPES pH7.4. A discontinuous sucrose gradient was layered over this by applying 3 ml of 65% and finally 1.25 ml of 10% sucrose in 20mM HEPES pH7.4. After centrifugation at 34,000 × g for ≥14 hr, 500 μl fractions were taken from the top. 20 μl of each fraction was used for SDS-PAGE and immunoblotting.

SDS-PAGE and immunoblotting—Samples were boiled in SDS-PAGE sample buffer (2% SDS, 60mM Tris pH 6.8, 0.01% bromophenol blue, 10% glycerol) with or without 1% β-mercaptoethanol for 5 min and spun for 2 min at 21,000 × g. CD63 immunoblotting required non-reducing conditions. Proteins were separated on 10% gels followed by transfer to

nitrocellulose. Membranes were blocked and probed in TBS, 0.05% Tween and 5% nonfat dry milk. Blots were imaged on a ChemiDoc MP imaging system (Bio-Rad).

References

1. Charrin, S., F. le Naour, O. Silvie, P. E. Milhiet, C. Boucheix, and E. Rubinstein. 2009. Lateral organization of membrane proteins: tetraspanins spin their web. *Biochem J* 420: 133-154.

2. Buschow, S. I., E. N. Nolte-'t Hoen, G. van Niel, M. S. Pols, T. ten Broeke, M. Lauwen, F. Ossendorp, C. J. Melief, G. Raposo, R. Wubbolts, M. H. Wauben, and W. Stoorvogel. 2009. MHC II in dendritic cells is targeted to lysosomes or T cell-induced exosomes via distinct multivesicular body pathways. *Traffic* 10: 1528-1542.

3. Deffit, S. N., and J. S. Blum. 2015. A central role for HSC70 in regulating antigen trafficking and MHC class II presentation. *Mol Immunol* 68: 85-88.

4. Geminard, C., A. de Gassart, L. Blanc, and M. Vidal. 2004. Degradation of AP2 during reticulocyte maturation enhances binding of Hsc70 and Alix to a common site on TfR for sorting into exosomes. *Traffic* 5: 181-193.

5. Taelman, V. F., R. Dobrowolski, J. L. Plouhinec, L. C. Fuentealba, P. P. Vorwald, I. Gumper, D. D. Sabatini, and E. M. De Robertis. 2010. Wnt signaling requires sequestration of glycogen synthase kinase 3 inside multivesicular endosomes. *Cell* 143: 1136-1148.

6. Murrow, L., R. Malhotra, and J. Debnath. 2015. ATG12-ATG3 interacts with Alix to promote basal autophagic flux and late endosome function. *Nat Cell Biol* 17: 300-310.

7. Eitan, E., C. Suire, S. Zhang, and M. P. Mattson. 2016. Impact of lysosome status on extracellular vesicle content and release. *Ageing Res Rev*

8. Fujita, H. 2002. A dominant negative form of the AAA ATPase SKD1/VPS4 impairs membrane trafficking out of endosomal/lysosomal compartments: class E vps phenotype in mammalian cells. *Journal of Cell Science* 116: 401-414.

9. Rusten, T. E., T. Vaccari, K. Lindmo, L. M. Rodahl, I. P. Nezis, C. Sem-Jacobsen, F. Wendler, J. P. Vincent, A. Brech, D. Bilder, and H. Stenmark. 2007. ESCRTs and Fab1 regulate distinct steps of autophagy. *Curr Biol* 17: 1817-1825.

10. Savina, A., M. Furlan, M. Vidal, and M. I. Colombo. 2003. Exosome release is regulated by a calcium-dependent mechanism in K562 cells. *J Biol Chem* 278: 20083-20090.

11. Wehman, A. M., C. Poggioli, P. Schweinsberg, B. D. Grant, and J. Nance. 2011. The P4-ATPase TAT-5 inhibits the budding of extracellular vesicles in C. elegans embryos. *Curr Biol* 21: 1951-1959.

12. Baietti, M. F., Z. Zhang, E. Mortier, A. Melchior, G. Degeest, A. Geeraerts, Y. Ivarsson, F. Depoortere, C. Coomans, E. Vermeiren, P. Zimmermann, and G. David. 2012. Syndecan-syntenin-ALIX regulates the biogenesis of exosomes. *Nat Cell Biol* 14: 677-685.

13. Colombo, M., C. Moita, G. van Niel, J. Kowal, J. Vigneron, P. Benaroch, N. Manel, L. F. Moita, C. Thery, and G. Raposo. 2013. Analysis of ESCRT functions in exosome biogenesis, composition and secretion highlights the heterogeneity of extracellular vesicles. *J Cell Sci* 126: 5553-5565.

14. Choudhuri, K., J. Llodra, E. W. Roth, J. Tsai, S. Gordo, K. W. Wucherpfennig, L. C. Kam, D. L. Stokes, and M. L. Dustin. 2014. Polarized release of T-cell-receptor-enriched microvesicles at the immunological synapse. *Nature* 507: 118-123.

15. Nabhan, J. F., R. Hu, R. S. Oh, S. N. Cohen, and Q. Lu. 2012. Formation and release of arrestin domain-containing protein 1-mediated microvesicles (ARMMs) at plasma membrane by recruitment of TSG101 protein. *Proc Natl Acad Sci U S A* 109: 4146-4151.

16. Trajkovic, K., C. Hsu, S. Chiantia, L. Rajendran, D. Wenzel, F. Wieland, P. Schwille, B. Brugger, and M. Simons. 2008. Ceramide triggers budding of exosome vesicles into multivesicular endosomes. *Science* 319: 1244-1247.

17. van Niel, G., S. Charrin, S. Simoes, M. Romao, L. Rochin, P. Saftig, M. S. Marks, E. Rubinstein, and G. Raposo. 2011. The Tetraspanin CD63 Regulates ESCRT-Independent and -Dependent Endosomal Sorting during Melanogenesis. *Dev Cell* 21: 708-721.

18. Clark, D. J., W. E. Fondrie, Z. Liao, P. I. Hanson, A. Fulton, L. Mao, and A. J. Yang. 2015. Redefining the Breast Cancer Exosome Proteome by Tandem Mass Tag Quantitative Proteomics and Multivariate Cluster Analysis. *Anal Chem* 87: 10462-10469.

19. Lin, Y., L. A. Kimpler, T. V. Naismith, J. M. Lauer, and P. I. Hanson. 2005. Interaction of the mammalian endosomal sorting complex required for transport (ESCRT) III protein hSnf7-1 with itself, membranes, and the AAA+ ATPase SKD1. *J Biol Chem* 280: 12799-12809.

Chapter 4 Figures

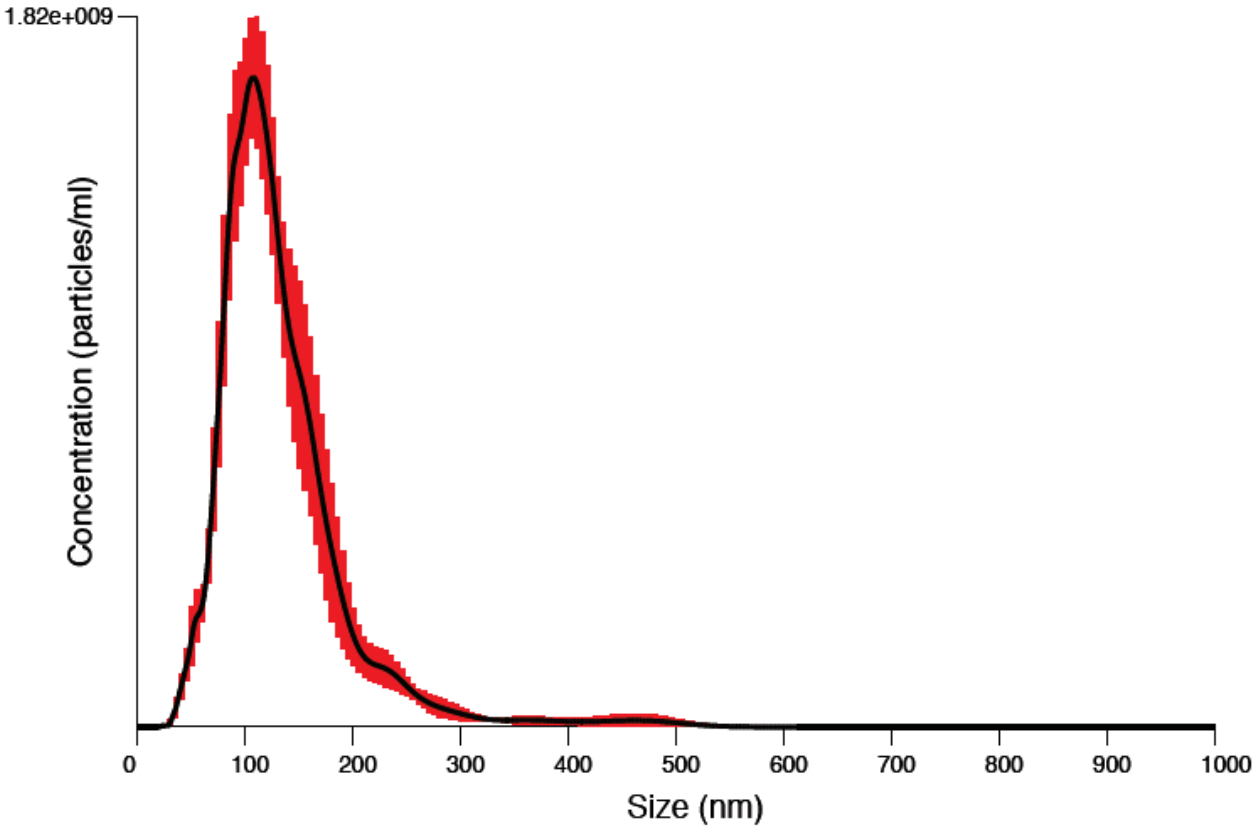

FIGURE 4-1. NanoSight particle tracking analysis of HEK293 EVs. EVs from HEK293 cells where isolated by differential centrifugation as described in Methods. The pellet was resuspended in HEPES buffer and a 1:500 dilution was applied to the NanoSight chamber. Average size = 132±7nm. Mode size = 100±5.5nm. Standard deviation = 58±6nm.

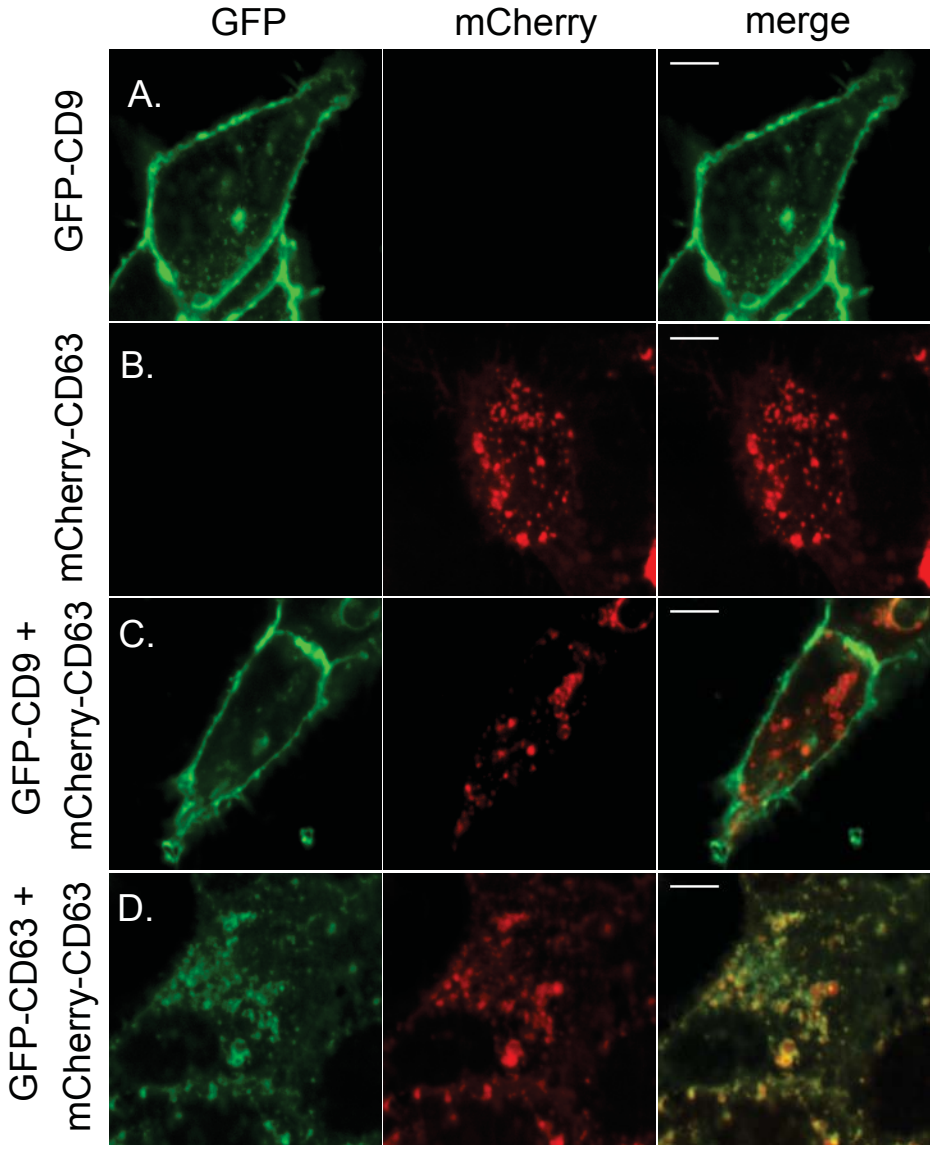

FIGURE 4-2. HEK293 cells expressing fluorescent tetraspanins. Images are single confocal planes. *A*, Cells expressing only GFP-CD9. *B*, Cells expressing only mCherry-CD63. *C*, Cells co-expressing GFP-CD9 and mCherry-CD63. *D*, Cells co-expressing GFP-CD63 and mCherry-CD63. Scale bar = 10μm.

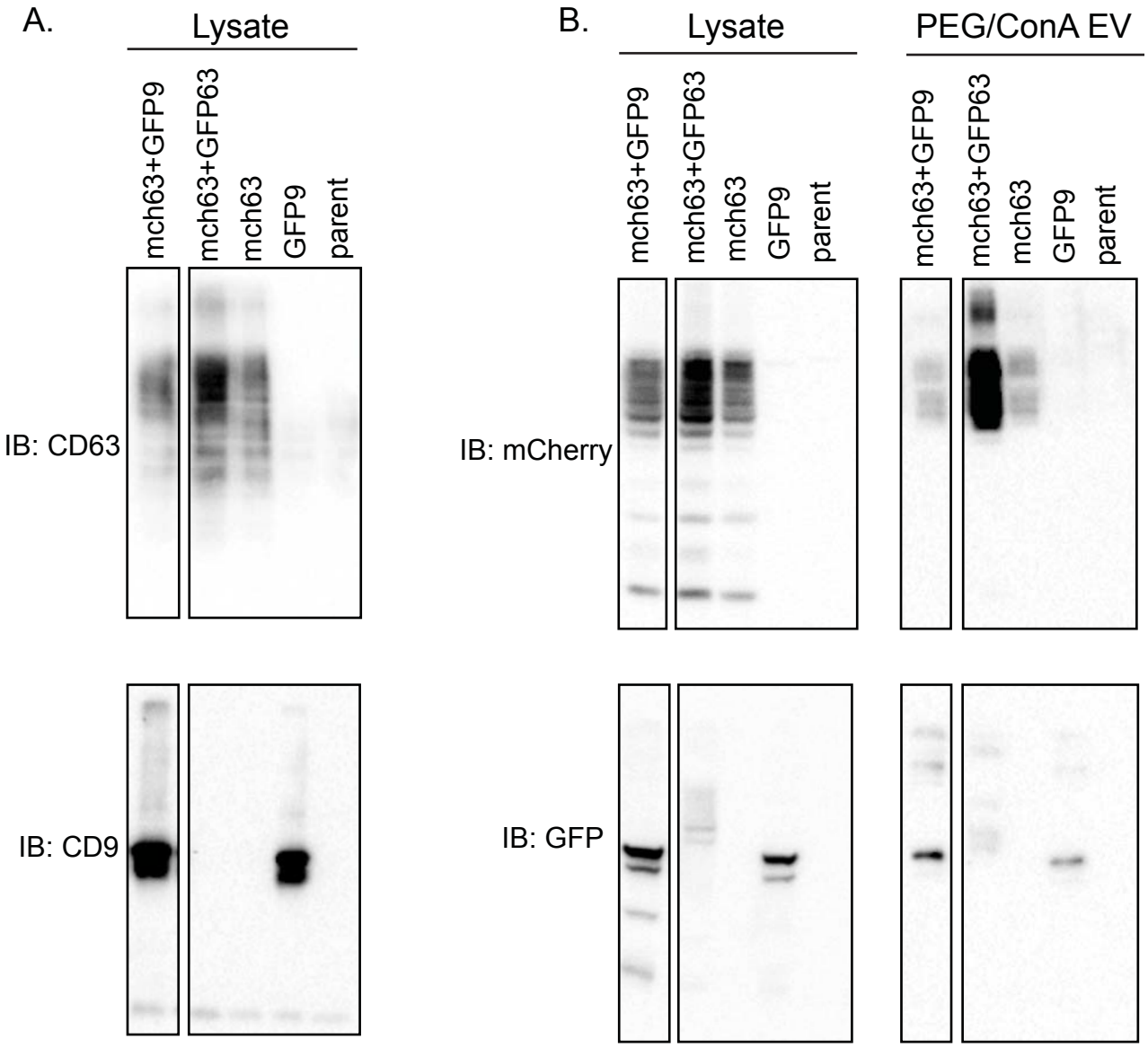

FIGURE 4-3. Fluorescently tagged tetraspanins are released on EVs. *A*, Cells from Figure 4-2 were solubilized as described in methods. Equal concentrations of whole cell protein from each cell line were immunoblotted for tetraspanins. *B*, EVs produced in 24hr by each cell line were collected by PEG/ConA. Volume of solubilized EVs was normalized to the total cellular protein concentrations. Equal concentrations of whole cell protein (Lysate) and equal volumes of EVs (PEG/ConA EVs) were immunoblotted with antibodies against GFP or mCherry.

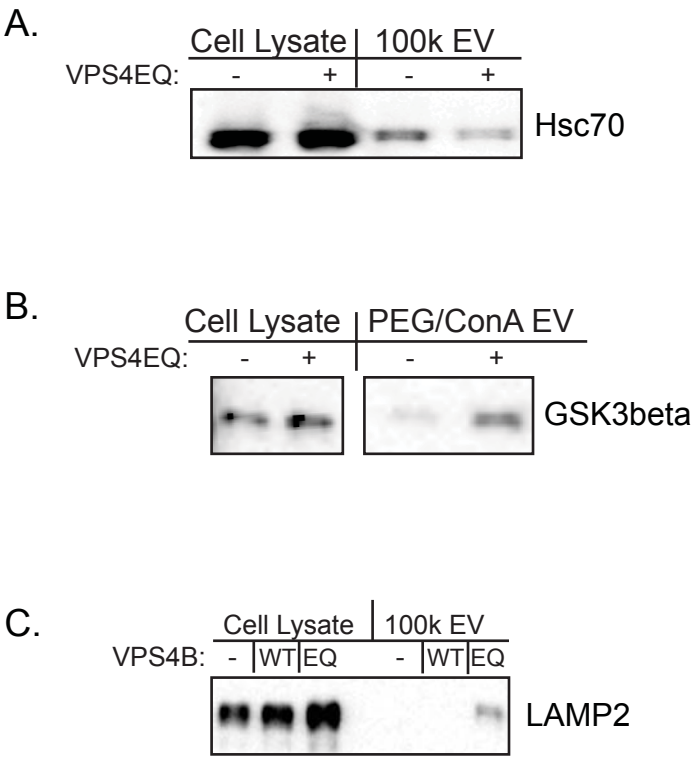

FIGURE 4-4. VPS4 inhibition alters EV protein composition. (A-C) EVs from VPS4EQ expressing cell over were harvested by differential centrifugation or PEG/ConA as described in methods. The EV resuspension volumes were normalized to the total protein concentration of the cells from which they derived. Equal concentrations of cellular protein and equal volumes of EV protein were immunoblotted with the indicated antibodies.

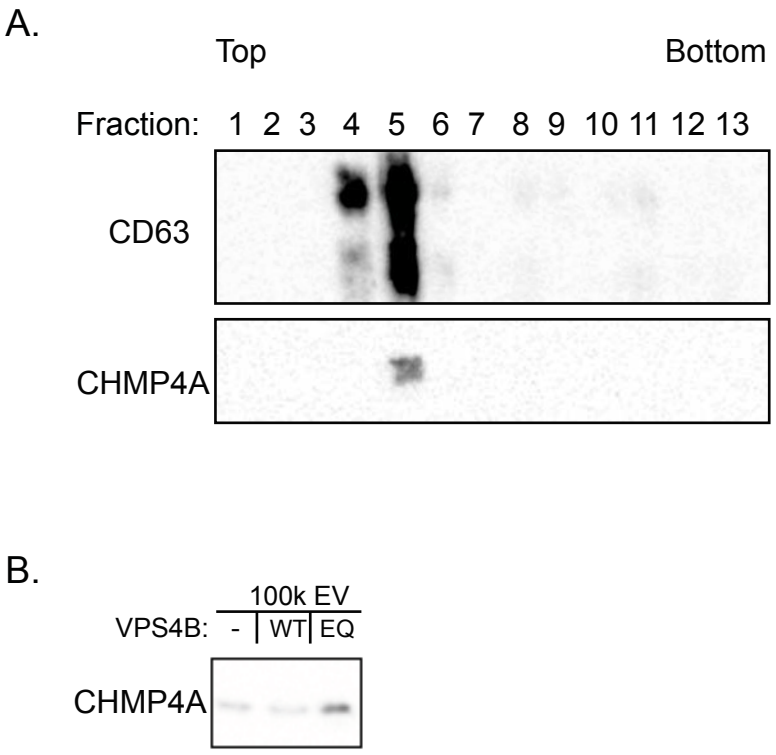

FIGURE 4-5. ESCRT-III is incorporated into EVs. *A*, EVs from SKBR3 cells were collected by differential centrifugation and floated into a sucrose gradient as described in Methods. Fractions were immunoblotted for CHMP4A and CD63. *B*, EVs from VPS4EQ expressing cells were harvested by differential centrifugation. The EV resuspension volumes were normalized to the total cellular protein concentration.

Chapter 5

Summary and Discussion

Summary of the Thesis

The extracellular environment is an important player in modulation of cellular activities. This statement is exemplified by our understanding of signaling processes requiring cell interactions with other cells, extracellular matrix, secreted soluble ligands, and hormones. As discussed above, EVs are emerging as intriguing components of the extracellular milieu which an increasing body of evidence points to as signaling units capable of eliciting phenotypic responses in the cells with which they come into contact. While evidence supports the capability of EVs to cause such changes, the specific roles proposed for exosomes in cell-cell signaling are difficult to test given that so little is known about their biogenesis.

A major challenge that limits investigations of EV biology is the lack of simple methods to reproducibly collect and quantify EVs. The most common method for concentrating EVs from culture medium is differential centrifugation (Chapter 1). We used typical procedures to collect EVs released from cultured cell lines by differential centrifugation followed in some cases by flotation into sucrose gradients (Chapter 2). We found that proteins characteristic of EVs were recovered in differing amounts from conditioned media, depending on the cell line studied and consistent with previously reported differences in EV production. However, differential centrifugation requires relatively large quantities of cells and/or long incubation time. These requirements preclude acute analysis of EV production and limit the repertoire of manipulations that can be tested since many pharmacological treatments are toxic to cells after long times. To

address this problem I developed a protocol for concentrating EVs from small volumes of culture medium using polyethylene glycol precipitation followed by lectin affinity isolation (Chapter 2).

At the time I began my thesis, mechanisms of EV biogenesis were only beginning to be investigated. Given the topology of EV budding, the MVB origin of exosomes, and the well-characterized roles of ESCRT in MVB biogenesis, ESCRT proteins were commonly invoked as cellular machinery likely to be involved in generating EVs. However, seminal work by Trajkovic and colleagues suggested an ESCRT-independent mechanism for budding of proteolipid protein into the MVB lumen prior to exocytosis (1). This gave rise to the concept that ESCRTs were unlikely to be generally required for forming the MVBs that give rise to exosomes. Over the course of my thesis work, studies from other groups have taken different approaches to address the question of ESCRT function in EV biogenesis with varying results limited by both the techniques and the complexity of ESCRT function in endosomal maturation

Our interest in studying EV biogenesis grew out of the lab's interest in how ESCRT-III and Vps4 work together and with other factors to promote vesicle (and virus) biogenesis and release. If ESCRT-III and Vps4 are directly responsible for creating ILVs within multivesicular bodies, a straight-forward prediction was that they should be necessary for exosome formation (and therefore release). Additionally, as part of the lab's effort to connect ESCRT-III filament structure to function in vesicle biogenesis we explored the localization and structure of ESCRT-III filaments stabilized by depleting Vps4 and found spirals likely to represent "scars" left behind by released vesicles on both endosomes and the plasma membrane (2). Together with the known role of ESCRT-III in viral particle budding from both the plasma membrane and the MVB, these observations led us to suspect a general involvement of ESCRT-III at both sites.

Attempts to assess ESCRT-III role in EV biogenesis have typically relied on siRNA-mediated depletion of individual ESCRT-III subunits. Interpreting results of these studies is complicated, since ESCRT-III is a dynamic polymer comprised of multiple closely related subunits, the precise stoichiometry of which is largely unknown. Furthermore, studies on ESCRT-III function in other biological processes suggest that not all subunits are required in each process and further that the function of some may be redundant. To broadly and efficiently inhibit ESCRT-III function, I employed the dominant-negative, ATPase-defective Walker B mutant of VPS4 (here referred to as VPS4EQ), which is the AAA+ ATPase master regulator of ESCRT-III disassembly that is required for all ESCRT-dependent processes. Using cell lines in which VPS4EQ is inducibly expressed, I was able to achieve timely and coordinated inhibition of ESCRT-III disassembly. I found that this manipulation decreased release of canonical EV proteins CD63 and CD9 as well as of representative miRNA cargo (Chapter 2). Importantly, VPS4EQ also reduced the number of membranous vesicles secreted into the culture medium. The consistent recovery of ESCRT proteins by EV proteomics is a primary impetus for investigating their role in EV biogenesis. Our finding that ESCRT-III proteins were more concentrated in EVs released by VPS4EQ expressing cells, despite the decrease in vesicle number, suggests that ESCRT-III polymer disassembly is important for membrane fission during EV formation.

Cells release two types of EVs that can be defined by their intracellular membrane of origin. I was intrigued by the contrasting localization of the tetraspanin proteins CD63 and CD9, which have become widely accepted as markers of exosomes. Indeed, CD63 localizes to endosomes and is enriched on lumenal vesicles within MVBs (3). In contrast, CD9 localizes primarily to the plasma membrane (4). Therefore, I hypothesized that CD63 is released on

exosomes while CD9 marks ectosomes. Using continuous sucrose gradient fractionation I show that these proteins are present on different populations of physically separable EVs. Further support for this interpretation came from finding that treating cells with nocodazole to interfere with MVB trafficking reduced CD63 but not CD9 release. In addition, I characterize serum as a specific trigger of VPS4-dependent ectocytosis (Chapter 2). Altogether, these findings implicate VPS4, and by extension ESCRT-III, in biogenesis of both exosomes and ectosomes. In order to further probe the extent to which CD63 and CD9 segregate on different EVs, I developed and characterized cell lines expressing these proteins fused to GFP or mCherry in different combinations.

With specific regard to exosome release, a further mystery is the question of what distinguishes a MVB destined for exocytosis from one destined for degradation. Currently, the most well characterized factors involved in the actual trafficking and release of exocytic MVBs are Rab27a and Rab27b. I have identified Rab27b as a likely marker of exocytic MVBs in U87 cells (Chapter 3). Rab27b localizes to a subset of late endosomes that also contain the exosomal protein CD63. I have provided evidence that these specialized MVBs are less acidic than canonically degradative MVBs. Furthermore, endosome pH appears to play a direct role in recruiting Rab27b since chloroquine neutralization increases both Rab27b endosomes and CD63 release.

Discussion

Understanding ESCRT-III function during EV biogenesis—Current thinking about how ESCRT-III and VPS4 act to create and release intralumenal vesicles has generally supported a model in which ESCRT-III filaments spiral on the membrane to surround cargo and eventually promote membrane buckling, neck constriction, and ultimately membrane fission -- all from the

cytoplasmic side of the event (5)(6). A difficulty with this model is understanding how the nucleating component(s) within the nascent particle separate from the spiral that they nucleate. This has led to some confusion and at least one proposal for how ESCRTs might act from the other side, assembling (and departing) with a viral particle (and, by analogy, an EV) (Van Engelenburg et al., 2014). While the data supporting this alternative model for viruses are not particularly strong (together with a general failure to report/detect appearance of ESCRT-III factors in released viruses, albeit in decidedly limited numbers of incomplete studies), there is a major question here. The frequent and enriched recovery of Alix and the entire ESCRT-III/Vps4 machinery in EVs and our data indicating that ESCRT-III disassembly regulates ESCRT-III concentration in EVs motivates readdressing this question.

ESCRT-dependent ILV formation in yeast requires an initiating ubiquitin signal on cargo proteins that in turn recruits components of the 'canonical' ESCRT pathway ending with ESCRT-III and Vps4 (7). In the case of viruses, viral structural proteins contain so called 'late domain' motifs that recruit either Tsg101 (ESCRT-I) or Alix to engage and activate ESCRT-III (8). If ESCRT-III (alone among ESCRT complexes) is involved in EV biogenesis, how is it recruited? One answer comes from a study of syndecan/syntenin containing exosomes, where syntenin was found to contain YPxL Alix binding motifs essential for its ability to promote exosome release (9). By recruiting Alix, syntenin couples cargo and the domain that it forms to ESCRT-III. The fact that syntenin is frequently present in EVs, binds CD63, and was found to play a general role in exosome release (9) suggests that it may be an adaptor broadly relevant in EV formation. Our data are consistent with a role for VPS4/ESCRT-III in syntenin release in EVs (Chapter 2). ALIX binds directly to CHMP4, and this is the proposed mechanism of ESCRT-III recruitment during EV biogenesis (10) (9). One way to test this hypothesis could be

to directly interfere with ESCRT-III polymerization downstream of ALIX-CHMP4 binding. Furthermore, syntenin is not important for release of several EV proteins including CD9 and flotillin (11) (9). Future studies should aim at identifying other adaptor molecules capable of recruiting ALIX to determine if other EVs also depend on ALIX through different mechanisms. In the future, it will be important to understand whether and/or how ESCRT-III polymerization directly contributes to proposed mechanisms of EV budding.

Investigating the exocytic MVB—As discussed in Chapters 1 and 3, the machinery responsible for trafficking, docking, and fusion of MVBS with the plasma membrane includes small GTPases and their effectors, their regulating GEFs and GAPs, and exocytic SNAREs. Importantly, however, none of these factors are uniquely responsible for MVB exocytosis but instead have a variety of other client membranes including lysosomes (12) , lysosome related organelles (13), and recycling endosomes (14). Physiologic effects associated with depleting any of these can therefore not be uniquely attributed to a block in EV release. There is clearly still much to learn about proteins controlling MVB exocytosis for EV release.

In Chapter 3, I focused on Rab27b as a candidate marker for exocytic MVBs in a subset of cell-types that express this protein. Rab27a expression is high in endocrine pancreas, intestines, parotid gland, while Rab27b is high in brain, spleen, paralotid, platelets, exocrine pancrease (13). Elevated Rab27b expression has been connected to bladder cancer, which is in line with the notion that mis-regulated exosome secretion contributes to cancer progression (15). However, given that most or all cells secrete exosomes an important question is what factors take the place of Rab27b when it is not expressed.

In Chapter 1, I discussed various other small GTPases implicated in exosome secretion including Rab11, Rab35, Arf6 and RalA/B . Some common threads may provide hints as to how exosome secretion is regulated in different cell types. One possible explanation is overlap in the effector molecules that bind to these GTPases. For example, both Rab27 and Rab11 bind to Munc13-4 to regulate calcium-dependent docking of secretory vesicles to the plasma membrane (16, 17). Ral GTPases are involved in secretion events along with Rab27 in several systems (18). Rab27, RalA/B and Rab11 and Arf 6 each interact with subunits of the exocyst complex, which is broadly implicated in tethering secretory vesicles to the plasma membrane. RalA/B binds Sec5 and Exo84, Rab 11 and Rab27 bind to Sec15 and Arf6 binds to Sec10 (18, 19) (20) (21). It will be interesting to test the importance of exocyst function during exosome release across different cell types. Several exocyst subunits bind to phosphoinoitides or possess domains capable of binding phosphoinositides (22) (23) (24). In particular, PI(4,5)P2 regulates exocyst membrane association. Interestingly, Rab35 is involved in regulating PI(4,5)P2 levels through its effector OCRL, which contains an inositol polyphosphate 5-phasphotase domain. Therefore, it is likely that regulation of phosphoinositides is an important mechanism for recruiting exosome secretion factors. These observations demonstrate interconnections between different trafficking regulatory GTPases and highlight factors that may be common regulatory elements during exosome secretion from different cell types.

Sensitivity of EV detection—A major challenge in studying both EV biogenesis and function is that the current list of EV-associated material is huge (Choi et al., 2014; Kim et al., 2015), reflecting the ease with which high throughput –omics techniques can generate data describing extracellular material collected from any source. While common and abundant components are repeatedly identified, most of the thousands of other factors present in subsets of

EV datasets are the result of vesicle heterogeneity (e.g. collected from different cell types, released in response to different secretory cues, etc.), contamination by other non-EV material (e.g. other membranes, fragments of dead/dying cells, components of the extracellular matrix, or non-vesicular secretions), or simply differences in detection limits. Distinguishing among these explanations is in most cases impractical. Additionally, most studies of cultured cells examine EVs collected over an extended period of time (often a day or more) because of limitations imposed by sample handling and detection sensitivity. This averaging of release (over time in cell culture experiments, and among cell types in body fluids) masks connections to cargo-packaging and release-triggering events which again makes it difficult to explore the responsible molecular machinery. In order to study cellular mechanisms responsible for EV biogenesis and release, strategies are needed to reduce sample heterogeneity, improve assay sensitivity and throughput, and provide kinetic and spatial resolution to the analysis of EV release.

In this work, I developed a protocol for isolating heterogeneous EVs from small numbers of cells after relatively short incubation times (Chapter 2). Methods for monitoring EV release with much greater temporal resolution are needed for more detailed characterization. The ability to trigger EV release with serum was critical to my assessment of ectosome release kinetics. Future studies should be aimed at identifying other EV secretagogues. Growth factors, calcium ionophores , phorbol esters and lysosomal perturbants are all likely candidates for triggering release of different EV types (Gennebäck et al., 2013)(Jeppesen et al., 2014; Savina et al., 2003) (Mittelbrunn et al., 2011)(Savina et al., 2003).

References

1. Trajkovic, K., C. Hsu, S. Chiantia, L. Rajendran, D. Wenzel, F. Wieland, P. Schwille, B. Brugger, and M. Simons. 2008. Ceramide triggers budding of exosome vesicles into multivesicular endosomes. *Science* 319: 1244-1247.

2. Cashikar, A. G., S. Shim, R. Roth, M. R. Maldazys, J. E. Heuser, and P. I. Hanson. 2014. Structure of cellular ESCRT-III spirals and their relationship to HIV budding. *Elife* 3:

3. Escola, J. M., M. Kleijmeer, W. Stoorvogel, J. M. Griffith, O. Yoshie, and H. J. Geuze. 1998. Selective enrichment of tetraspan proteins on the internal vesicles of multivesicular endosomes and on exosomes secreted by human B-lymphocytes. *J Biol Chem* 273: 20121-20127.

4. Israels, S. J., E. M. McMillan-Ward, J. Easton, C. Robertson, and A. McNicol. 2001. CD63 associates with the alphaIIb beta3 integrin-CD9 complex on the surface of activated platelets. *Thromb Haemost* 85: 134-141.

5. Wollert, T., and J. H. Hurley. 2010. Molecular mechanism of multivesicular body biogenesis by ESCRT complexes. *Nature* 464: 864-869.

6. Chiaruttini, N., L. Redondo-Morata, A. Colom, F. Humbert, M. Lenz, S. Scheuring, and A. Roux. 2015. Relaxation of Loaded ESCRT-III Spiral Springs Drives Membrane Deformation. *Cell* 163: 866-879.

7. MacDonald, C., N. J. Buchkovich, D. K. Stringer, S. D. Emr, and R. C. Piper. 2012. Cargo ubiquitination is essential for multivesicular body intralumenal vesicle formation. *EMBO Rep* 13: 331-338.

8. Votteler, J., and W. I. Sundquist. 2013. Virus budding and the ESCRT pathway. *Cell Host Microbe* 14: 232-241.

9. Baietti, M. F., Z. Zhang, E. Mortier, A. Melchior, G. Degeest, A. Geeraerts, Y. Ivarsson, F. Depoortere, C. Coomans, E. Vermeiren, P. Zimmermann, and G. David. 2012. Syndecan-syntenin-ALIX regulates the biogenesis of exosomes. *Nat Cell Biol* 14: 677-685.

10. McCullough, J., R. D. Fisher, F. G. Whitby, W. I. Sundquist, and C. P. Hill. 2008. ALIX-CHMP4 interactions in the human ESCRT pathway. *Proc Natl Acad Sci U S A* 105: 7687-7691.

11. Roucourt, B., S. Meeussen, J. Bao, P. Zimmermann, and G. David. 2015. Heparanase activates the syndecan-syntenin-ALIX exosome pathway. *Cell Res* 25: 412-428.

12. Rao, S. K., C. Huynh, V. Proux-Gillardeaux, T. Galli, and N. W. Andrews. 2004. Identification of SNAREs involved in synaptotagmin VII-regulated lysosomal exocytosis. *J Biol Chem* 279: 20471-20479.

13. Fukuda, M. 2013. Rab27 effectors, pleiotropic regulators in secretory pathways. *Traffic* 14: 949-963.

14. Takahashi, S., K. Kubo, S. Waguri, A. Yabashi, H. W. Shin, Y. Katoh, and K. Nakayama. 2012. Rab11 regulates exocytosis of recycling vesicles at the plasma membrane. *J Cell Sci* 125: 4049-4057.

15. Ostenfeld, M. S., D. K. Jeppesen, J. R. Laurberg, A. T. Boysen, J. B. Bramsen, B. Primdal-Bengtson, A. Hendrix, P. Lamy, F. Dagnaes-Hansen, M. H. Rasmussen, K. H. Bui, N. Fristrup, E. I. Christensen, I. Nordentoft, J. P. Morth, J. B. Jensen, J. S. Pedersen, M. Beck,

D. Theodorescu, M. Borre, K. A. Howard, L. Dyrskjot, and T. F. Orntoft. 2014. Cellular disposal of miR23b by RAB27-dependent exosome release is linked to acquisition of metastatic properties. *Cancer Res* 74: 5758-5771.

16. Johnson, J. L., J. He, M. Ramadass, K. Pestonjamasp, W. B. Kiosses, J. Zhang, and S. D. Catz. 2016. Munc13-4 Is a Rab11-binding Protein That Regulates Rab11-positive Vesicle Trafficking and Docking at the Plasma Membrane. *J Biol Chem* 291: 3423-3438.

17. Elstak, E. D., M. Neeft, N. T. Nehme, J. Voortman, M. Cheung, M. Goodarzifard, H. C. Gerritsen, P. M. van Bergen En Henegouwen, I. Callebaut, G. de Saint Basile, and P. van der Sluijs. 2011. The munc13-4-rab27 complex is specifically required for tethering secretory lysosomes at the plasma membrane. *Blood* 118: 1570-1578.

18. Shirakawa, R., and H. Horiuchi. 2015. Ral GTPases: crucial mediators of exocytosis and tumourigenesis. *J Biochem* 157: 285-299.

19. Zhang, X. M., S. Ellis, A. Sriratana, C. A. Mitchell, and T. Rowe. 2004. Sec15 is an effector for the Rab11 GTPase in mammalian cells. *J Biol Chem* 279: 43027-43034.

20. Wu, S., S. Q. Mehta, F. Pichaud, H. J. Bellen, and F. A. Quiocho. 2005. Sec15 interacts with Rab11 via a novel domain and affects Rab11 localization in vivo. *Nat Struct Mol Biol* 12: 879-885.

21. Prigent, M., T. Dubois, G. Raposo, V. Derrien, D. Tenza, C. Rosse, J. Camonis, and P. Chavrier. 2003. ARF6 controls post-endocytic recycling through its downstream exocyst complex effector. *J Cell Biol* 163: 1111-1121.

22. Liu, J., X. Zuo, P. Yue, and W. Guo. 2007. Phosphatidylinositol 4,5-bisphosphate mediates the targeting of the exocyst to the plasma membrane for exocytosis in mammalian cells. *Mol Biol Cell* 18: 4483-4492.

23. Zhang, X., K. Orlando, B. He, F. Xi, J. Zhang, A. Zajac, and W. Guo. 2008. Membrane association and functional regulation of Sec3 by phospholipids and Cdc42. *J Cell Biol* 180: 145-158.

24. Jin, R., J. R. Junutula, H. T. Matern, K. E. Ervin, R. H. Scheller, and A. T. Brunger. 2005. Exo84 and Sec5 are competitive regulatory Sec6/8 effectors to the RalA GTPase. *EMBO J* 24: 2064-2074.